Image Cover Sheet

CLASSIFICATION	SYSTEM NUMBER 513041
UNCLASSIFIED	

TITLE

A Procedure for Assessing the Structure of the CPF Considering the Loss of Strength Due to Corrosion

System Number:

Patron Number:

Requester:

Notes:

DSIS Use only:

Deliver to:

REPRODUCTION QUALITY NOTICE

This document is the best quality available. The copy furnished to DRDCIM contained pages that may have the following quality problems:

: Pages smaller or Larger than normal

: Pages with background colour or light coloured printing

: Pages with small type or poor printing; and or

: Pages with continuous tone material or colour photographs

Due to various output media available these conditions may or may not cause poor legibility in the hardcopy output you receive.

☒ If this block is checked, the copy furnished to DRDCIM contained pages with colour printing, that when reproduced in Black and White, may change detail of the original copy.

Copy No. 9

DEFENCE R&D DÉFENSE

A PROCEDURE FOR ASSESSING THE STRUCTURE OF THE CPF CONSIDERING THE LOSS OF STRENGTH DUE TO CORROSION

D.R. Smith

DEFENCE RESEARCH ESTABLISHMENT ATLANTIC

Contractor Report

DREA CR 1999-111

April 1999

National Defence Défense nationale

Canada

National Defence
Research and Development Branch

Défense nationale
Bureau de recherche et développement

DREA CR 1999-111

A PROCEDURE FOR ASSESSING THE STRUCTURE OF THE CPF CONSIDERING THE LOSS OF STRENGTH DUE TO CORROSION

D.R. Smith

Scientific Authority
Layton GILROY

W7707-8-5853
Contract Number

April 1999

CONTRACTOR REPORT

Prepared for

Defence Research Establishment Atlantic

Centre de Recherches pour la Défense Atlantique

Canada

Abstract

The report describes the effect of possible corrosion of the hull plating and stiffeners on the structural strength of the Canadian Patrol Frigate in deep departure hogging and light operational sagging conditions. Balance on an eight meter wave was the sea state loading case considered. A MAESTRO analysis was carried out to obtain the initial structural strength, then the effects of corrosion were assessed. To model corrosion, areas of plating and the attached stiffeners were reduced in cross-section and modelled in detail. After each reduction, the structure was analysed using the finite element analysis program, VAST, to determine the effect on strength when applying the boundary conditions and loading from the MAESTRO analysis. The adequacy parameters and stresses with and without corrosion are presented in graphical form as a measure of the hull strength.

Résumé

Dans le rapport, on décrit l'effet de la corrosion possible du bordé de coque et des raidisseurs sur la résistance structurale d'une Frégate canadienne de patrouille, dans des conditions d'arc prononcé et de contre-arc léger lors de l'utilisation normale du navire. L'état de mer considéré correspondait à l'équilibre du navire sur une vague de huit mètres. On a procédé à une analyse MAESTRO en vue de déterminer la résistance structurale initiale, puis on a évalué les effets de la corrosion. Pour modéliser la corrosion, la surface de la section transversale des bordés et des raidisseurs qui y étaient fixés a été réduite et modélisée de façon détaillée. Après chaque réduction, on a analysé la structure à l'aide du programme d'analyse des éléments finis VAST, pour déterminer l'effet sur la résistance de l'application des conditions aux limites et de la charge utilisées lors de l'analyse MAESTRO. Les paramètres de conformité et les contraintes avec et sans corrosion sont présentés, sous forme graphique, comme une mesure de la résistance de la coque.

Contents

List of Tables

List of Figures

1 Introduction

The possible effect on the structural strength of the Canadian Patrol Frigate caused by different degrees of corrosion at chosen locations was assessed. The assessment was carried out initially by using the finite element analysis program MAESTRO[1] to perform a global analysis for two loading cases on a MAESTRO model of the CPF. The loading cases were deep departure hogging and light operational sagging conditions when balanced on an eight-meter wave. The stresses and adequacy parameters were obtained from this initial analysis.

The adequacy parameters used in MAESTRO are based on the design code modes of failure listed in Table 1. They are calculated using the following equation, which compares stresses originating from the loading with the allowable stresses for each of the failure modes.

$$g = \frac{1 - \left(\frac{Q}{Q_l}\right) sf}{1 + \left(\frac{Q}{Q_l}\right) sf}$$

where: g is the adequacy parameter, sf is the safety factor, Q is the stress due to the loading, and Q_l is the allowable limit.

Adequacy parameters of zero or greater are considered satisfactory as the safety factor has been exceeded. Parameters less than 0.0 are less than satisfactory indicating the actual safety factor is lower than that set for the design, indicating a high possibility of failure as g approaches -1.00.

Regions for detailed investigation were identified from this analysis and from reports of corrosion from hull inspections. These regions were extracted and the MAESTRO elements were converted to quadrilateral plate elements from the VAST[2] finite element program, using the Detailed Stress Analysis modelling feature of MAESTRO. The elements were then refined as required to model possible corrosion. Top-down analyses were carried out on each of the extracted regions using boundary conditions and loading obtained from the initial MAESTRO analysis.

2 MAESTRO Model of the CPF

The MAESTRO finite element model of the CPF is shown in Figure 1. It was made up of three substructures as shown in Figure 2. The substructures were divided into modules. Each module was divided into MAESTRO strake elements which stretch from one end of the module to the other. The strakes are assembled to form the hull shell, decks, and longitudinal bulkheads as shown in Figure 3. Each strake consists of a plate of uniform thickness with or without uniformly spaced stiffeners. The stiffeners are smeared into the strake cross-section area by MAESTRO to resist in-plane loads. The strakes can not resist loadings that cause bending. The lateral or bending loads and a portion of the in-plane loads were carried by girders located at strake edges. Additional elements, in the form of quadrilateral and triangular membranes and

beams, were used to model bulkheads and vertical structure such as uptakes and the forward portion of the bow. Large transverse bulkheads, as shown in Figure 4, were also modelled by groups of co-planar membrane elements. These groups of elements were considered entities called superelements.

3 Procedure

The assessment was carried out in two steps. Initially the stresses along with the adequacy of the entire structure were determined by a MAESTRO analysis of the two loading cases. Then four regions were chosen for examination of the effects of possible corrosion. Each region was extracted and refined using the modeller MAESTRO/DSA[3] which replaced strake and girder elements with plate elements from the finite element program, VAST. The effects of possible corrosion were simulated by locally reducing the plate thicknesses in the chosen areas of the refined models. A top-down analysis was carried out on each detailed model for each of the two loading cases where displacements from the MAESTRO analysis were applied to the matching nodes at the boundaries of the detail models. Loads, if any, were automatically transferred from the MAESTRO load cases and refined and applied to the refined models.

4 Loading

4.1 Load Case 1

The weight distribution, in MAESTRO load file format, for the deep departure condition is given in Appendix A. It includes all fluids, the structural weight, point loads and buoyancy loads due to submerged components other than the hull. The external pressure loads due to hogging immersion are shown in Figure 5. The internal tank pressure loads from stored fluids for the deep departure hogging case are shown in Figure 6.

4.2 Load Case 2

The weight distribution, in MAESTRO load file format, for the light operational condition is given in Appendix B. The structural weights remain the same with changes in the non-structural loads to reflect the lighter loading condition. The external pressure loads due to sagging immersion are shown in Figure 7. The internal tank pressure loads from stored fluids for the light operational sagging condition are shown in Figure 8.

5 Model Boundary Conditions

The boundary conditions applied to the MAESTRO model were located to obtain a positive definite system with as little reaction force as possible due to the static balance between

buoyancy forces and structural plus non-structural weight. The boundary conditions are shown located on a wire frame drawing of the model in Figure 9.

6 Results of the Initial Assessment for Stress and Structural Adequacy

The initial MAESTRO analysis for the two load cases was carried out as a basis for comparison of the effect of local reduction in the hull plating thickness due to possible corrosion. The as-built plate thicknesses of the main deck are shown in Figure 10 and for the bottom in Figure 11.

6.1 Results of the MAESTRO Analysis of the Hogging Load Case

The longitudinal stress distribution in the deck for the hogging load case is shown in Figure 12. An enlarged view of the region of the highest deck stresses, with a list of the highest stress components and their location, is shown in Figure 13. The acronyms for the stresses are defined in Table 2.

The longitudinal stress distribution in the bottom is shown in Figure 14. Enlarged views of the regions of the highest bottom stresses, with a list of the highest stress components and their location, are shown in Figure 15 and Figure 16.

The minimum adequacy parameters from the hogging load for the deck strength case are shown in Figure 17 and for the bottom in Figure 18. The FORENSIC option in MAESTRO was used which imposed a safety factor of 1. Therefore any adequacy parameters less than zero indicate a possibility of failure for the load case.

6.2 Results of the MAESTRO Analysis of the Sagging Load Case

The longitudinal stress distribution in the deck for the sagging load case is shown in Figure 19. An enlarged view of the region of the highest deck stresses, with a list of the highest stress components and their location, is shown in Figure 20.

The longitudinal stress distribution in the bottom is shown in Figure 21. Enlarged views of the regions of the highest bottom stresses, with a list of the highest stress components and their location, are shown in Figure 22 and Figure 23.

The minimum adequacy parameters from the hogging load for the deck strength are shown in Figure 24 and for the bottom in Figure 25.

7 Regions Selected for Detailed Analysis of Corrosion Effects

From the results of the MAESTRO analysis, four regions in the model were selected for detailed analysis of corrosion effects. Their selection was based on high concentration of stress,

the possibility of buckling, and corrosion identified in hull surveys. Regions 1 and 2 are high stress concentrations located on the bottom as shown in Figure 26. Region 3 bounds a high stress concentration on the main deck as shown in Figure 27. Region 4, shown in Figure 28, includes the gray water tank where corrosion has actually occurred.

8 Refined Region 1 of the Bottom

Region 1 of the bottom was extracted and refined using MG/DSA. The MAESTRO strakes, strake stiffeners, frames and girders were replaced with VAST quadrilateral and triangular elements to more accurately model these components as shown in Figure 29. In addition, an area of the region, shown to have the highest stress by the MAESTRO analysis, was refined further as shown in Figure 30. A top-down analysis was initially performed for the two loading cases without any changes to the plate thickness. The plate thickness was then reduced locally in stages to represent corrosion, and the analyses were repeated.

8.1 Results from the Loadings on the Uncorroded Refined Region 1

The stress results from the top-down analysis of region 1 for the two load cases are shown in Figure 31 and Figure 32. The maximum stress in hogging was compressive at -115 MPa. The maximum stress in sagging was tensile at 111 MPa. The stress concentration shown in the MAESTRO results was not present in the detailed model. The stress concentration was due to an error in the MAESTRO model caused by connecting girder elements to longitudinal strake elements in this region. The moment at the connection could not be carried over between the two MAESTRO element types. The detail model was therefore a much more accurate representation of the structure in the region than the MAESTRO model.

8.2 Results from the Simulated Corrosion in Refined Region 1

Three corrosion examples were modelled in the 12 mm thick plate in the bottom . One was a localized reduction of plating to form a pit, starting at an area 161 mm by 333 mm at 9mm thick down to an area 40 mm by 80 mm at 5 mm thick. The second was localized corrosion of a longitudinal stiffener with the web and flange and part of the bottom reduced in cross-section as shown in Figure 33. The third was severe uniform corrosion of a panel from 12 mm down to 5 mm.

8.2.1 Localized Reduction of Plate Thickness to a Pit

The stress distribution in the 12 mm plate corroded into a pit is shown for the two loading cases in Figure 34 and Figure 35. The maximum stress for the hogging case was -154 MPa at the bottom of the pit. The maximum stress for the sagging case was 120 MPa.

8.2.2 Localized Reduction of the Stiffener Cross-section

The stresses resulting at the reduced cross-section of stiffener for the two load cases are shown in Figure 36 and Figure 37. The maximum stress was compressive at -152 MPa for the hogging case. It occurred in the bottom plating at the junction with the stiffener web. The flange stress was -121 MPa.

The maximum stress for the sagging case was a tensile stress of 142 MPa which occurred in the flange and upper web. In this case, the stresses in the flange due to the bottom pressure were additive while in the hogging case they were subtractive.

8.2.3 Uniform Reduction of the Bottom Panel

The stresses for the panel are shown in Figure 38 and Figure 39. The maximum stress occurred during hogging in the form of a compression stress of -373 MPa. The maximum stress from sagging was a tensile stress of 154 MPa. The large difference was due to the bottom pressure which was much higher in the hogging case.

8.2.4 Comparison of the Results from Region 1

The stresses for all three cases of severe corrosion in Region 1 are compared in Table 3. They reached a maximum compressive stress of -373 MPa. The yield stress for the steel used is 350 MPa.

Buckling of the uniformly corroded panel was checked and found to have a critical buckling stress of 108 MPa for simply supported edges and 189 MPa when fully clamped. If the edge constraint lies halfway between, the stress would be 148 MPa with a possibility of buckling as the maximum compressive stress due to the hogging load was -373 MPa.

9 The Refined Region 2 of the Bottom

Region 2 of the bottom was extracted as shown in Figure 40 and refined using MAESTRO/DSA. The MAESTRO strakes, strake stiffeners, frames and girders were replaced with VAST quadrilateral and triangular elements to more accurately model these components as shown in Figure 41. In addition, an area of the region, shown to have the highest stress by the MAESTRO analysis, was refined further as shown in Figure 42. A top-down analysis was performed for the two loading cases without any changes to the plate thickness.

9.1 Results from Loading on Refined Region 2

The results from the top-down analysis of Region 2 for the hogging and sagging load cases are shown in Figure 43 and Figure 44. The detailed model results show a tranverse redistribution of the the stress concentration found in the MAESTRO model, with the maximum of 261 MPa

occurring in the grid refinement transition elements in the hogging case, and -229 MPa in the sagging case. The stress concentration in the MAESTRO model was, as in Region 1, due to an error in the MAESTRO model where longitudinal strake elements were incorrectly connected to girder elements. This together with the unreasonably high stresses found in the refined model derived from it, indicated that neither the MAESTRO model nor the refined model properly represent the state of stress in this region. For these reasons, an investigation of possible corrosion was not carried out in this region.

10 The Refined Region 3 of the Main Deck

Region 3 of the main deck was extracted as shown in Figure 45. This region was chosen because of the high stress concentration observed in the MAESTRO results. It was refined using MAESTRO/DSA. The MAESTRO strakes and strake stiffeners were replaced with VAST quadrilateral elements and the frames and additional beams were modelled as VAST general beam elements, as shown in Figure 46. Again a top-down analysis was initially performed for the two loading cases without any changes to the plate thickness.

10.1 Results from Loading of Refined Region of the Main Deck

The results from the top-down analysis of Region 3 for the hogging and sagging load cases are shown in Figure 47 and Figure 48. In this case, the stress concentration observed in the MAESTRO analysis was confirmed in the detail model. The stresses were much higher and more concentrated and moved into the superstructure. The maximum stresses for hogging and sagging in the superstructure of the detail model were 215 MPa and -227 MPa compared to 58 MPa and -74 MPa for the MAESTRO results. The maximum stress in the detail model of the deck plating for the two load cases was 202 MPa and -246 MPa compared to 135 MPa and -154 MPa for the MAESTRO results.

10.2 Results from the Simulated Corrosion in Refined Region 3

Three corrosion examples were modelled. One was localized reduction of the plate thickness in the area of the stress concentration. The second was localized corrosion of a longitudinal stiffener and the third was a localized pit.

10.2.1 Localized Reduction of Plate Thickness

The localized reduction in plate thickness under a hogging load was done in three steps. The first step was to reduce the thickness in the deck by 2 mm to 7 mm as shown in Figure 49. The stresses resulting from this reduction are shown in Figure 50 and were slightly greater rising from 215 MPa to 219 MPa in the superstructure.

The local plating on the superstructure was then reduced from 4 mm to 3 mm as shown in Figure 51. The stresses increased slightly to 233 MPa as shown in Figure 52.

The grid was then further refined locally, as shown in Figure 53, and the superstructure plate was locally reduced to 2 mm and the edge at the superstructure to deck juncture was reduced to 6 mm The resulting stresses due to the hogging load as shown in Figure 54 reached a maximum of 378 MPa in the superstructure and 241 MPa in the deck.

The effect of the sagging load on the most severally reduced model is shown in Figure 55, where the stress reached a maximum element compression stress of -427 MPa in the superstructure, and -272 MPa in the deck. Because this region of the superstructure was more complex than represented by the MAESTRO model, it could not be easily converted into an accurate detail model. The results are therefore, more an indication of the high sensitivity to loss of strength due to corrosion than an accurate prediction of the actual stress occurring.

10.2.2 Localized Reduction of a Deck Stiffener Cross-section

A deck stiffener and a portion of the deck were reduced in cross-section to model corrosion, as shown in Figure 56. The uncorroded flange and the web were 8.4 mm and 6.1 mm thick. The stresses from the hogging load are shown in Figure 57 with maximum stress of 243 MPa compared to the uncorroded stiffener stress of 110 MPa. The stresses due to sagging are shown in Figure 58 with a maximum element stress of -266 MPa compared to the uncorroded stiffener stress of 99 MPa. A fringe plot of the stiffener stresses for hogging is shown in Figure 59 indicating a maximum stress of 235 MPa. The fringe stresses are somewhat lower than the element stress results which are considered to be more accurate.

10.2.3 Localized Reduction of Plate Thickness to a Pit

A local area of plating 333 mm by 370 mm was reduced in thickness in three steps from 9 mm to 3 mm to form a corrosion pit. The area of the 3 mm thickness was 92 mm by 83 mm. The stresses resulting from the hogging and sagging loads are shown in Figure 60 and Figure 61 as 185 MPa and -207 MPa compared to the uncorroded plate stresses of 85 MPa and -108 MPa.

10.2.4 Comparison of the Results from Region 3

The stresses for the three cases of corrosion in Region 3 are compared in Table 4. The highest stress moved from the deck into the superstructure reaching a maximum compressive stress of -427 MPa compared to a stress of -227 MPa in the uncorroded plate. This result is not accurate because the area of the superstructure in which it occurred was not modelled by MAESTRO to account for a hatch present in the area. The refinement was therefore much simpler than would be required. It did however indicate an area to be checked for corrosion.

The fore and aft deck plate at the junction with the superstructure reached a stress of -247 MPa in a material with a yield strength of 350 MPa. The tranverse plate at the junction

with the superstructure reached a stress of -271 MPa in a material with a yield strength of 700 MPa.

The stress in the locally corroded deck plate, in an area away from the superstructure, was less affected by corrosion, rising in the hogging load case, from a stress of 112 MPa in the uncorroded condition to 185 MPa when reduced to a thickness of 2 mm in the corroded condition. In the sagging case the stessses rose from -126 MPa when uncorroded to -207 MPa when corroded.

The stress under hogging in the uncorroded stiffener was 99 MPa in the flange and the web. Under sagging it was -110 MPa in the flange and the web. The stress under hogging in the corroded stiffener flange was 243 MPa. Under sagging the stress was -266 MPa in the flange.

11 The Refined Region 4 the Gray Water Tank

The gray water tank and surrounding structure were extracted from the bottom of the MAESTRO model as shown in Figure 62. It was refined and converted to a VAST model using quadrilateral, triangular and general beam elements as shown in Figure 63. The refinement of the gray water tank itself is shown in Figure 64. Because the MAESTRO model did not load the gray water tank, the DSA load file was modified to more truly represent the hydrostatic pressure from the stored fluid as shown in Figure 65. Thus the tank sides were loaded with the pressure applied to the refined elements. A top-down analysis was then performed on the uncorroded refined model for the two load cases to establish the initial stress condition.

11.1 Results from the Hogging and Sagging Loads on Refined Region 4

A top down analysis of Region 4 showed that stresses in the gray water tank from the hull bending for an empty tank were as high as -67 MPa for hogging, as shown in Figure 66, and 61 MPa for sagging as shown in Figure 67. The maximum stresses in the full gray water tank, for the hogging case, are shown to be -72 MPa for the port side in Figure 68 and -66 MPa for the starboard side in Figure 69. The maximum stresses in the bottom are shown to be -72 MPa in Figure 70.

The stresses in the full gray water tank for the sagging case are shown to be 69 MPa for the port side in Figure 71 and 69 MPa for the starboard side in Figure 72. The maximum stresses in the bottom are 75 MPa as shown in Figure 73. The results show that the hull bending stresses contributed a much larger portion of the combined stress in the tank than did the stresses due to the fluid in the tank.

11.2 Results of Simulated Corrosion in the Gray Water Tank

The port and starboard walls and the bottom of the gray water tank were modelled for pitting corrosion in high stress areas. Starboard side and bottom pits were created by graduated

mesh refinement using elements to effect the transition from coarse to fine grid as shown in Figure 74. The transition between coarse and fine grid was accomplished on the port side with the use of multipoint constraints, as shown in Figure 75. To form the pits in the port and starboard sides, the plate thickness was reduced in steps from the original 8 mm to 3 mm The 3 mm thickness had an area of 6 mm by 5 mm on the port side and 10 mm by 10 mm on the starboard side. The corrosion in the bottom of the tank was simulated in a high stress area by gradually reducing the plate thickness from 7 mm to 3 mm to an area 10 mm by 10 mm. A typical element grid showing the variation in the plate thickness in the corrosion pit in the bottom is shown in Figure 76.

The maximum stresses in the full gray water tank resulting from the corrosion in the hogging case are shown to be -102 MPa for the port side in Figure 77 and -101 MPa for the starboard side in Figure 78. The stresses in the bottom are -91 MPa as shown in Figure 79.

The maximum stresses in the full gray water tank for the sagging case are shown to be 109 MPa for the port side in Figure 80 and 108 MPa for the starboard side in Figure 81. The stresses in the bottom are 89.2 MPa as shown in Figure 82.

11.3 Comparison of the Results from Region 4

The stresses in the corroded areas of the full gray water tank are compared with the stresses in the full uncorroded gray water tank in Table 5. The stresses in the pits, considering the considerable loss of plate thickness due to the simulated corrosion, did not increase to serious levels.

12 Conclusions

The MAESTRO model was found to have modelling errors in the bottom structure where strake elements were connected to girder elements. In Region 3 the MAESTRO model of the superstructure was not detailed enough to allow a simple conversion to a refined detailed model of the superstructure where the structure appeared to be very sensitive to loss of strength due to corrosion. The quadrilateral and triangular elements used in the transition between coarse and refined grids (used to model corrosion) were sensitive to corner angles. It was seldom possible to meet the criteria for these elements when used for this purpose. This often resulted in the transition elements having stresses greater than the ambient stress for the areas in which they were used. This problem was particularly noticable in the grids used to model corrosion pits in the gray water tank. The use of multipoint constraints in the modeling of the pit in the port side of the gray water tank appears to produce a better result in determining the stresses as all the elements are in good proportions.

The results from the static analysis show that, except in the superstructure and the junction of the deck and superstructure in Region 3, the structure can withstand severe localized corrosion without serious effect as the stress increased more or less in proportion to the loss

Table 1: Limit State Checks and Definitions

Limit State Acronyms	Definition	Comments
PCSF	Panel Collapse - Stiffener Flexure	
PCCB	Panel Collapse - Combined Buckling	
PCMY	Panel Collapse - Membrane Yield	
PCSB	Panel Collapse - Stiffener Buckling	
PYTF	Panel Yield - Tension, Flange	
PYTP	Panel Yield - Tension, Plate	
PYCF	Panel Yield - Compression, Flange	
PYCP	Panel Yield - Compression, Plate	
PSPBT	Panel Serviceability - Plate Bending	Tranverse
PSPBL	Panel Serviceability - Plate Bending	Longitudinal
PFLB	Panel Failure - Local Buckling	
GCT	Girder Collapse - Tripping	
GCCF	Girder Collapse - Compression,Flange	
GCCP	Girder Collapse - Compression, Plate	
GYBF	Girder Yield - Bending, Flange	
GYBP	Girder Yield - Bending, Plate	
GYTF	Girder Yield - Tension, Flange	
GYTP	Girder Yield-Tension, Plate	
FCPH1,2,3	Frame Collapse-Plastic Hinge	1 = Strake Edge 1
FYCF1,2,3	Frame Yield-Compression, Flange	2 = Strake Edge 2
FYTF1,2,3	Frame Yield-Tension, Flange	and
FYCP1,2,3	Frame Yield-Compression Plate	3 = midlength of
FYTP1,2,3	Frame Yield-Tension, PLate	frame section

of material without appreciable stress concentration. Failure from fatigue, however, may occur under cyclic loads due to the loss of material, and due to imperfections such as plate roughness, caused by corrosion.

Acknowlegement

I wish to acknowledge the assistance given me by Terry MacFarlane and Alex Ritchie of the DREA SAS Group, in the generation of the corrosion models.

Table 2: Stress Acronyms Definitions

Stress Acronyms	Definition
SIGX	element local X stress
SIGY	element local Y stress
TAU	element local shear stress
SIGVM	element Von Mises stress
AVSIGX	bay average local X stress
AVSIGY	bay average local Y stress
AVTAU	bay average shear stress
AVSIGVM	bay average Von Mises stress
PRES	bay average pressure stress

Table 3: Region 1 Stress Results in Bottom

Location	Plate Thickness Reduction	Stresses MPa		Comments
		Hog	Sag	
Uncorroded Plate	0 mm	-115	111	12 mm thick plate at keel
Corrosion Pit	7 mm	-154	121	in 12 mm plate in keel
Uncorroded Stiffener	0 mm	-76	88	in flange and web
Corroded Stiffener	4 mm	-152	142	in plate, flange and web
Uncorroded Panel	0 mm	-105	87	1274 mm by 1602 mm bottom panel
Corroded Panel	8 mm	-373	154	1274 mm by 1602 mm bottom panel

Table 4: Region 3 Stress Results in Deck

Location	Plate Thickness Reduction	Stresses MPa Hog	Sag	Comments
Uncorroded Deck Plate	0 mm	202	-246	9 mm plate at superstructure
Corroded Deck Plate	3 mm	219	-247	350 yield, at superstructure
Corroded Deck Plate	3 mm	241	-271	700 yield, at superstructure
Uncorroded Superstructure	0 mm	215	-227	5 mm plate
Corroded Superstructure	2 mm	378	-427	at junction with deck
Uncorroded Deck Plate	0 mm	112	-126	9 mm plate
Corrosion Pit in Deck Plate	6 mm	185	-207	in 9 mm plate in deck
Uncorroded Stiffener	0 mm	99	-110	in flange and web
Corroded Stiffener	4 mm	243	-266	in flange and web

Table 5: Region 4 Stress Results in the Full Gray Water Tank

Location	Plate Thickness Reduction	Stresses MPa Hog	Sag	Comments
Uncorroded Port Side Plate	0 mm	-72	69	8 mm thick plate
Corrosion Pit Port Side Plate	5 mm	-102	109	pit 6 mm by 5mm
Uncorroded Star'b Side Plate	0 mm	-66	69	8 mm thick plate
Corrosion Pit Star'b Side Plate	5 mm	-101	108	pit 10 mm by 10 mm
Uncorroded Bottom Plate	0 mm	-72	75	7 mm thick plate
Corrosion Pit Bottom Plate	4 mm	-91	89	pit 10 mm by 10 mm

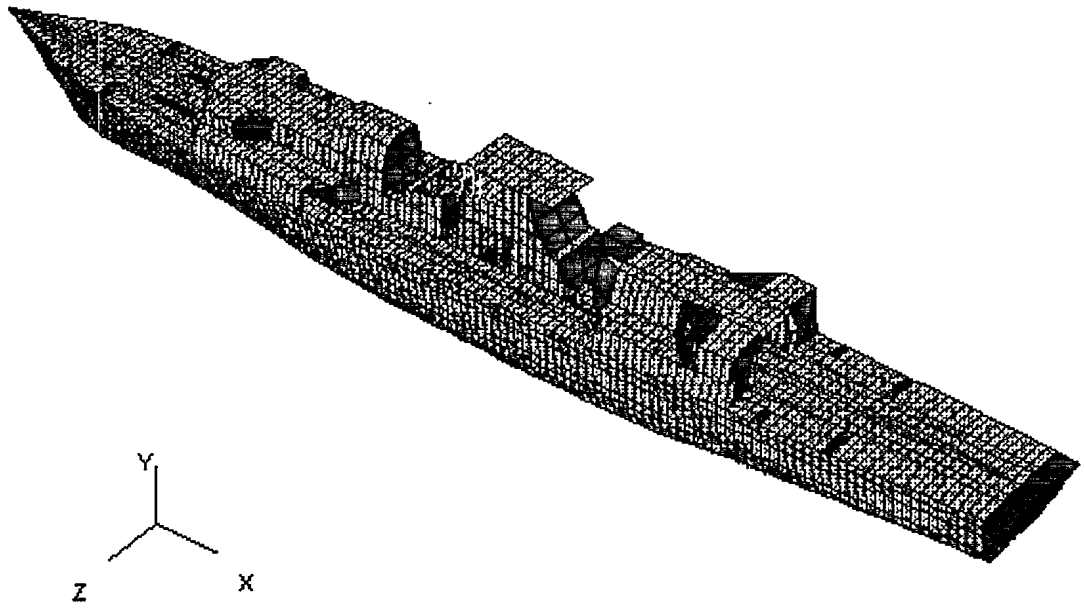

Figure 1: The MAESTRO Model of the CPF

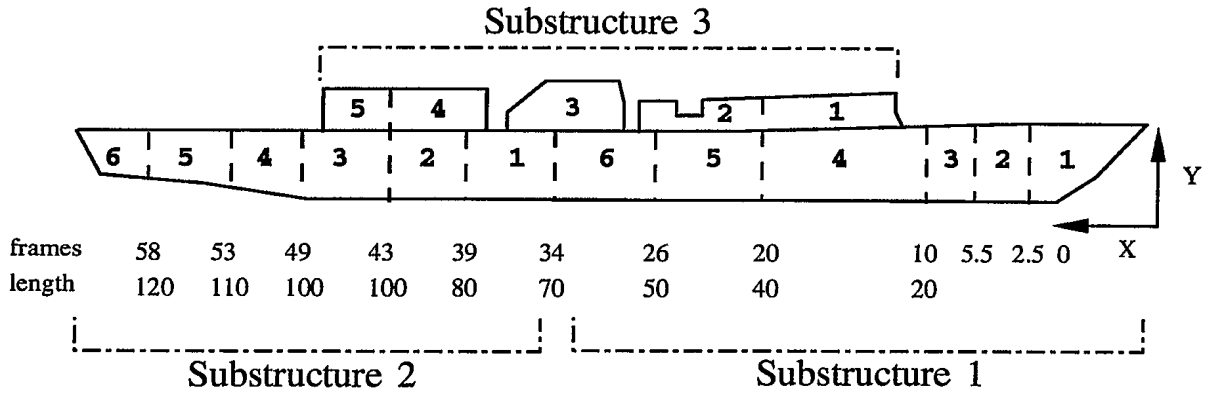

Figure 2: The Substructures and Modules of the MAESTRO Model

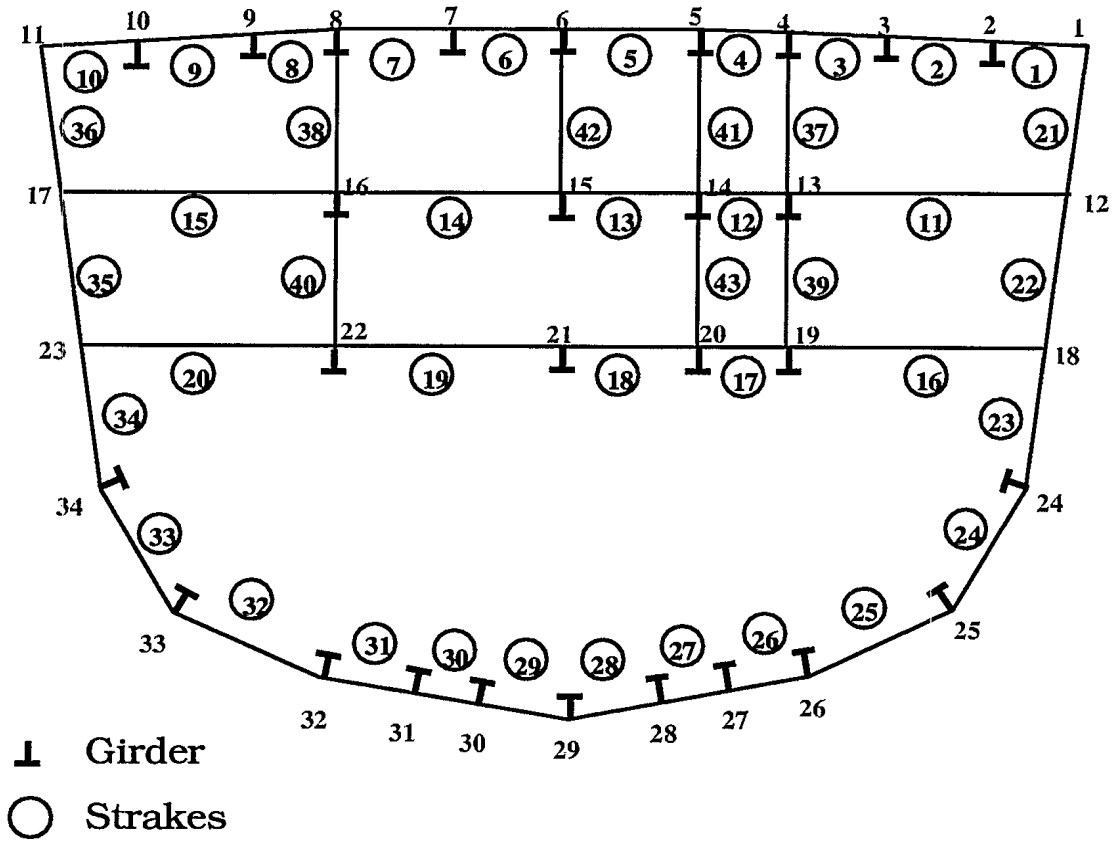

Figure 3: A Typical Model Crossection Showing Strakes, Girders and Endpoints

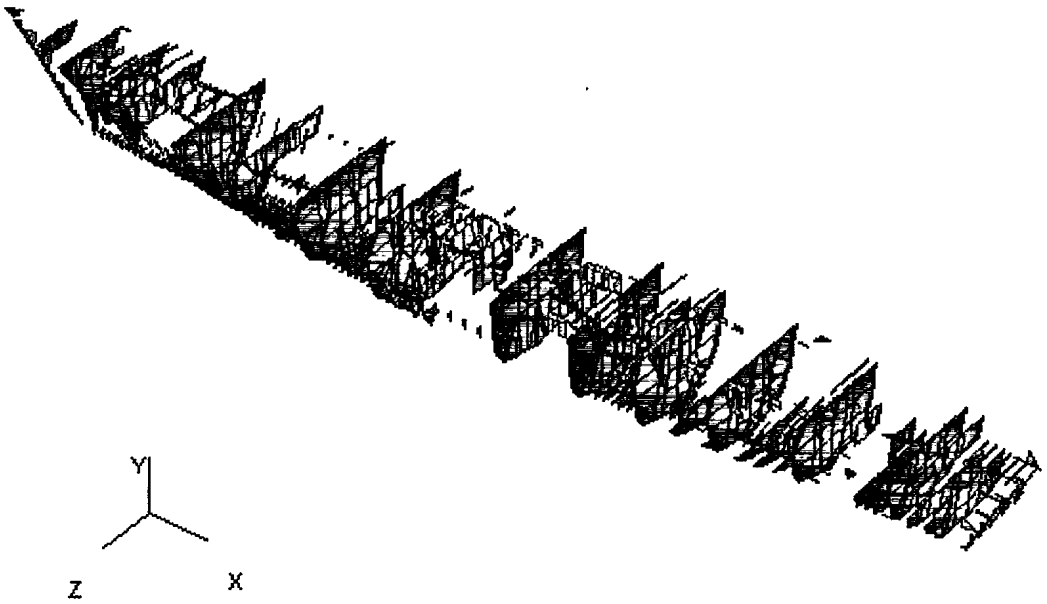

Figure 4: The Tranverse Bulkheads in the MAESTRO Model

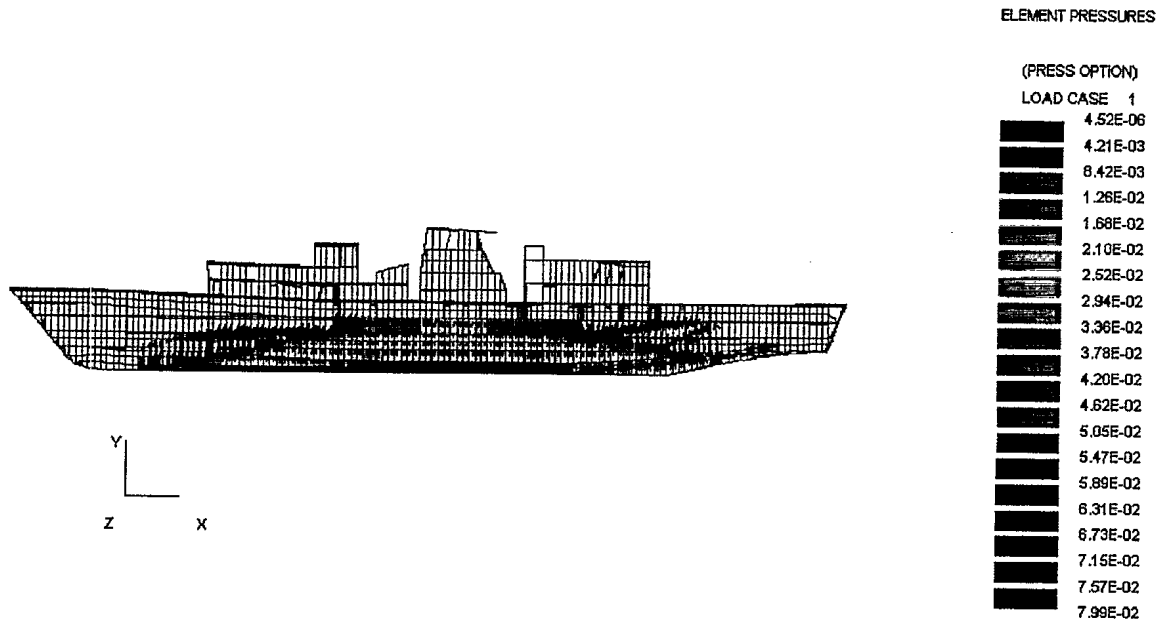

Figure 5: The Immersion Pressures (MPa) for Deep Departure Hogging

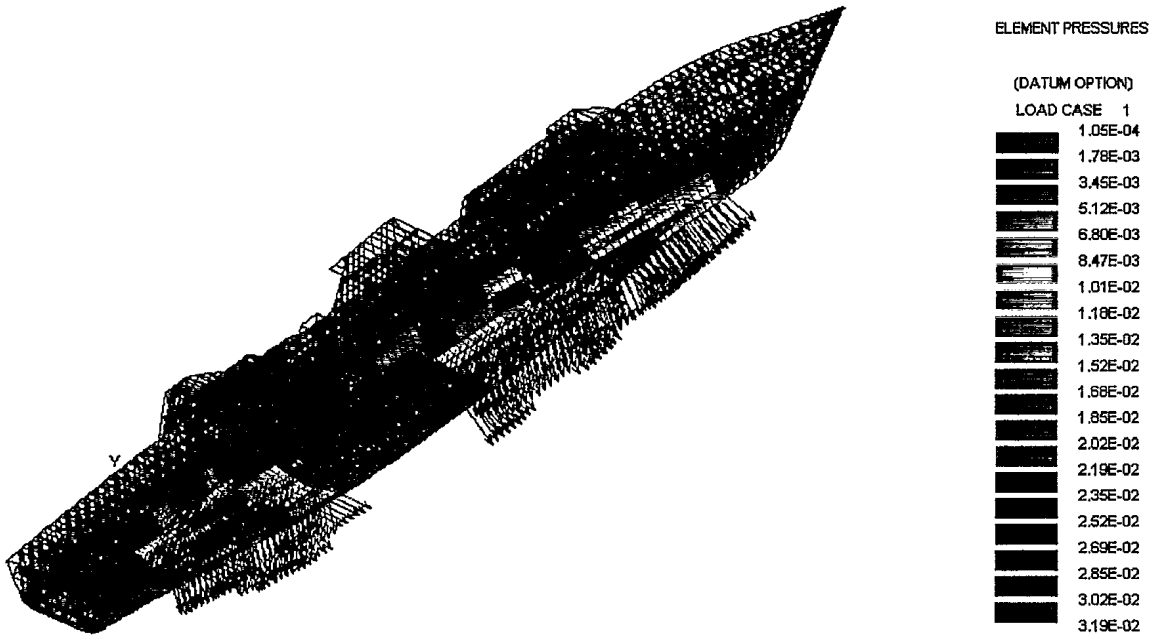

Figure 6: Internal Tank Pressures (MPa) for Deep Departure Hogging

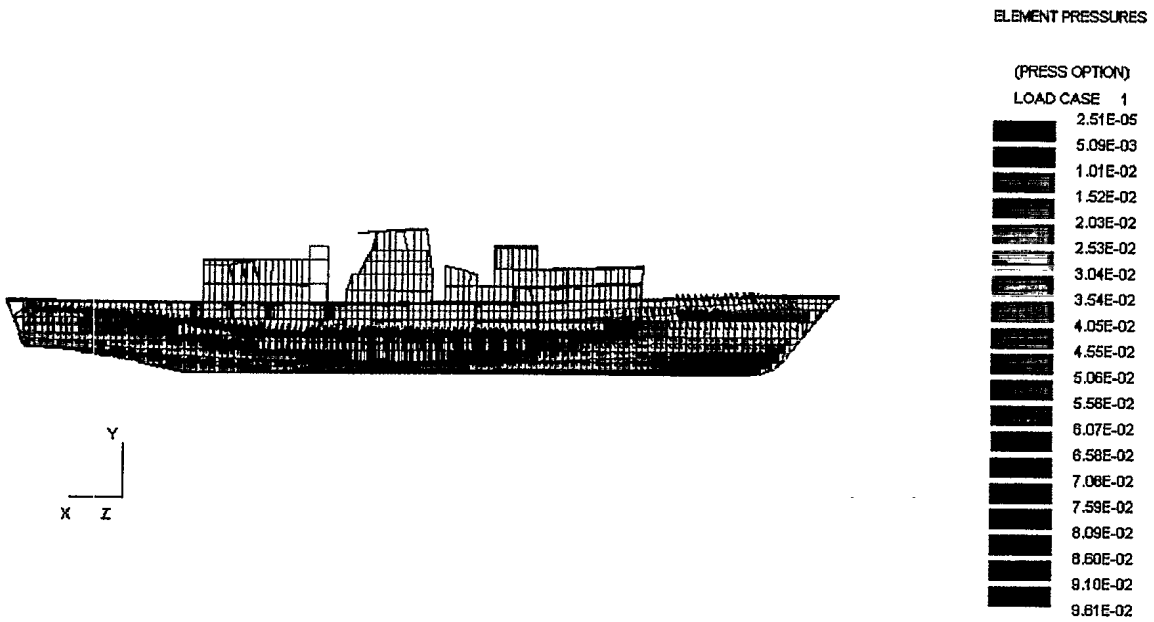

Figure 7: The Immersion Pressures (MPa) for Light Operational Sagging

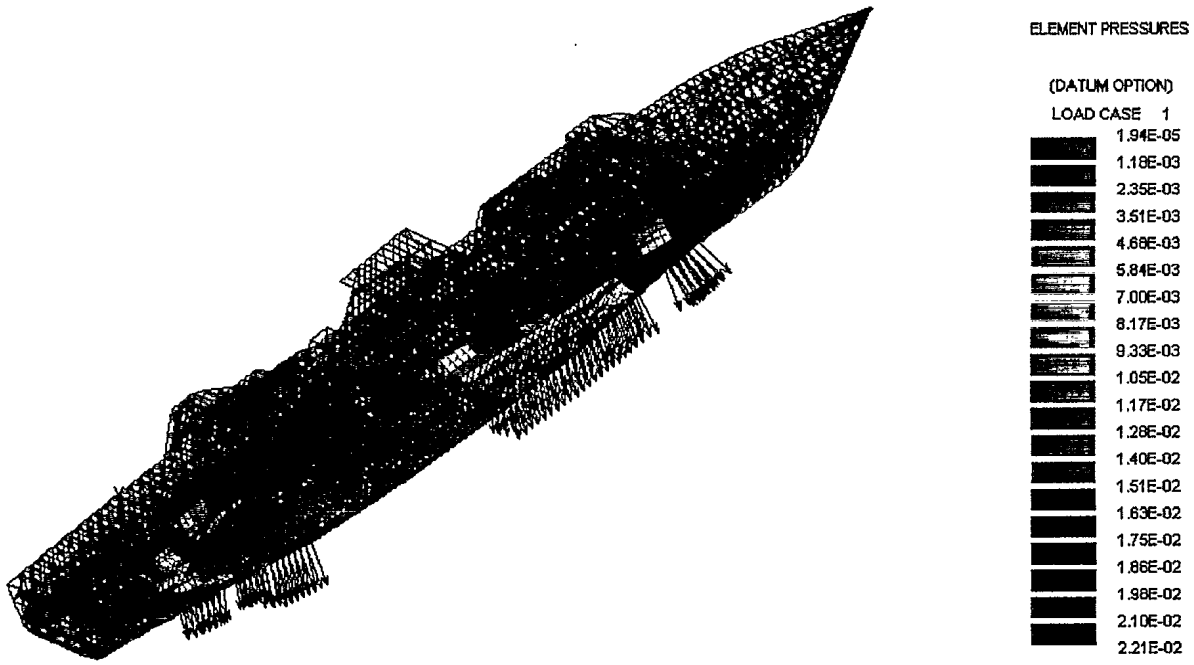

Figure 8: Internal Tank Pressures (MPa) for Light Operational Sagging

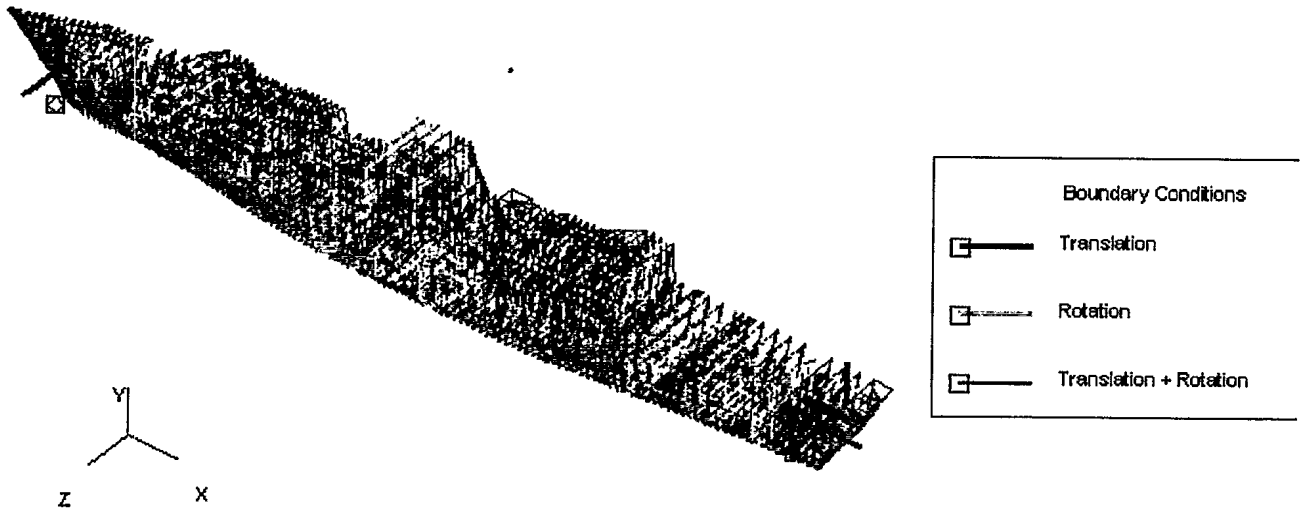

Figure 9: A Wire Frame Drawing of the Model Showing the Boundary Conditions

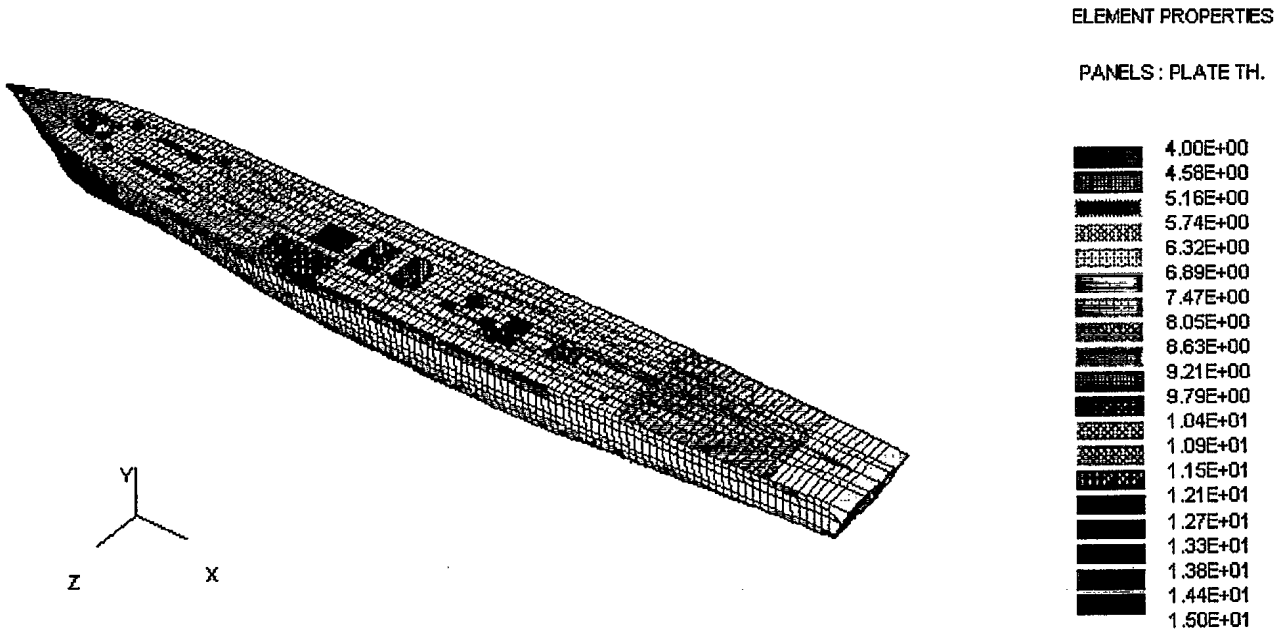

Figure 10: The As-Built Initial Plate Thickness of the Deck

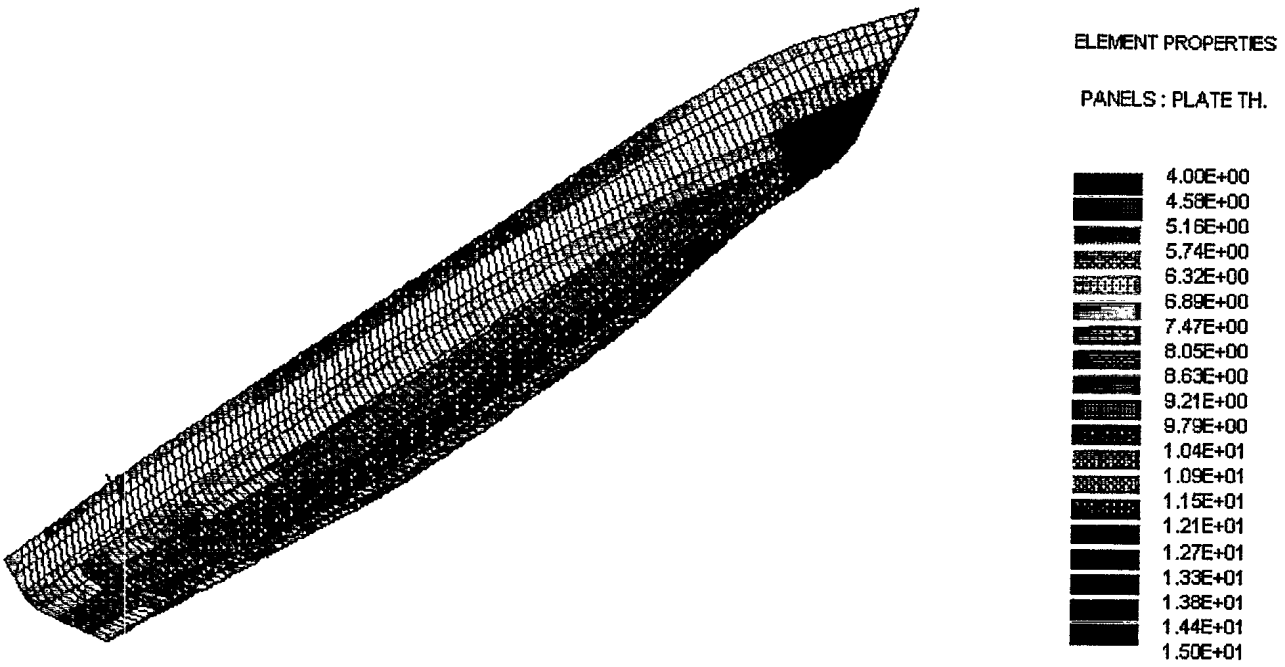

Figure 11: The As-Built Initial Plate Thickness of the Bottom

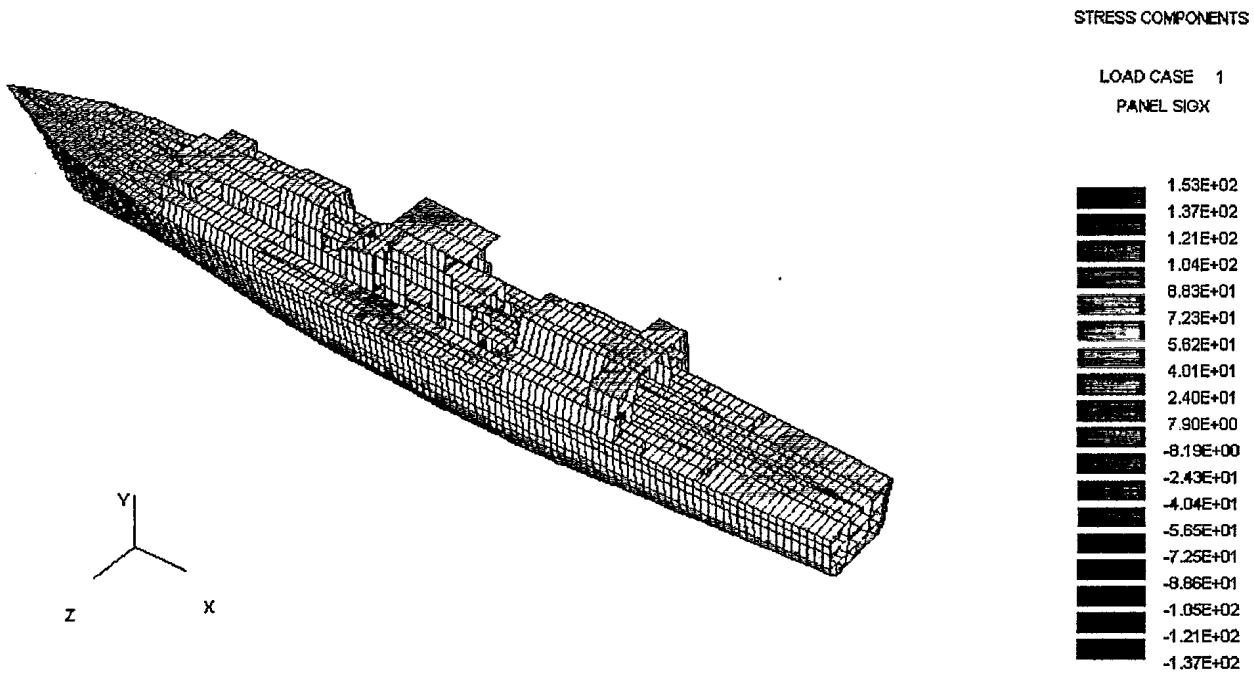

Figure 12: The Longitudinal Stress (MPa) Distribution in the Deck for the Hogging Case

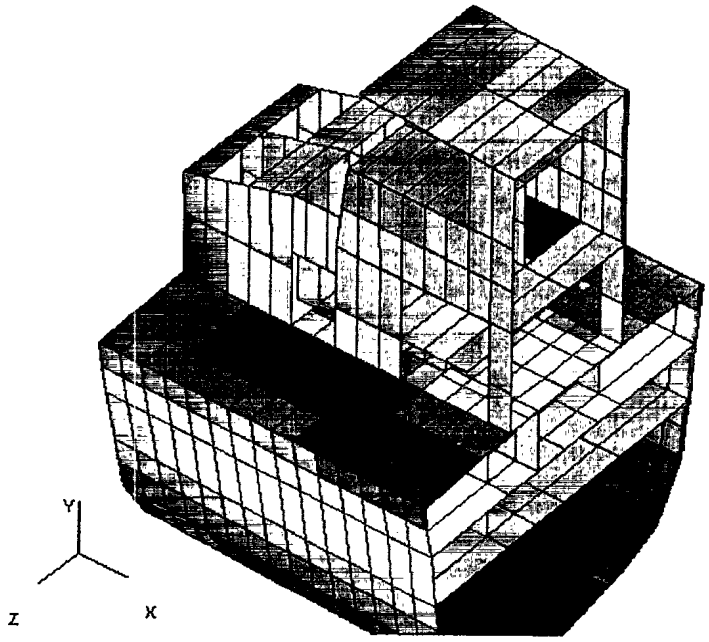

STRESS INQUIRY

STRAKE PANEL
Substructure : 1
Module : 6
Strake : 3
Section : 7
Load Case : 1

SIGX	1.350E+02
SIGY	-3.446E+00
TAU	1.282E+01
SIGVM	1.385E+02
AVSIGX	1.350E+02
AVSIGY	-3.446E+00
AVTAU	1.282E+01
AVSIGVM	1.385E+02
PRES	0.000E+00

Figure 13: An Enlarged View of the Highest Stresses (MPa) in the Main Deck for the Hogging Case

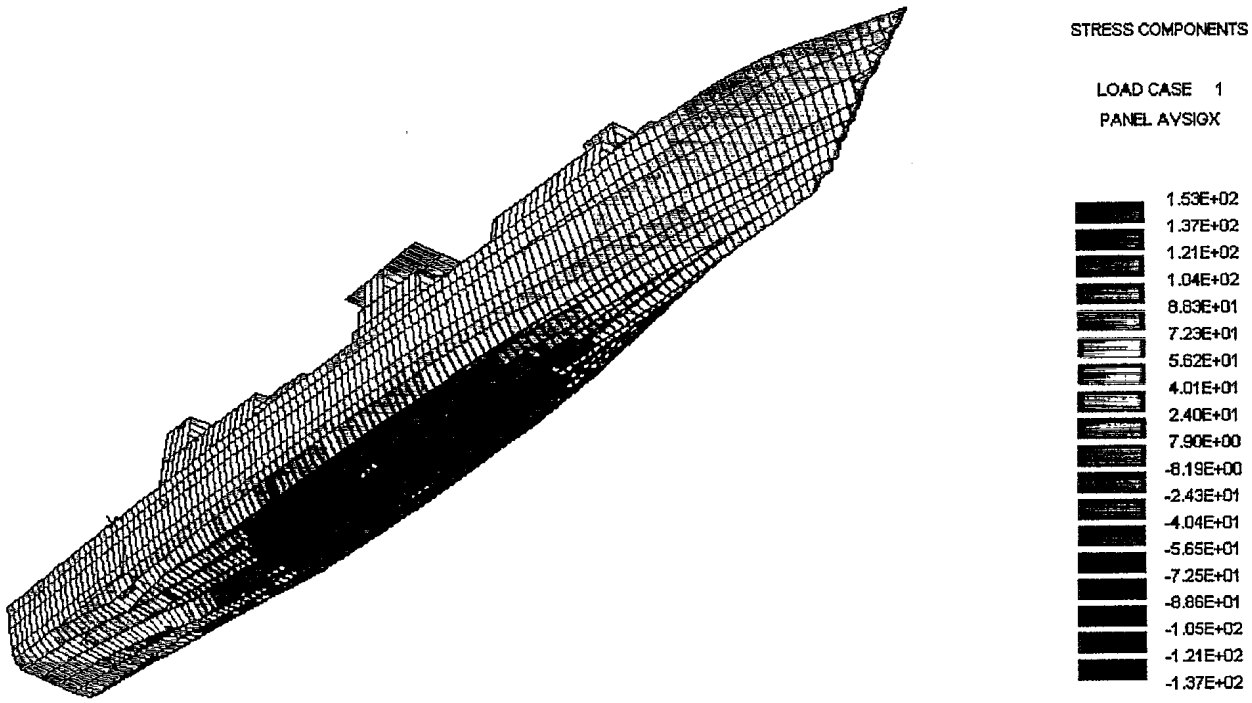

Figure 14: The Longitudinal Stress (MPa) Distribution in the Bottom for the Hogging Case

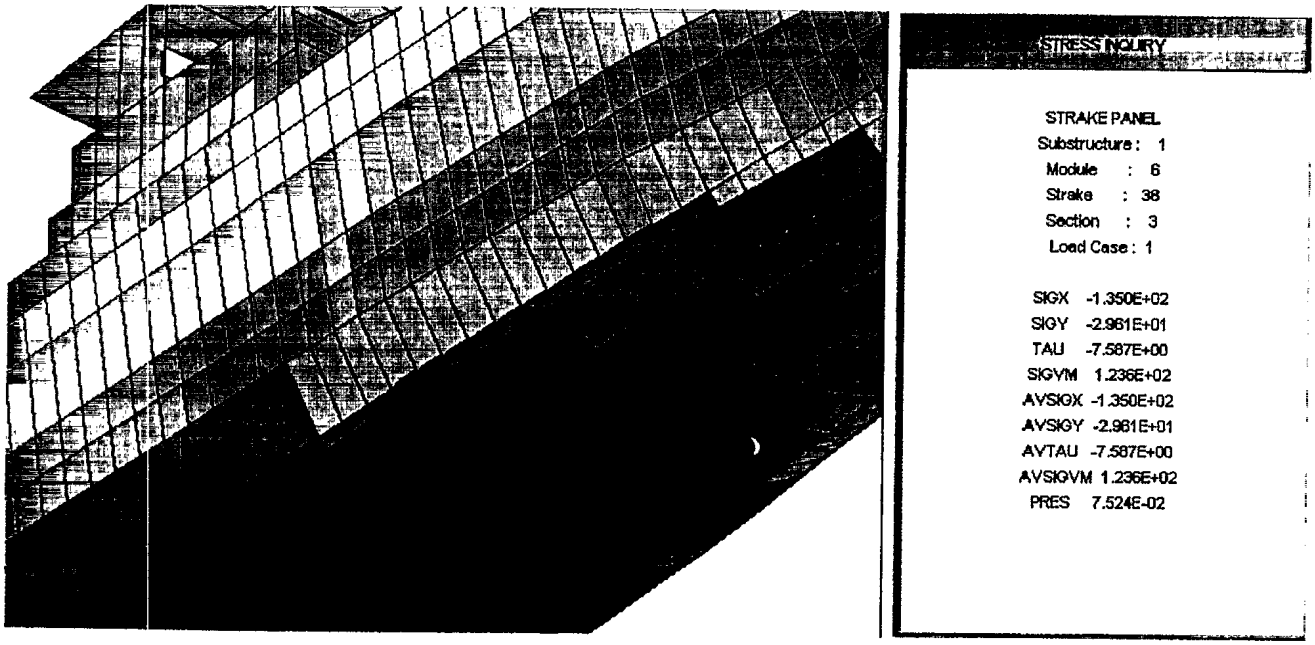

Figure 15: An Enlarged View of the Forward Location of the Highest Stresses (MPa) in the Bottom for the Hogging Case

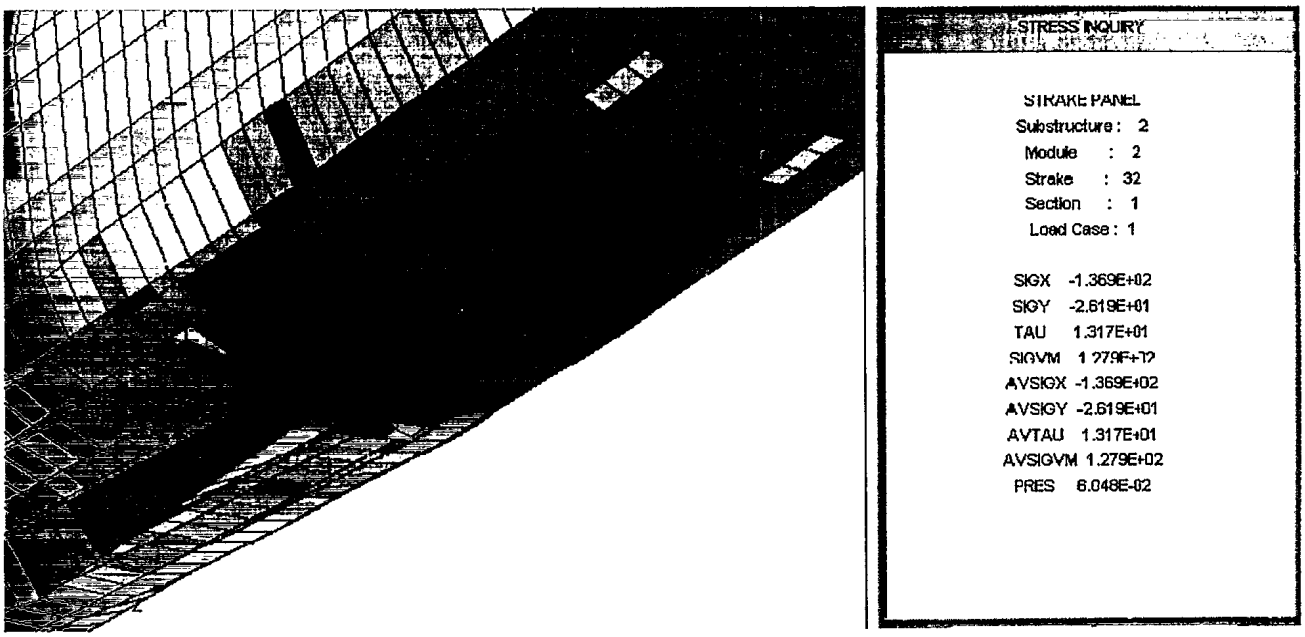

Figure 16: An Enlarged View of the Aft Location of the Highest Stresses (MPa) in the Bottom for the Hogging Case

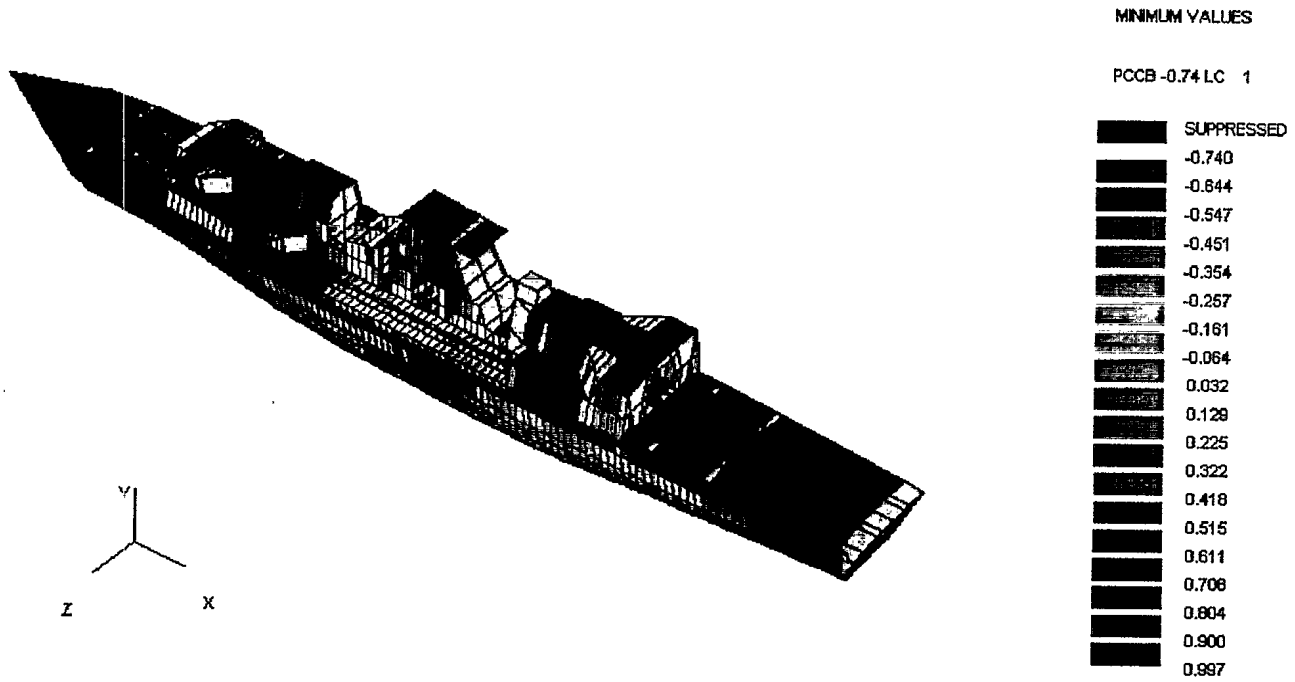

Figure 17: The Minimum Adequacy Parameters for the Deck for the Hogging Case

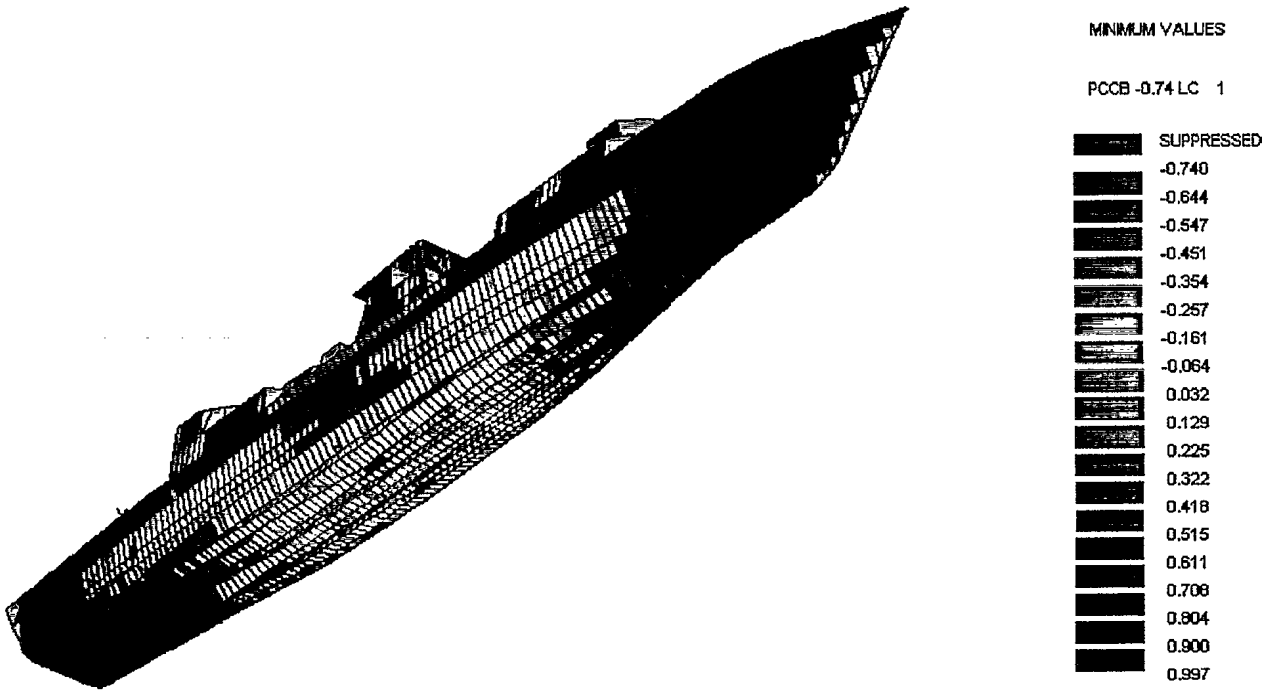

Figure 18: The Minimum Adequacy Parameters for the Bottom for the Hogging Case

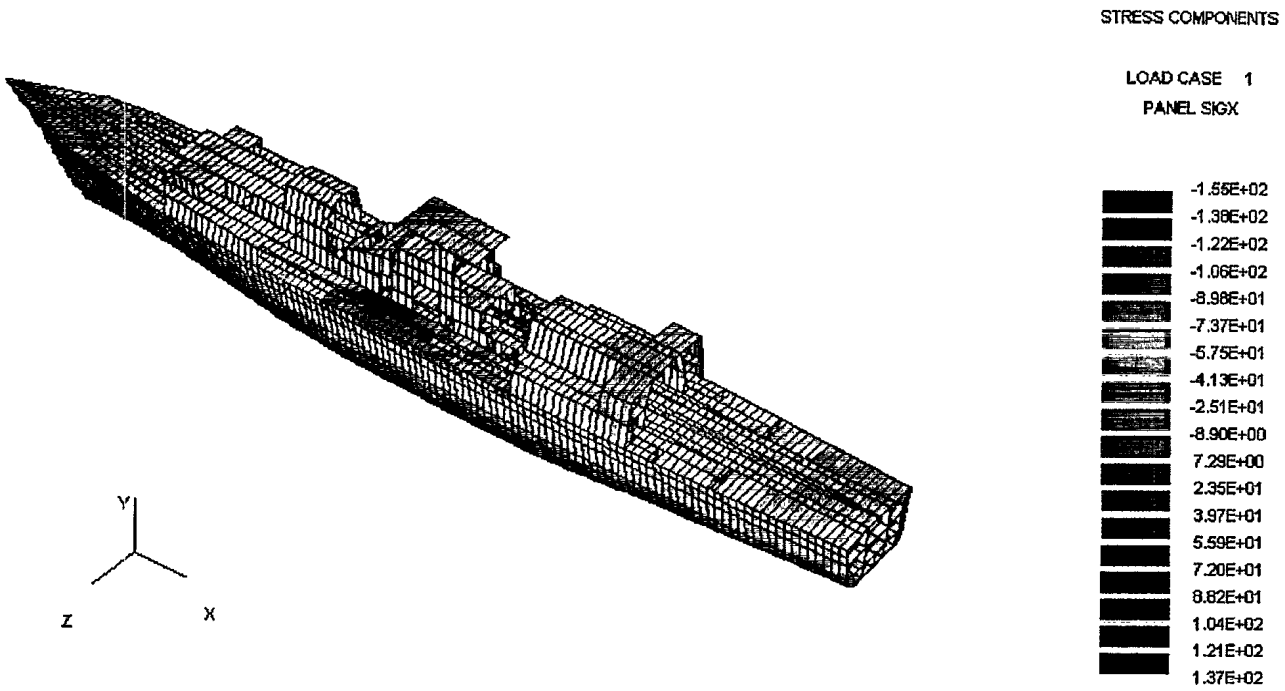

Figure 19: The Longitudinal Stress (MPa) Distribution in the Deck for the Sagging Case

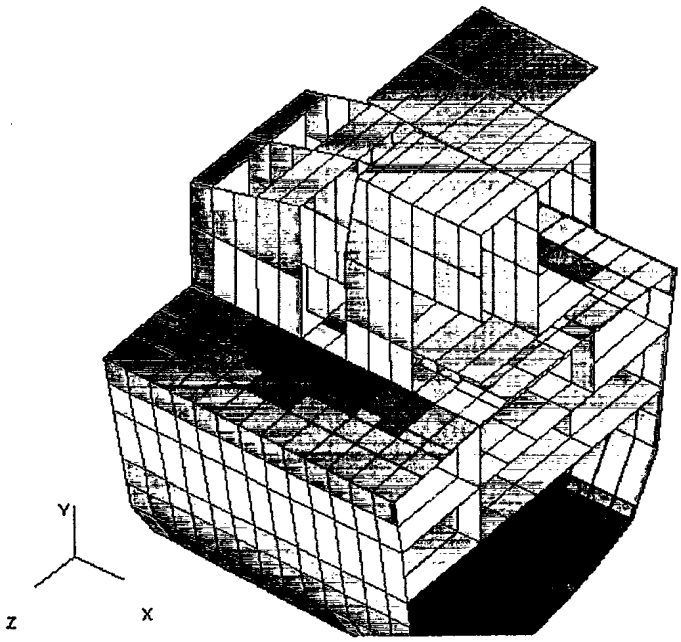

STRESS INQUIRY

STRAKE PANEL
Substructure : 1
Module : 6
Strake : 3
Section : 7
Load Case : 1

SIGX	-1.546E+02
SIGY	2.936E+00
TAU	-1.245E+01
SIGVM	1.576E+02
AVSIGX	-1.546E+02
AVSIGY	2.936E+00
AVTAU	-1.245E+01
AVSIGVM	1.576E+02
PRES	0.000E+00

Figure 20: An Enlarged View of the Highest Stresses (MPa) in the Main Deck for the Sagging Case

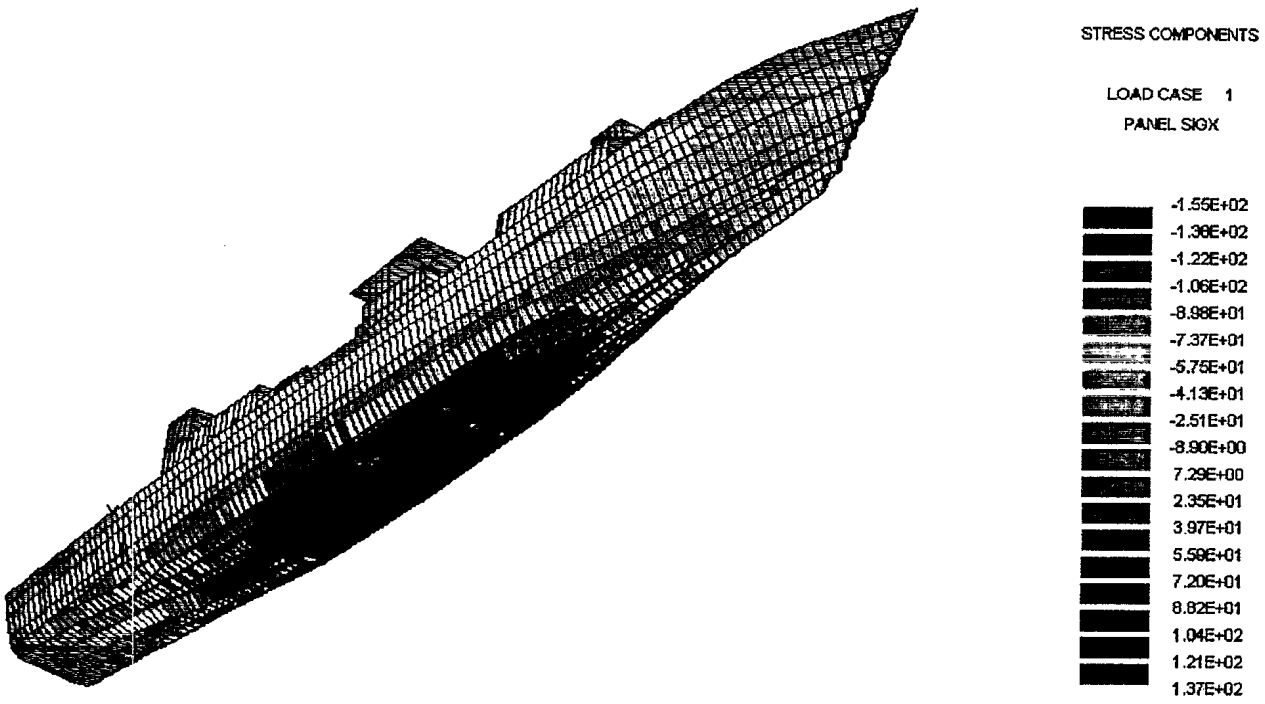

Figure 21: The Longitudinal Stress (MPa) Distribution in the Bottom for the Sagging Case

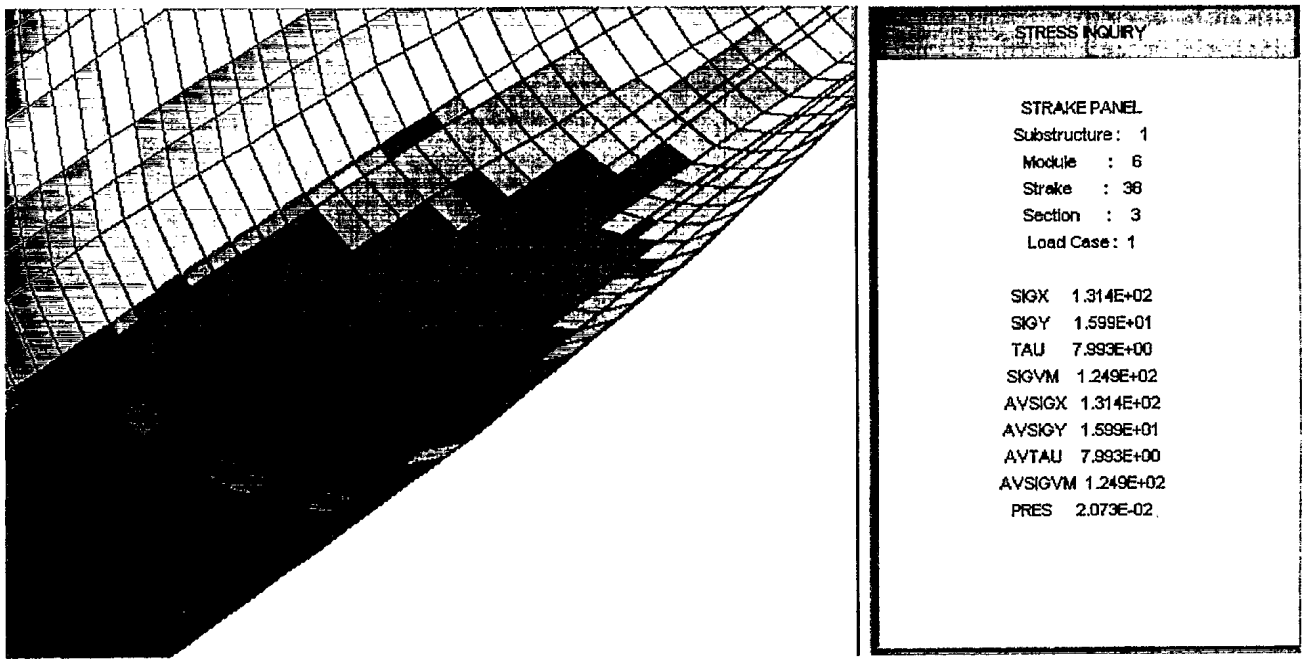

Figure 22: An Enlarged View of the Forward Location of the Highest Stresses (MPa) in the Bottom for the Sagging Case

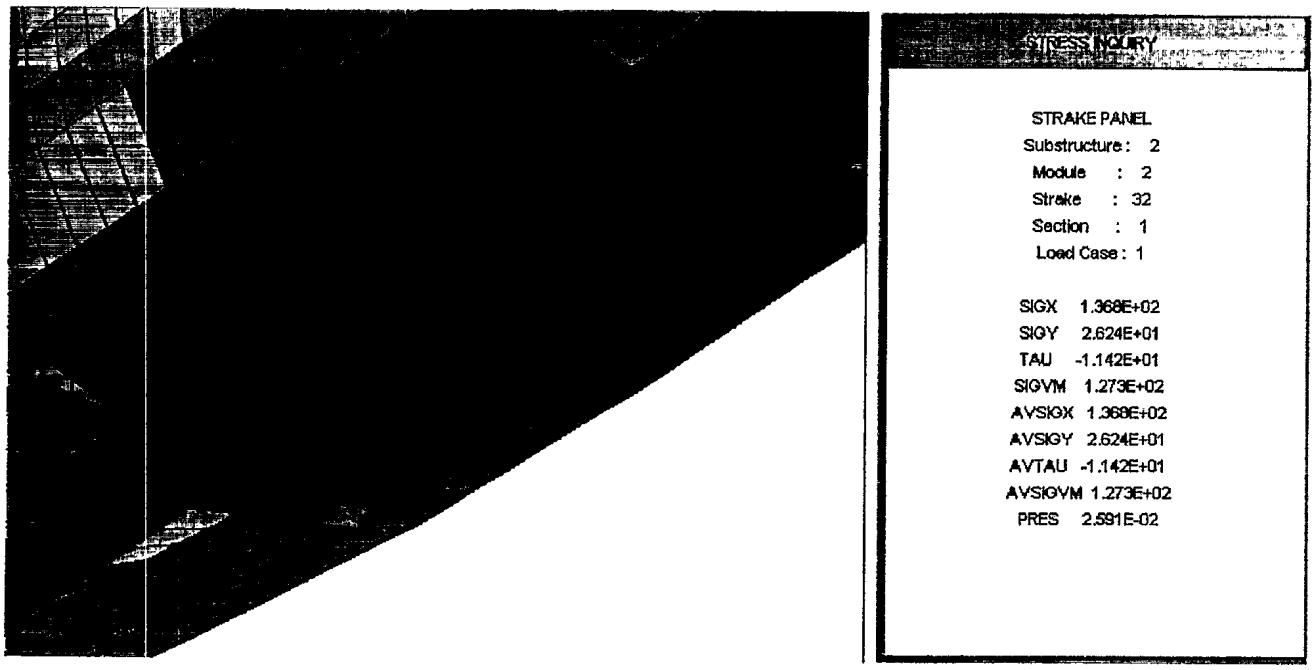

Figure 23: An Enlarged View of the Aft Location of the Highest Stresses (MPa) in the Bottom for the Sagging Case

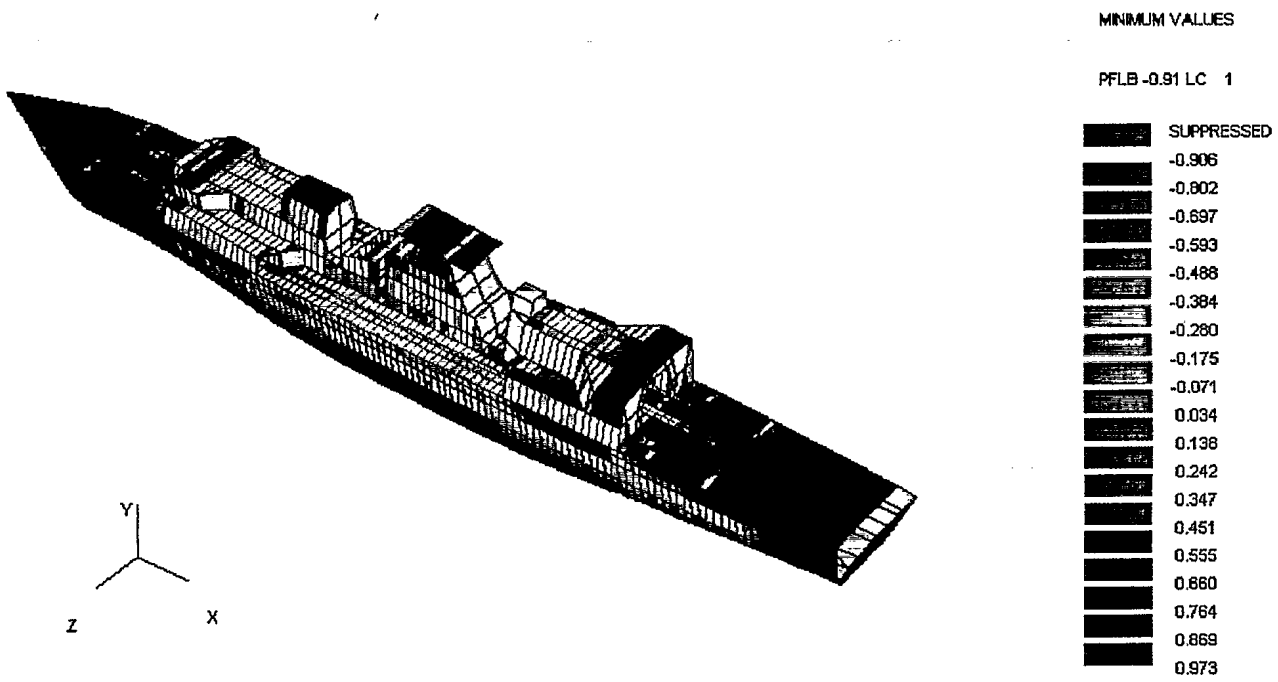

Figure 24: The Minimum Adequacy Parameters for the Deck for the Sagging Case

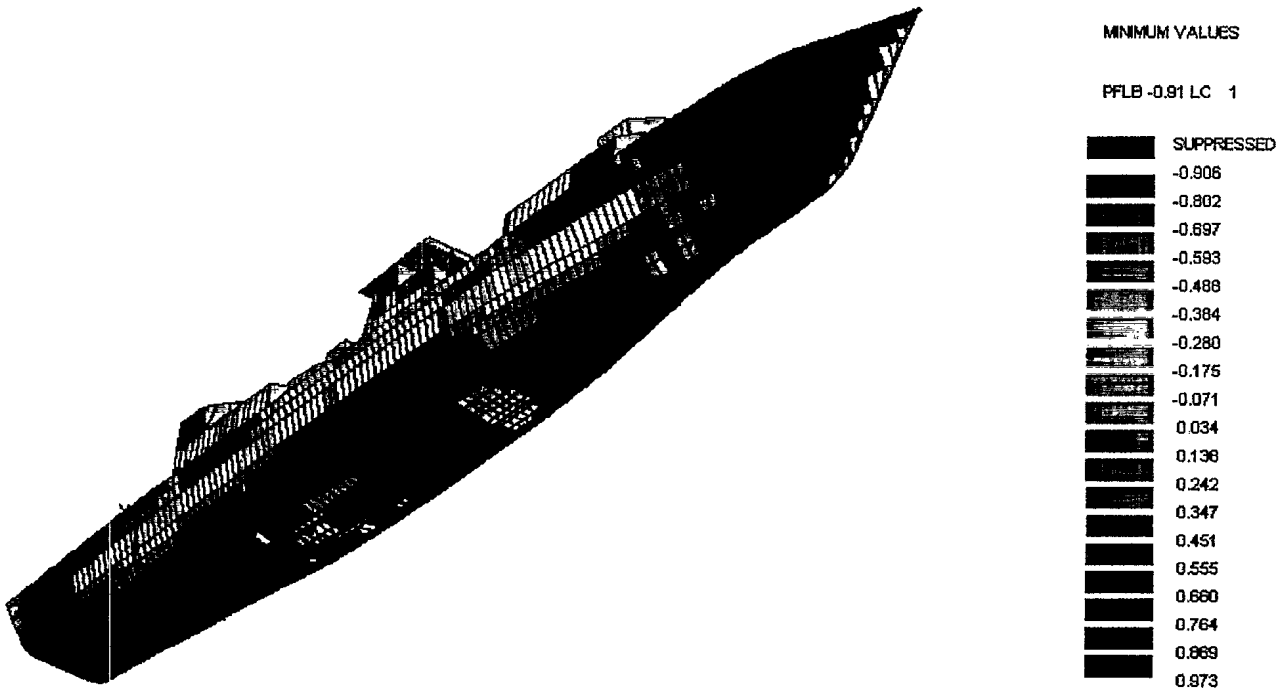

Figure 25: The Minimum Adequacy Parameters for the Bottom for the Sagging Case

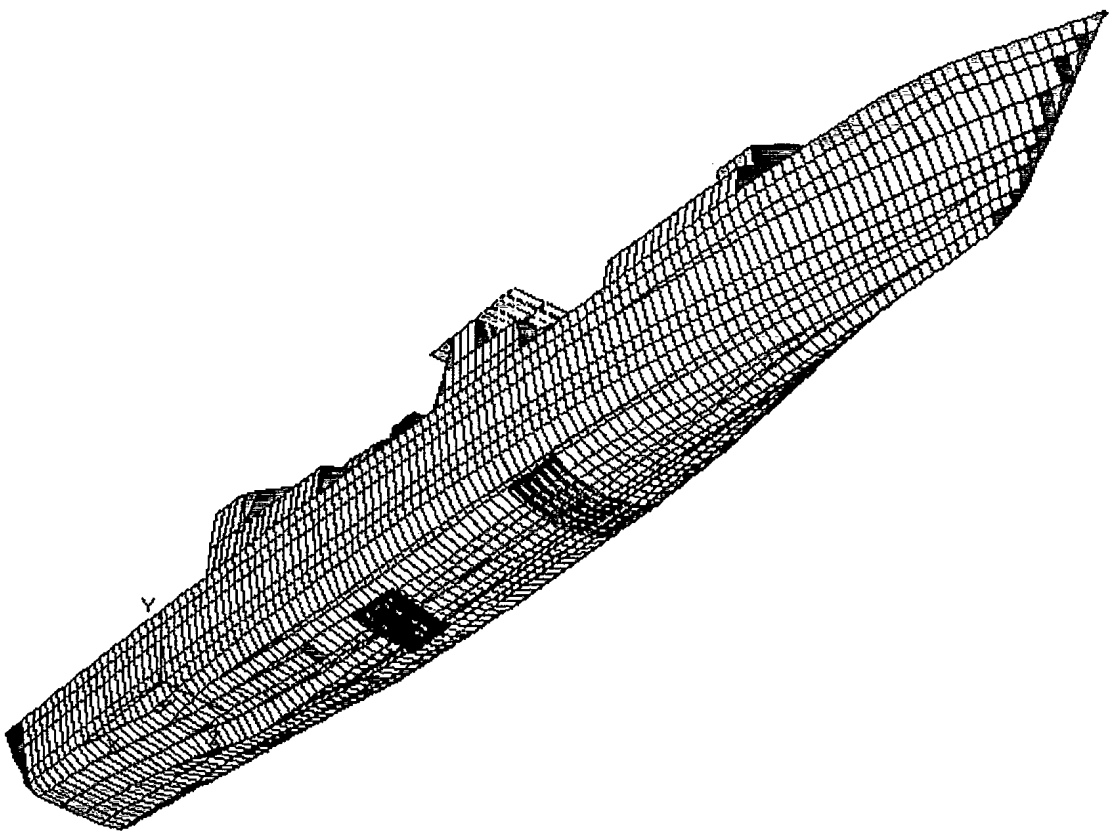

Figure 26: Regions 1 and 2 Bounding the MAESTRO High Stresses in the Bottom

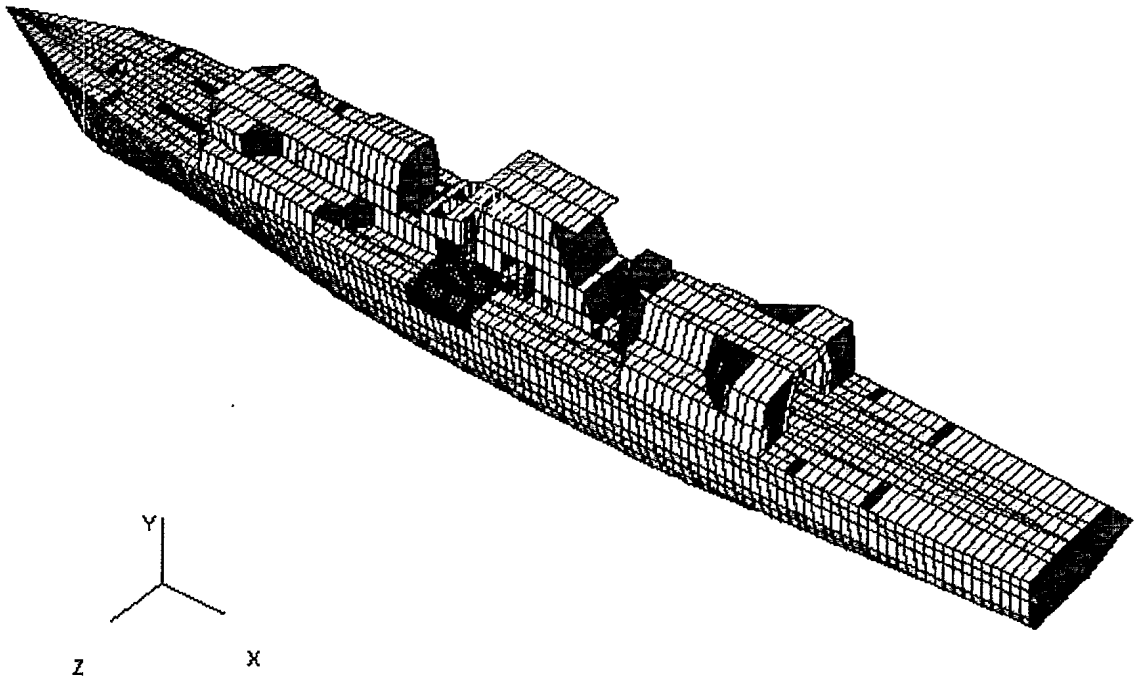

Figure 27: Region 3 Bounding the MAESTRO High Stresses in the Deck

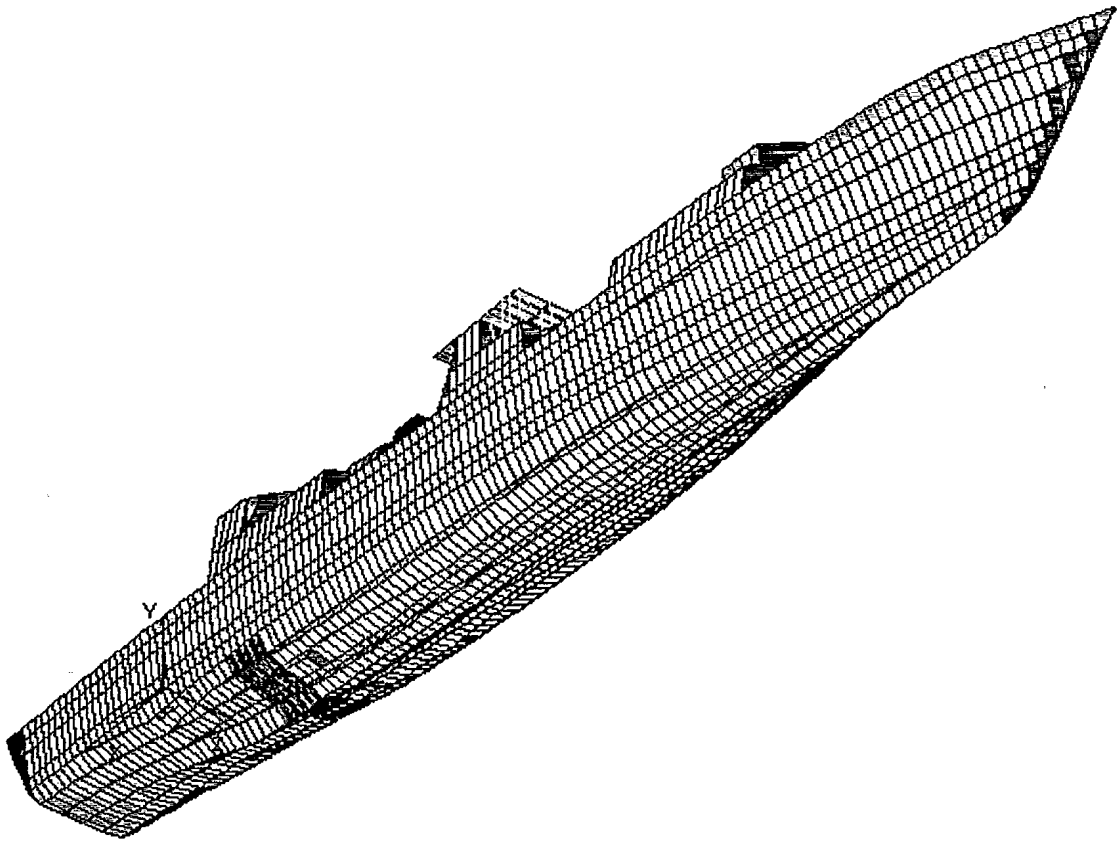

Figure 28: Region 4, the Black Water Tank in the Bottom at Frame 25

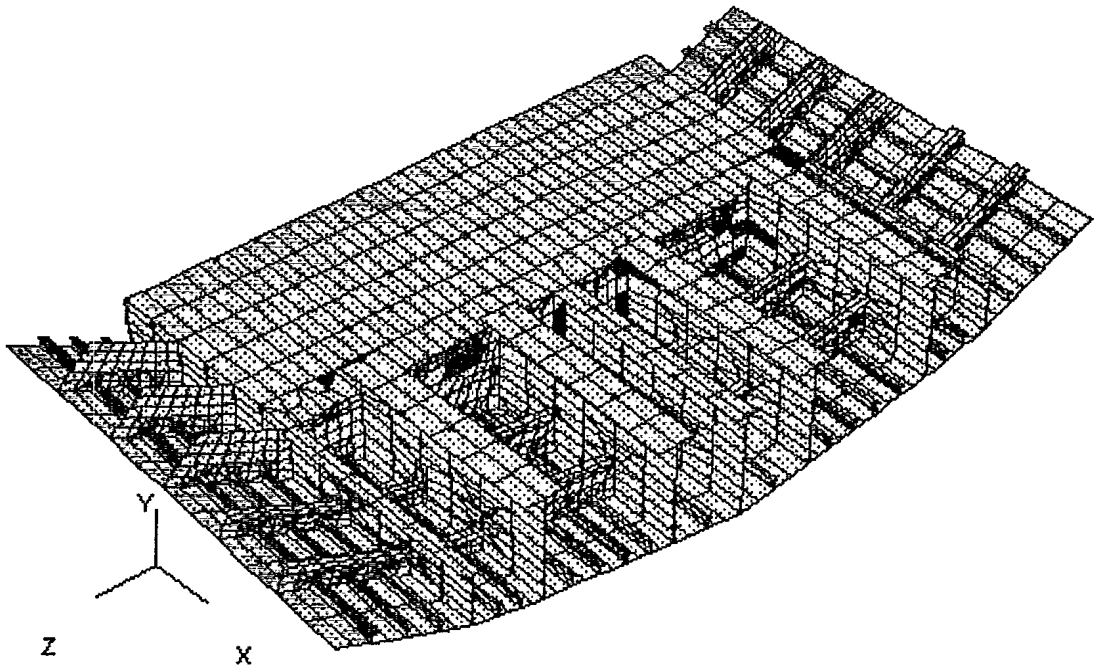

Figure 29: Refined Model of Region 1

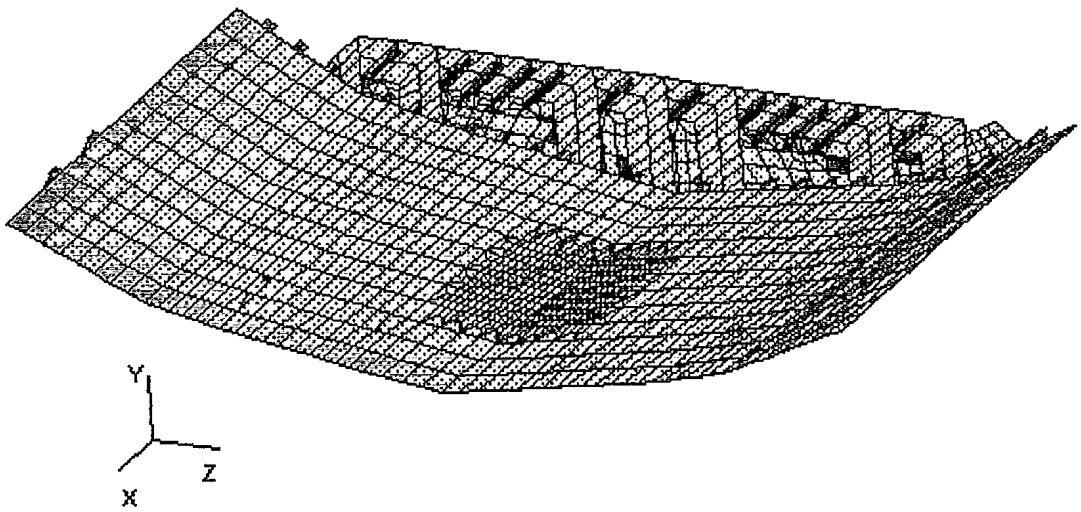

Figure 30: Additional Refinement of the High Stress Area of Region 1

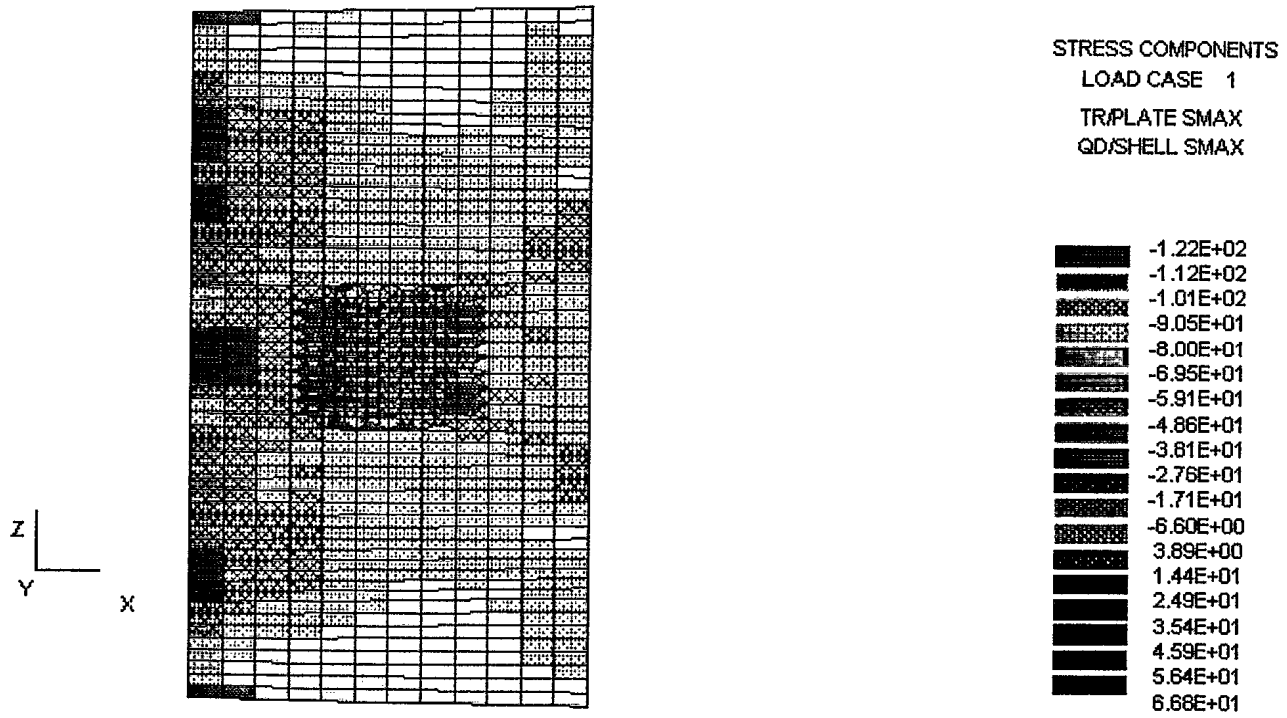

Figure 31: Stress (MPa) Results in the Locally Refined Area of Region 1 Due to the Hogging Load

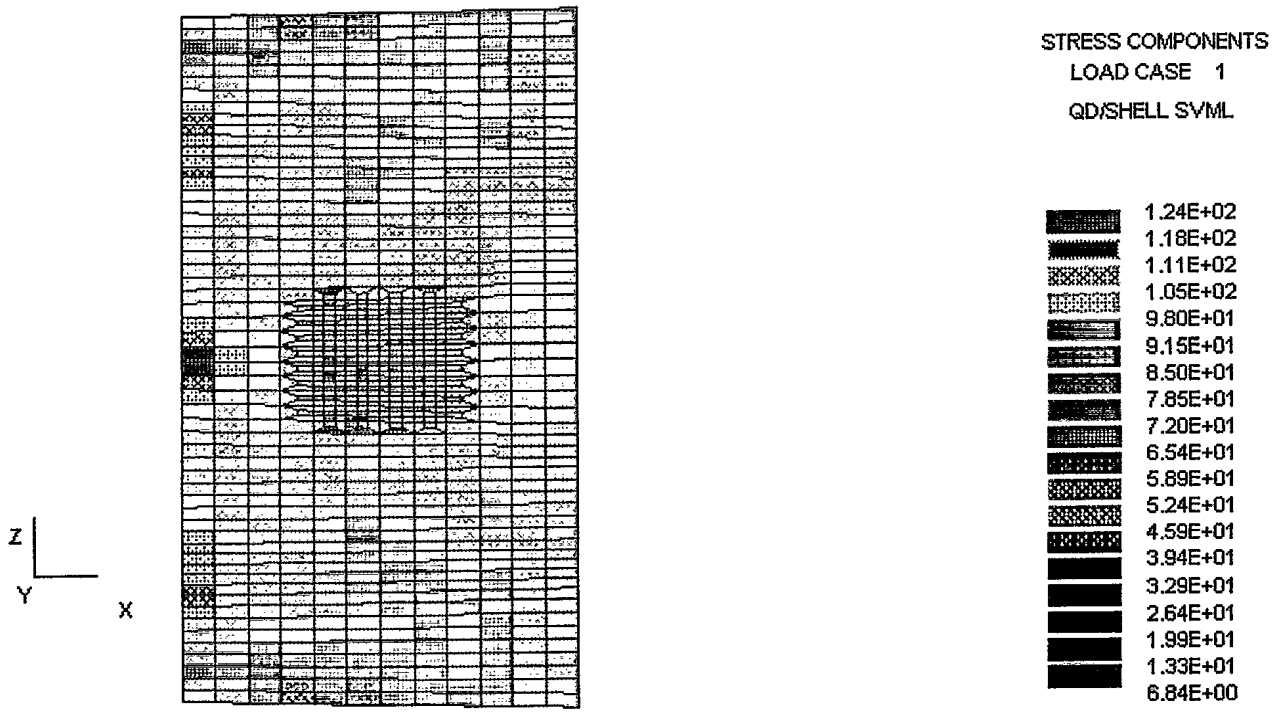

Figure 32: Stress (MPa) Results in the Locally Refined Area of Region 1 Due to the Sagging Load

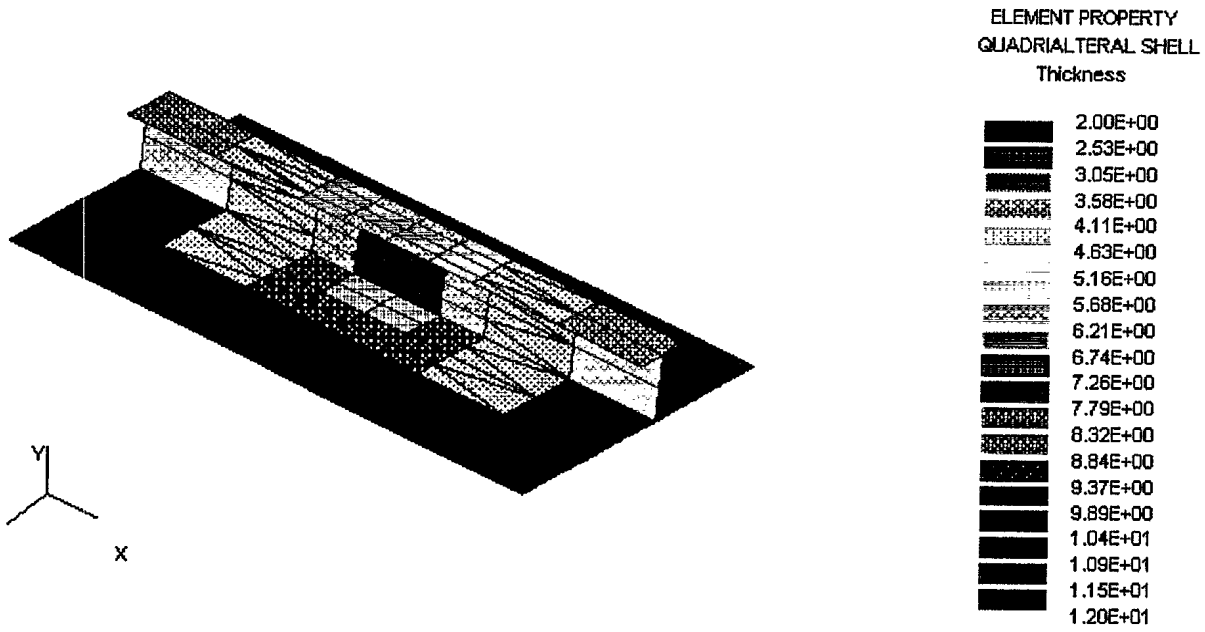

Figure 33: Local Reduction of the Stiffener Cross-section to Simulate Corrosion

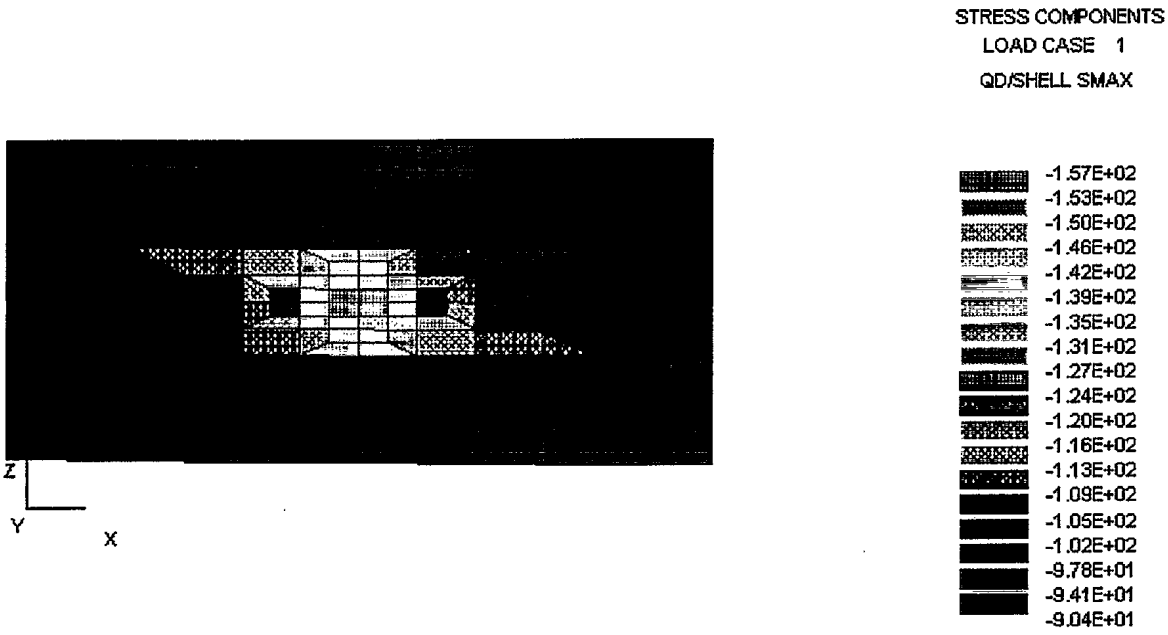

Figure 34: Stresses (MPa) in a Corrosion Pit in Region 1 Due to the Hogging Load

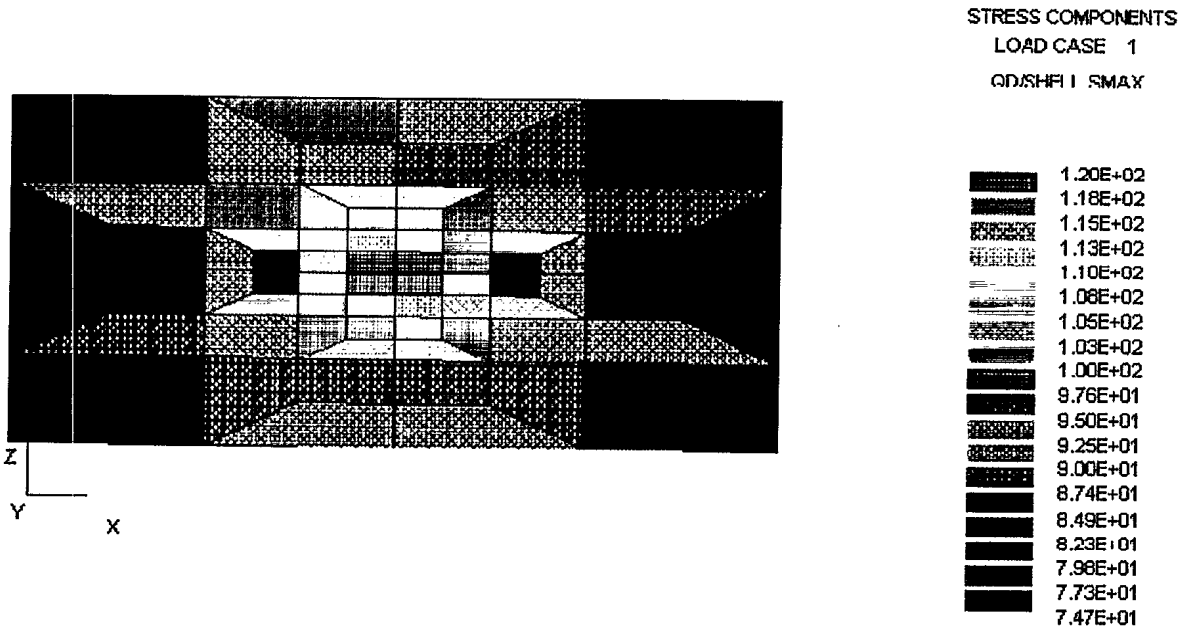

Figure 35: Stresses (MPa) in a Corrosion Pit in Region 1 Due to the Sagging Load

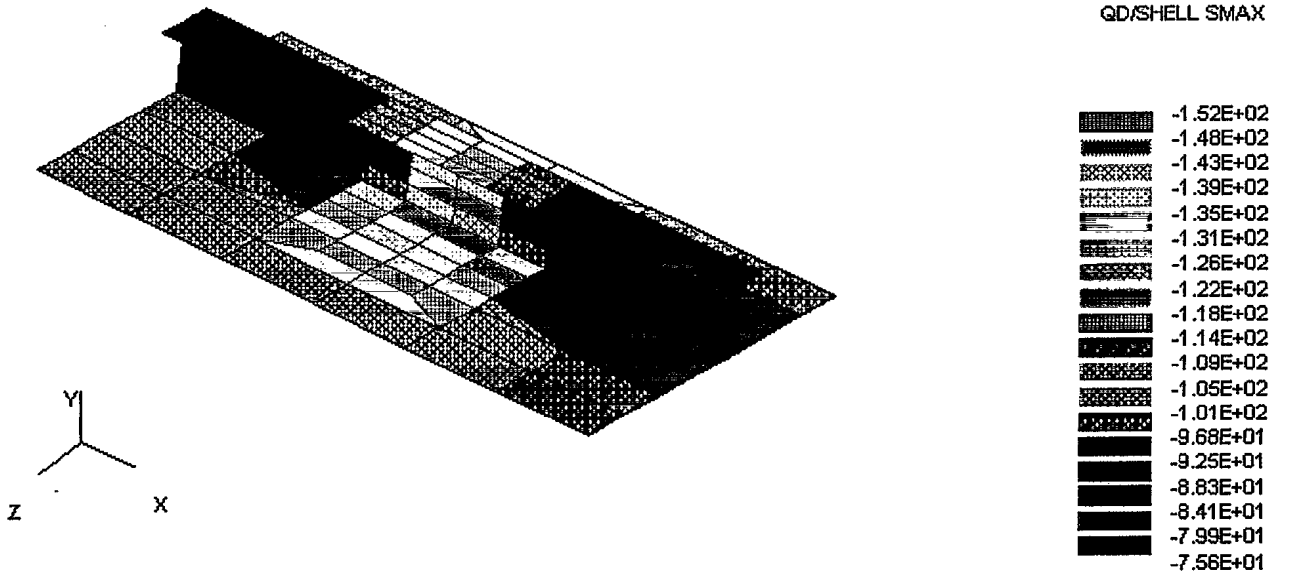

Figure 36: Stresses (MPa) Resulting from Localized Corrosion of Stiffener Cross-section in Region 1 Due to the Hogging Load

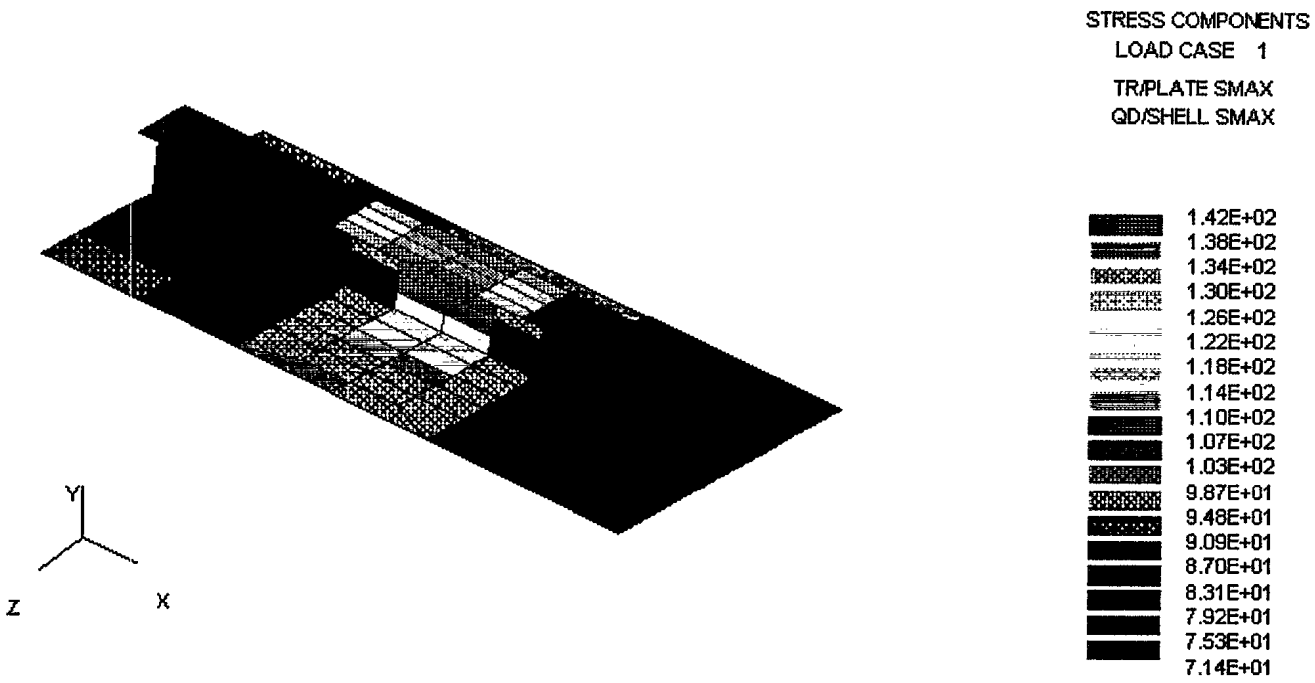

Figure 37: Stresses (MPa) Resulting from Localized Corrosion of the Stiffener Cross-section in Region 1 Due to the Sagging Load

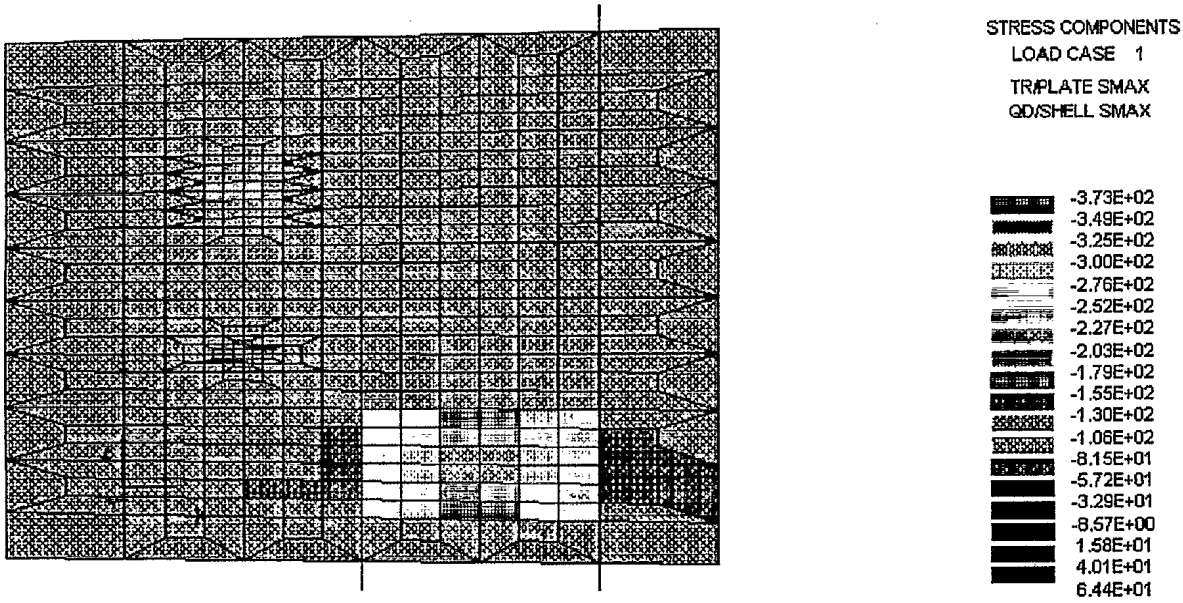

Figure 38: Stresses (MPa) Resulting from Severe Uniform Corrosion, from 12 mm to 5 mm, of a Panel in Region 1 Due to the Hogging Load

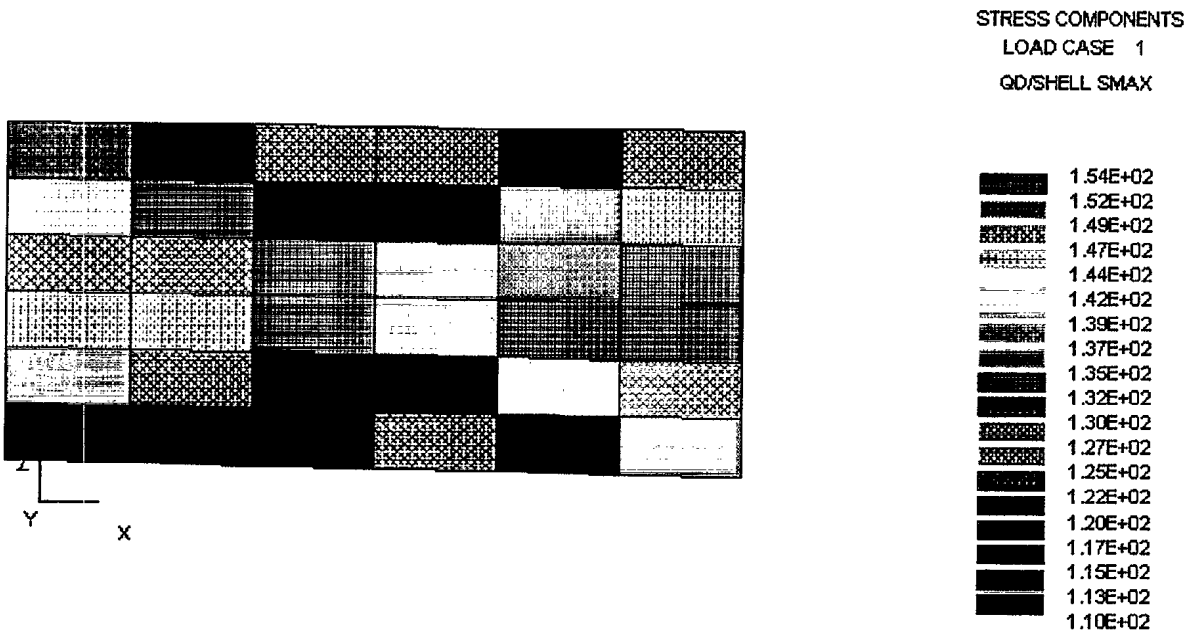

Figure 39: Stresses (MPa) Resulting from Severe Uniform Corrosion, from 12 mm to 5 mm, of a Panel in Region 1 Due to the Sagging Load

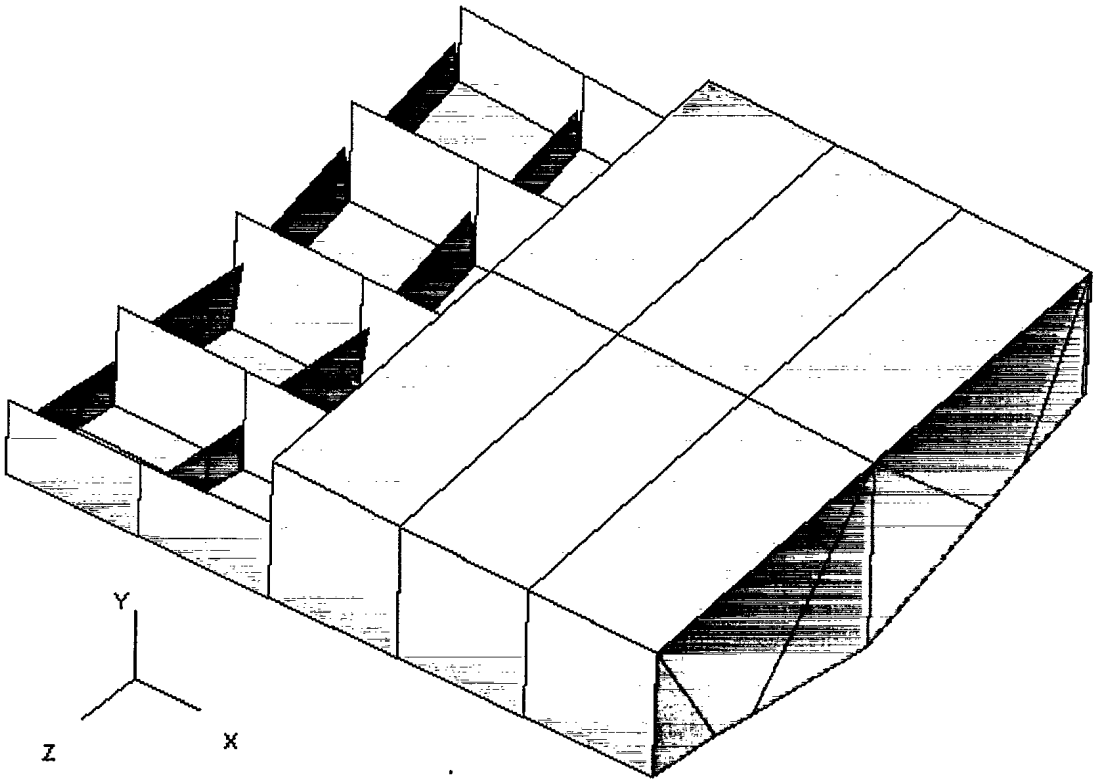

Figure 40: Region 2 of Bottom Extracted from the MAESTRO Model

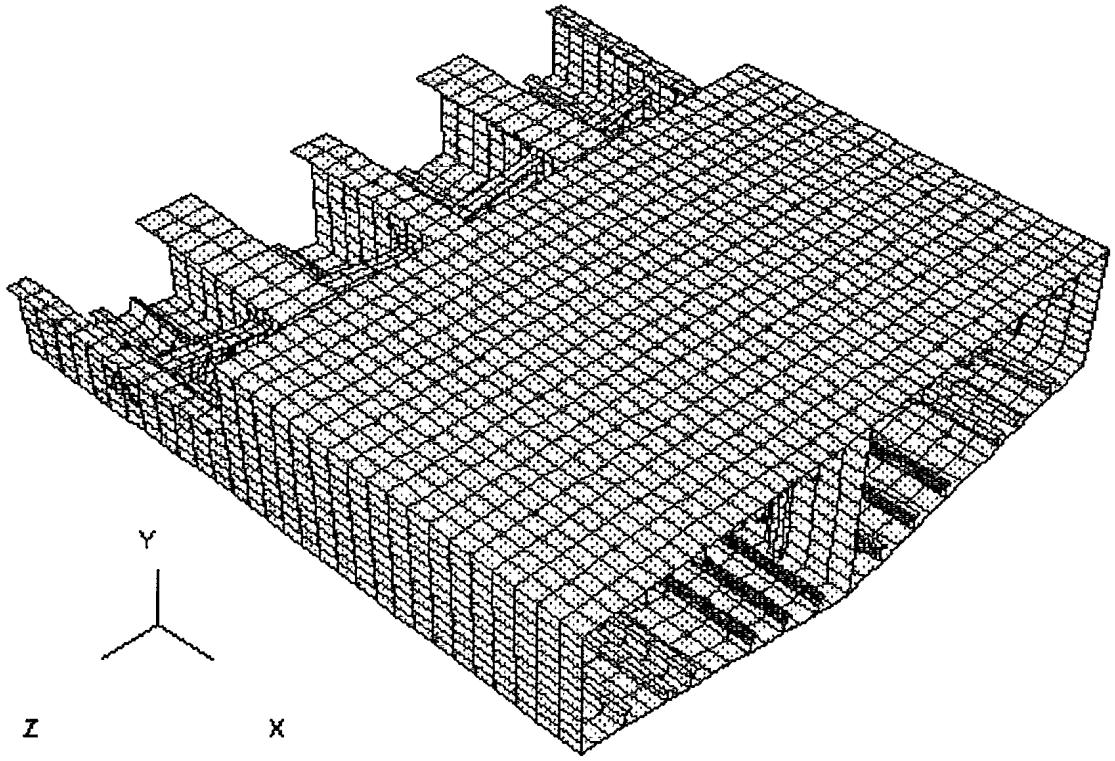

Figure 41: The Refined Model of Region 2

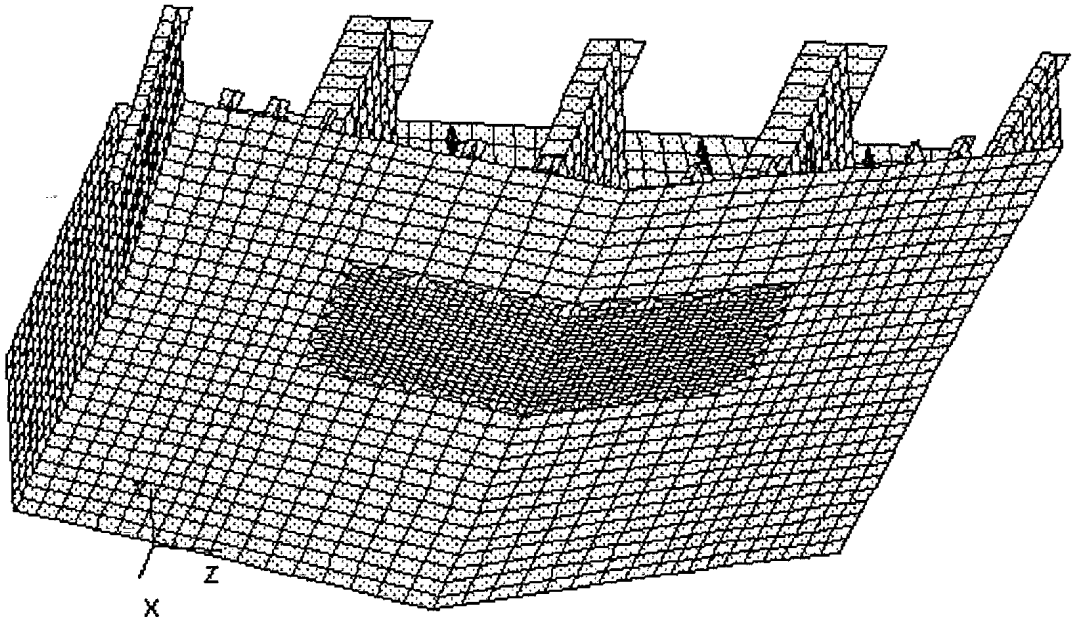

Figure 42: Additional Refinement of Region 2 in the Area of High Stress in the MAESTRO Model

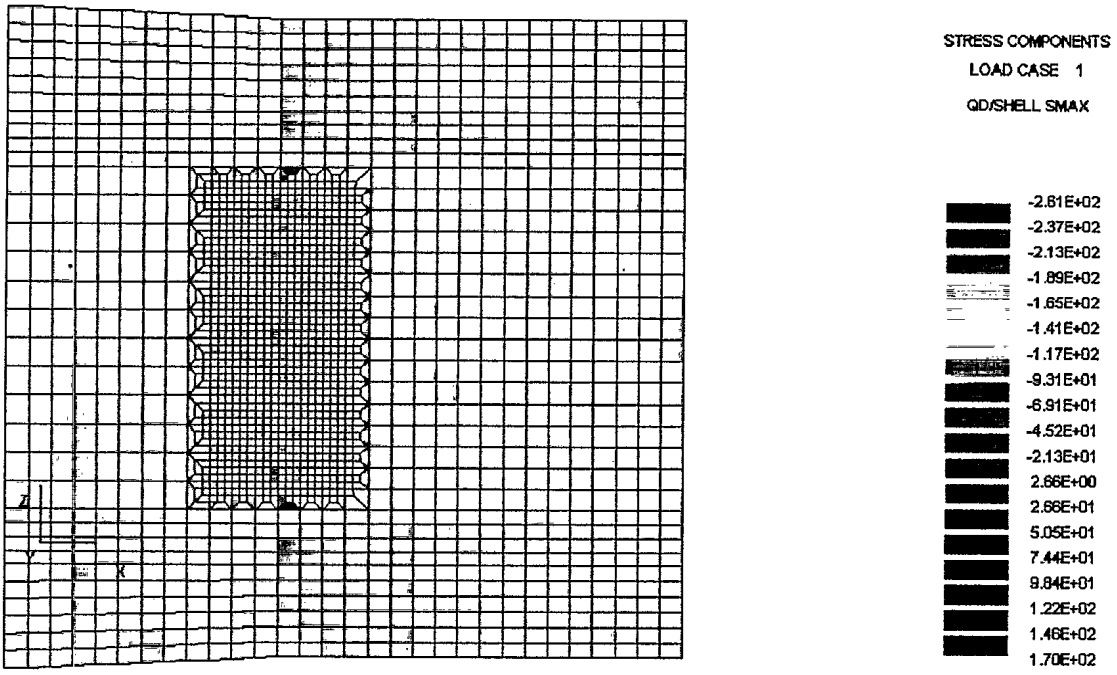

Figure 43: Stresses (MPa) in the Refined Region 2 Resulting from the Hogging Load Case

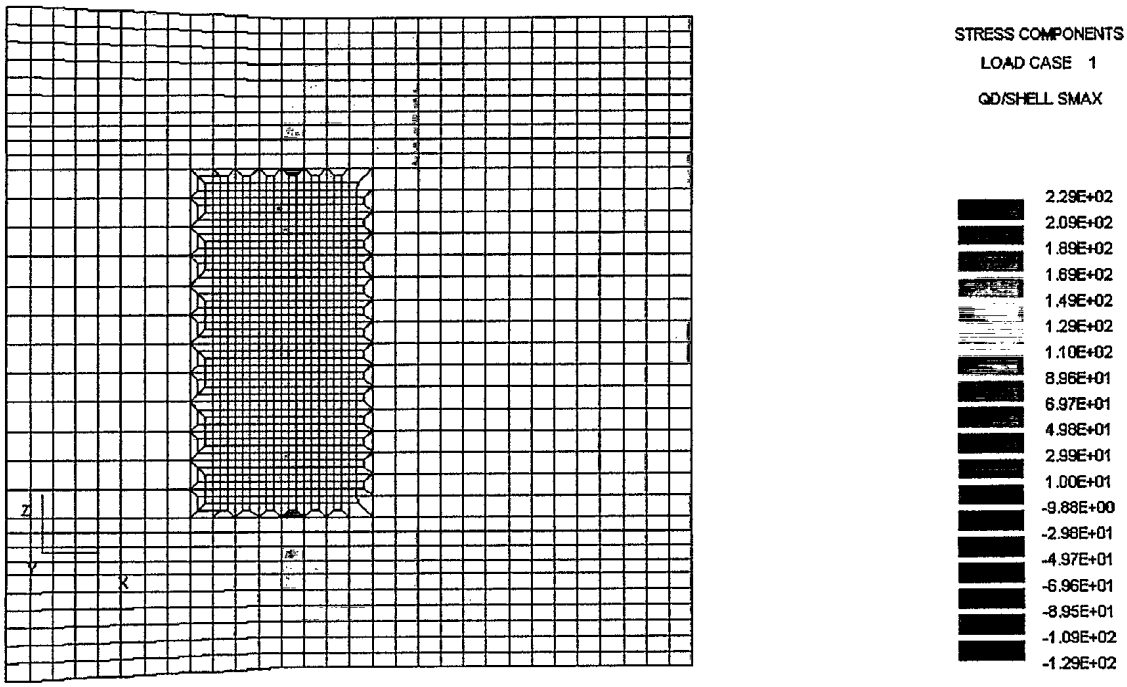

Figure 44: Stresses (MPa) in the Refined Region 2 Resulting from the Sagging Load Case

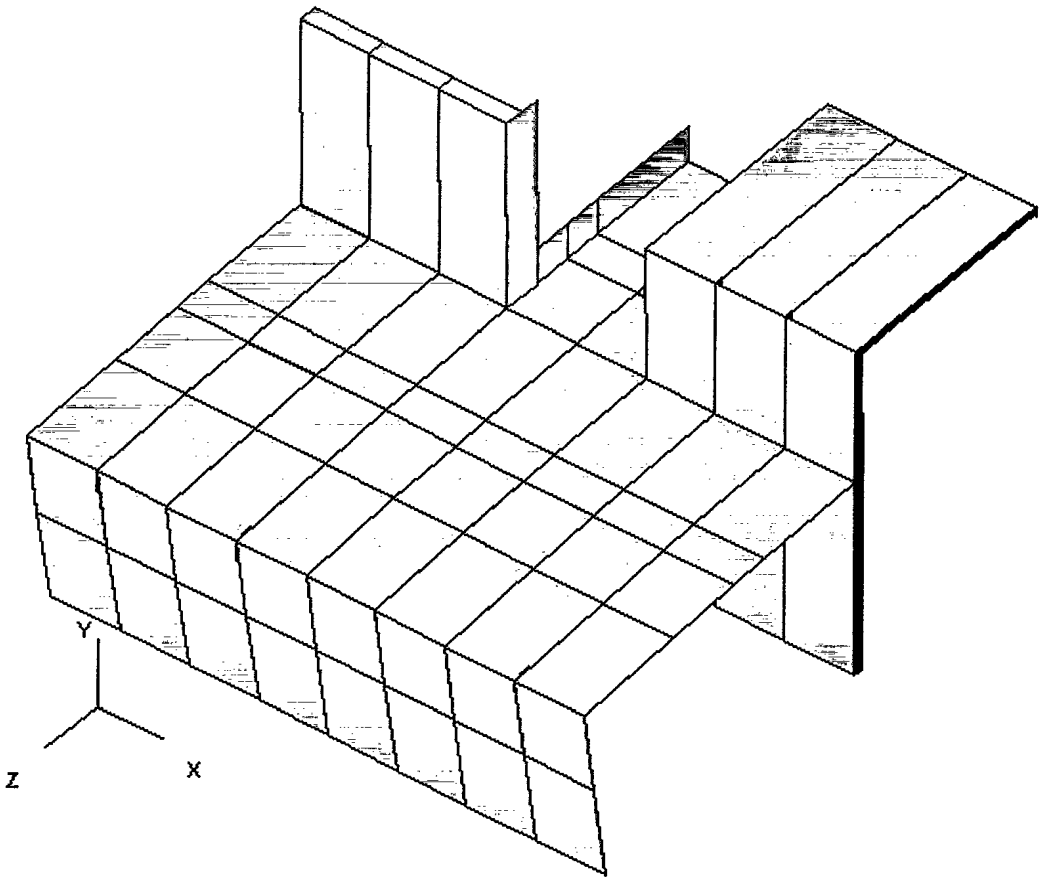

Figure 45: Region 3 Extracted from the MAESTRO Model

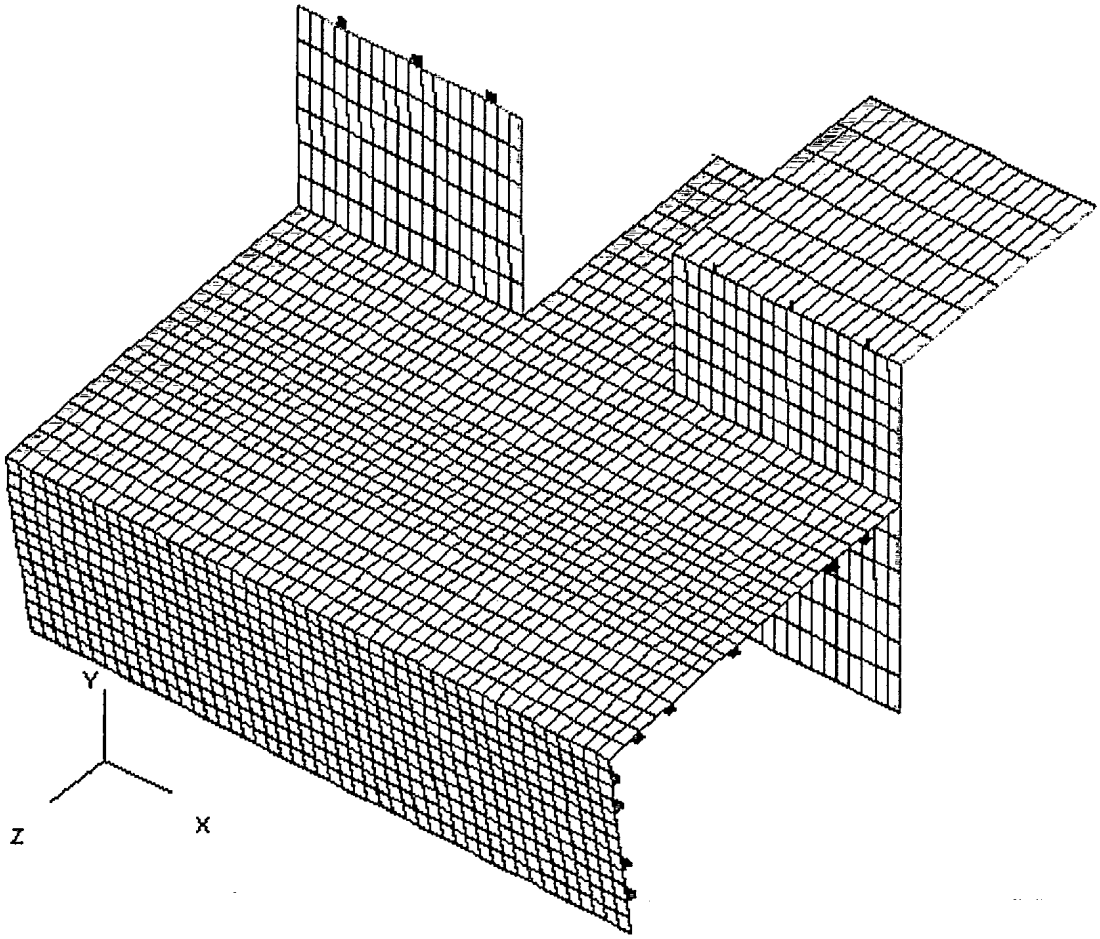

Figure 46: The Refined Model of Region 3

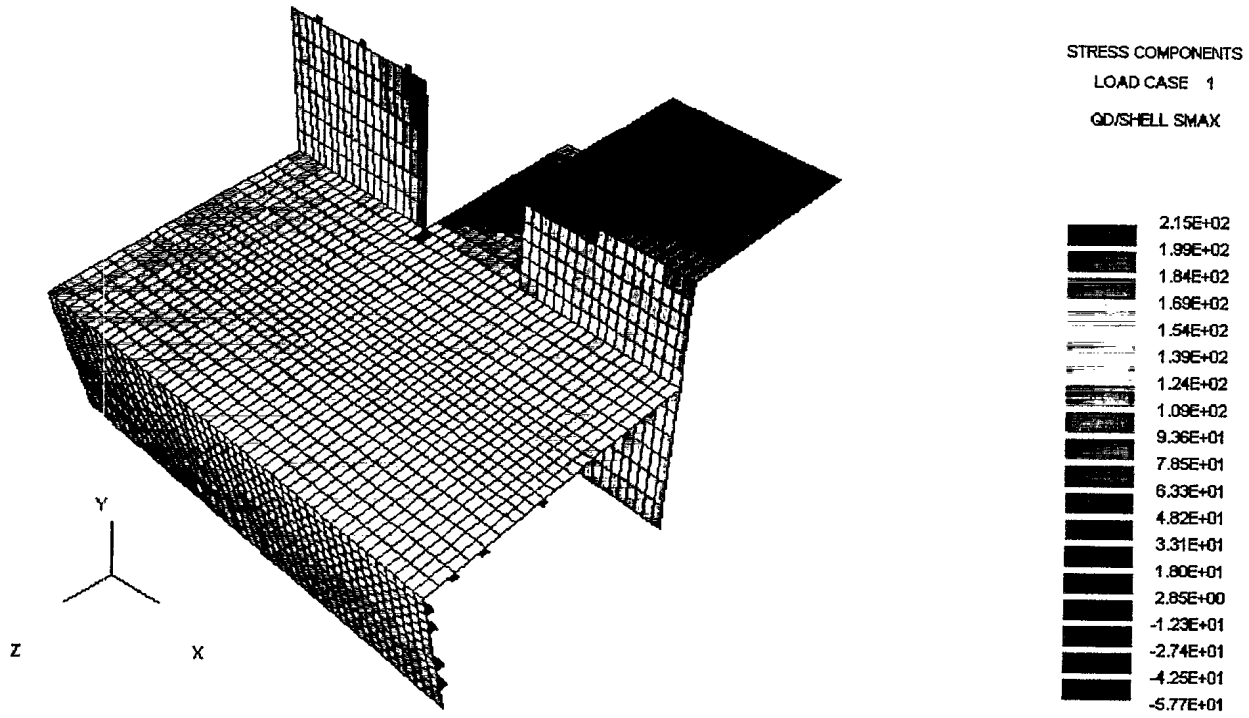

Figure 47: The Stresses (MPa) Resulting from the Hogging Load on the Refined Model of Region 3

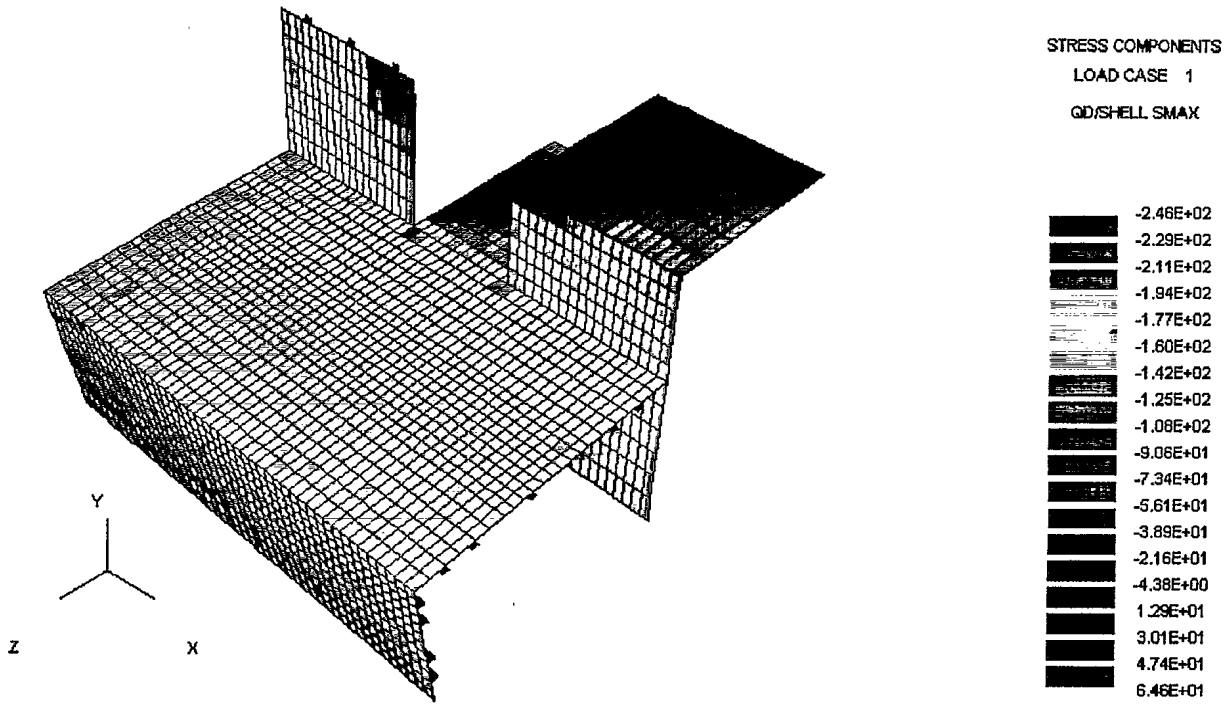

Figure 48: The Stresses (MPa) Resulting from the Sagging Load on the Refined Model of Region 3

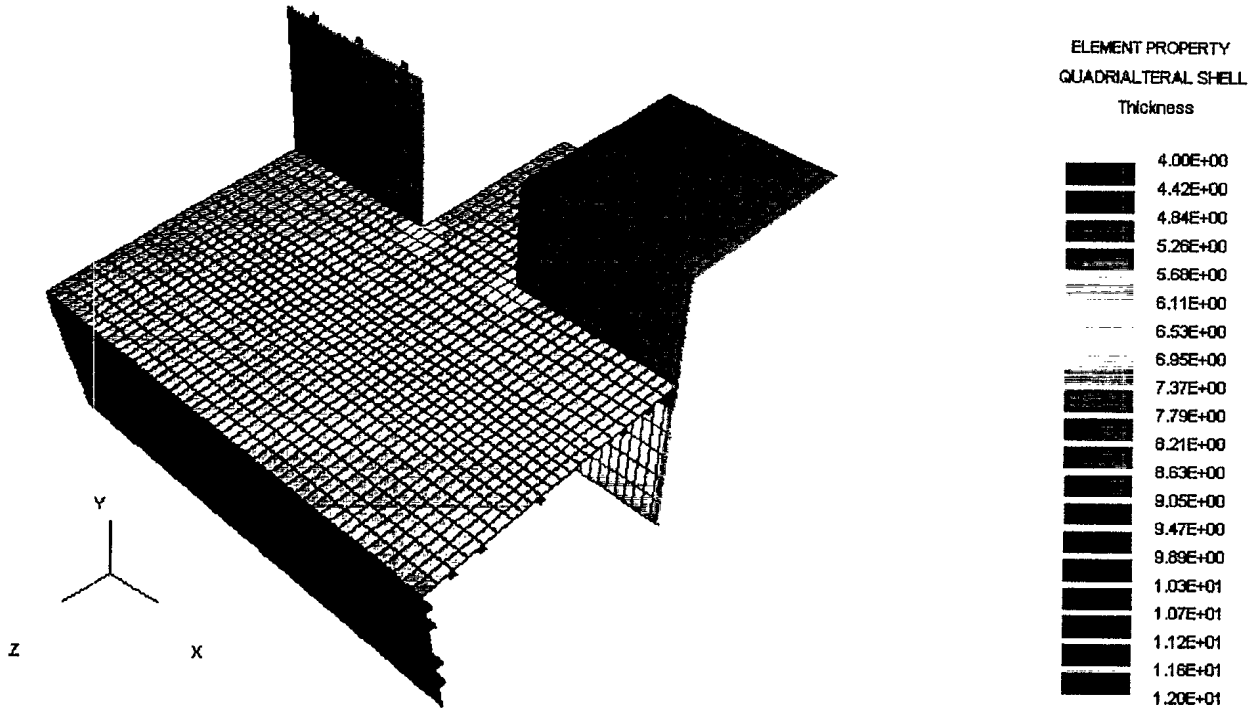

Figure 49: The Reduction in Plate Thicknesses in Local High Stress Area of the Deck to 7 mm

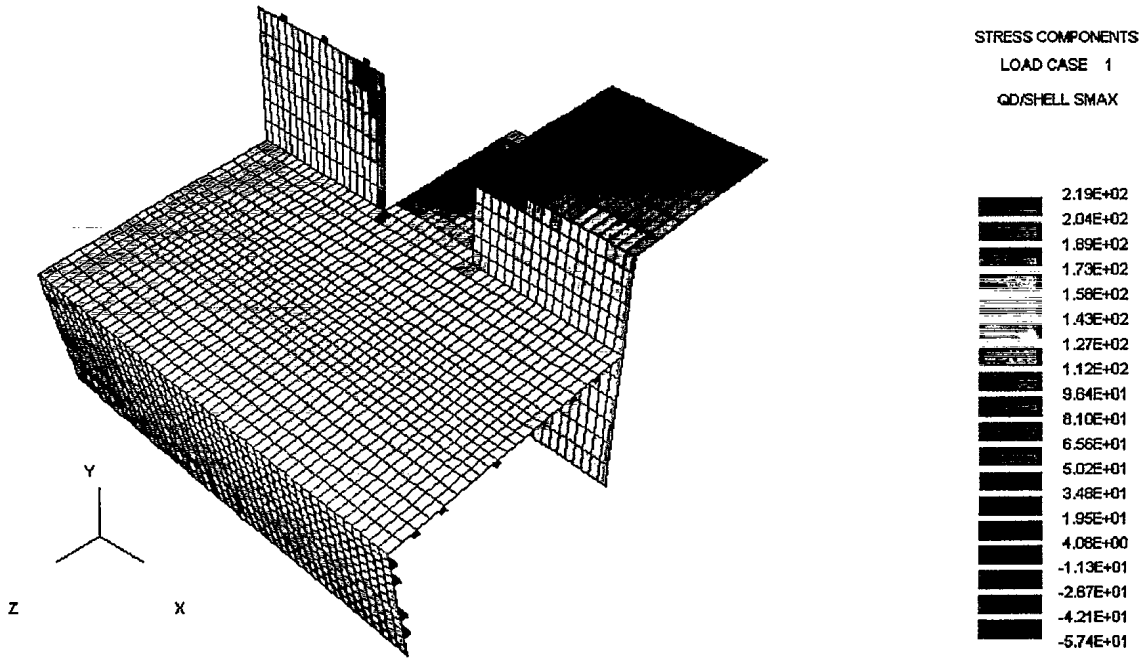

Figure 50: The Stresses (MPa) Resulting from the Plate Thickness Reduction to 7 mm in the Deck Due to the Hogging Load

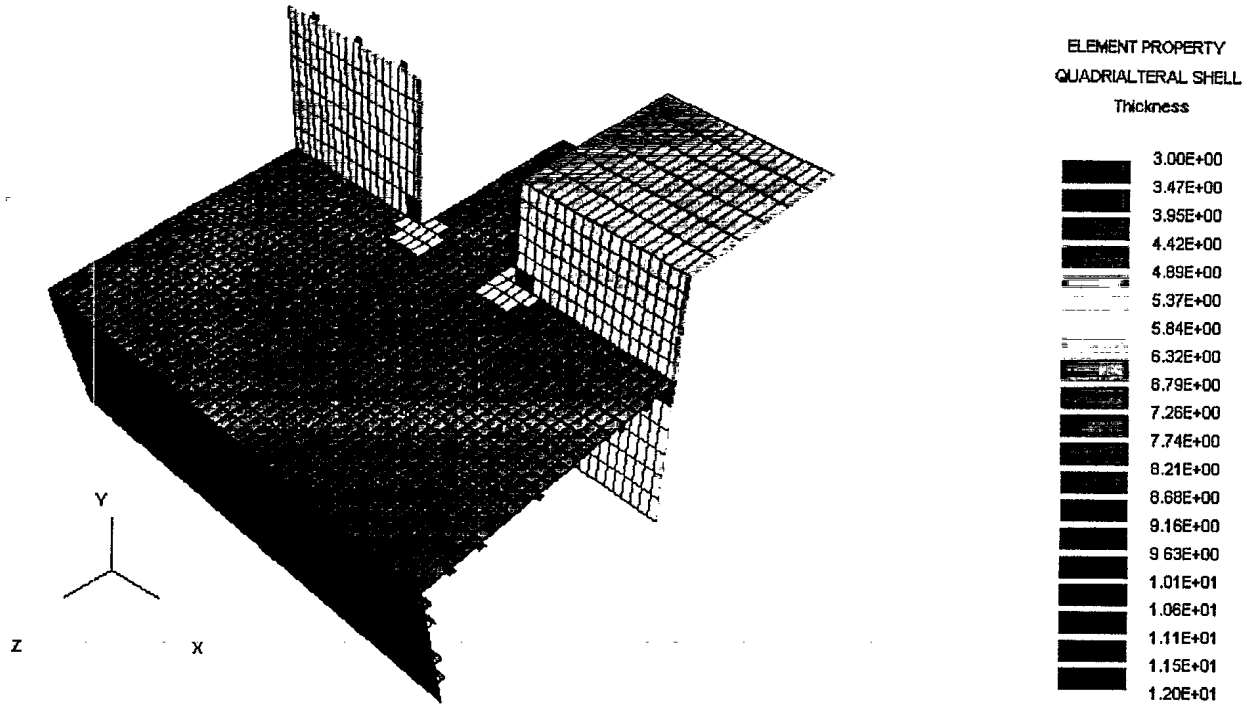

Figure 51: The Local Reduction in the Plate Thickness to 3 mm in the Superstucture

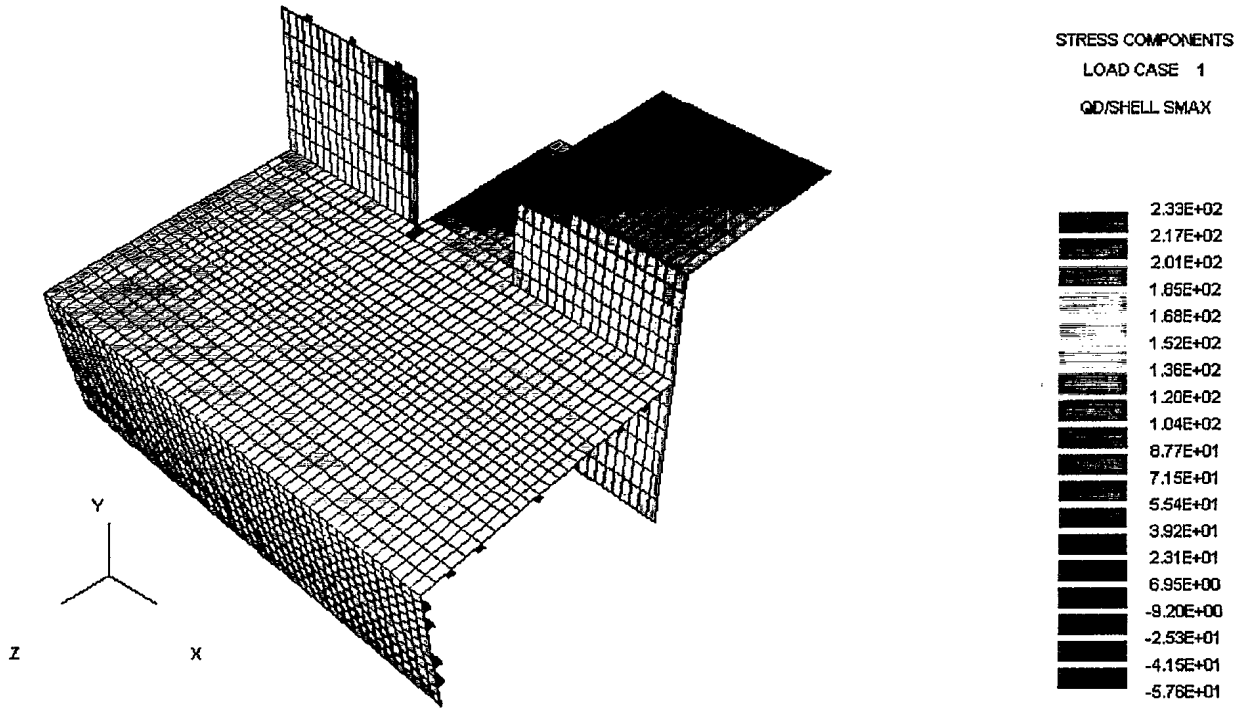

Figure 52: The Stresses (MPa) Resulting from the Plate Thickness Reduction to 3 mm in the Superstructure Due to the Hogging Load

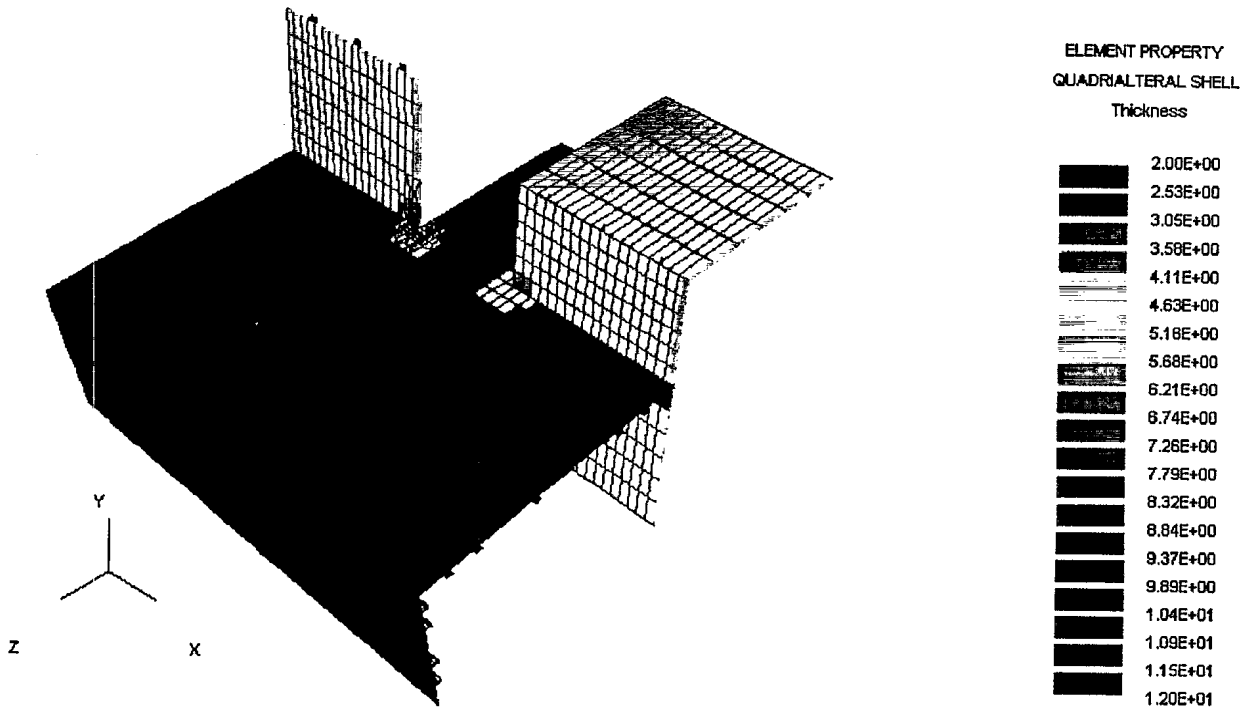

Figure 53: The Local Reduction in the Plate Thickness to 2 mm in the Superstructure and 6 mm in the Deck

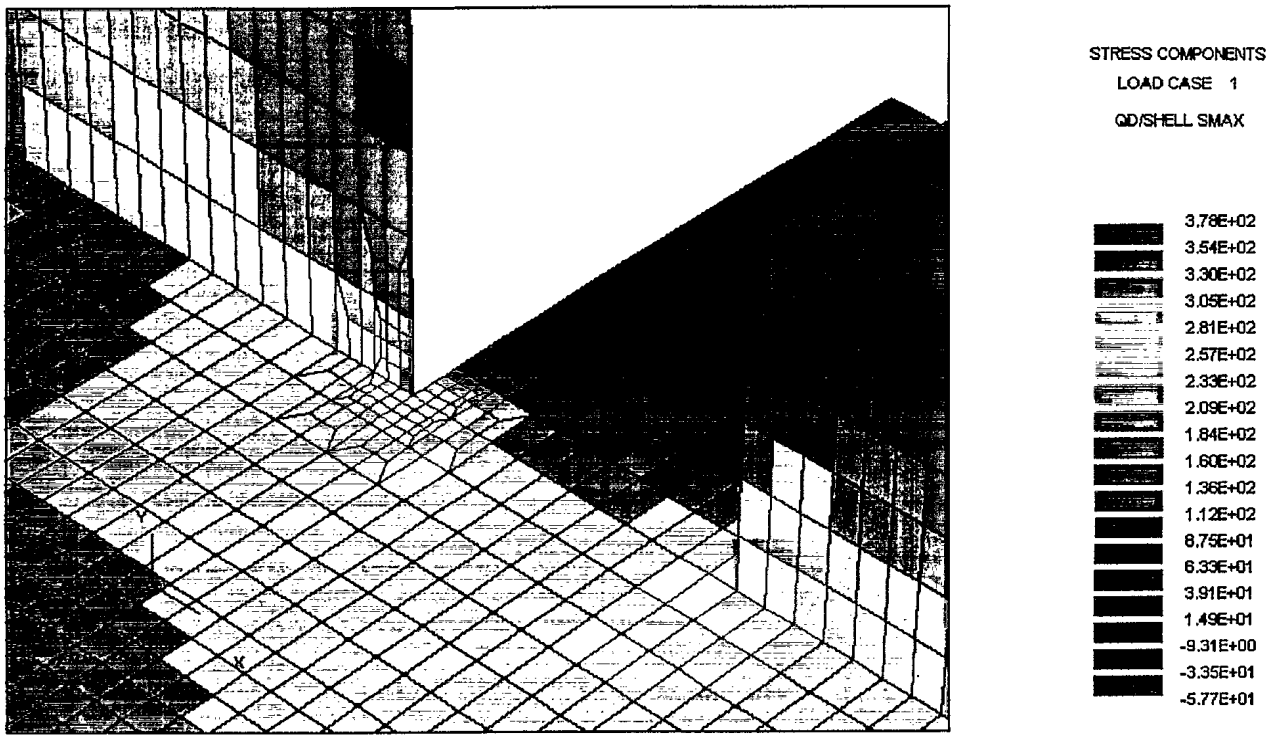

Figure 54: The Element Stresses (MPa), Resulting from the Plate Thickness Reduction in the Superstructure and Deck, Due to the Hogging Load

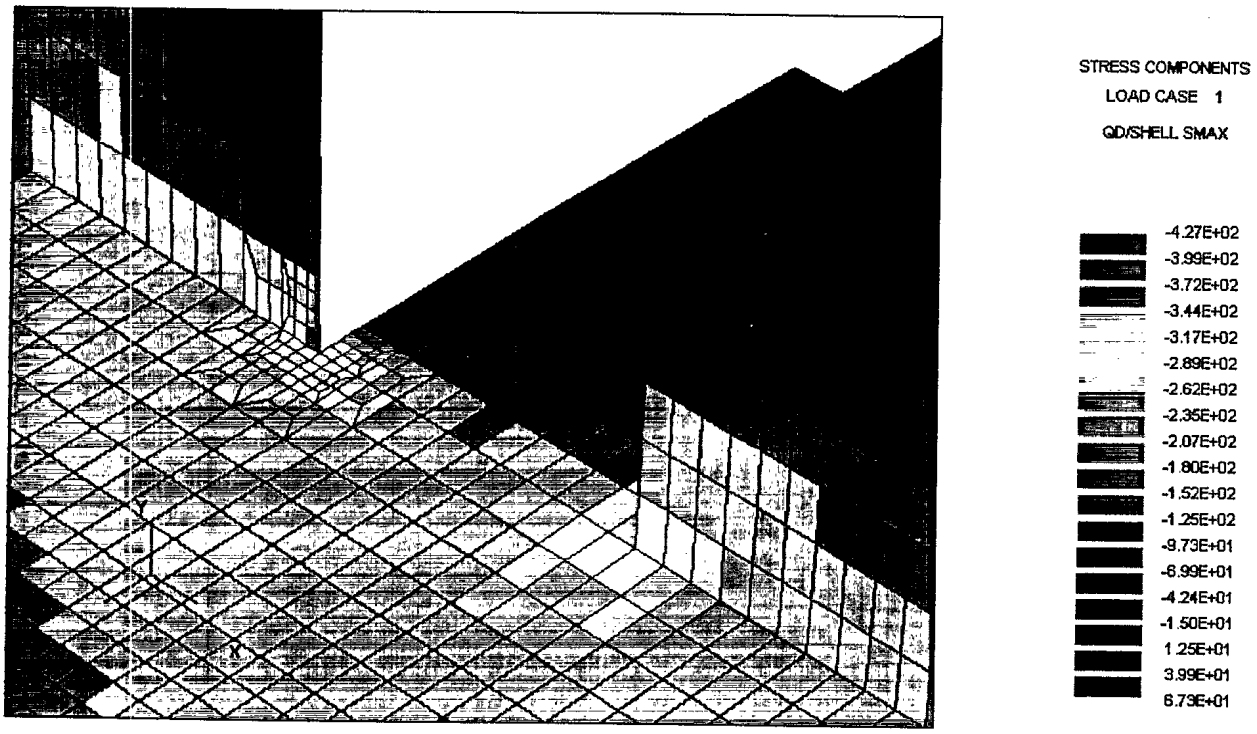

Figure 55: The Stresses (MPa), Resulting from the Plate Thickness Reduction in the Superstructure and Deck, Due to the Sagging Load

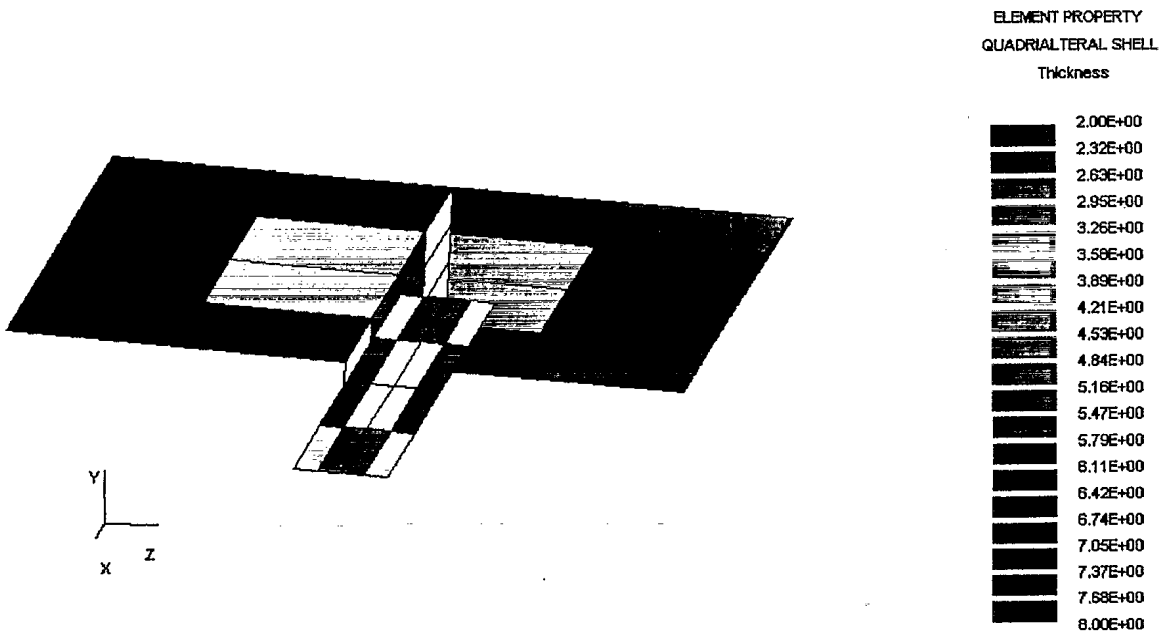

Figure 56: Reduced Cross-section of Deck Stiffener and Deck

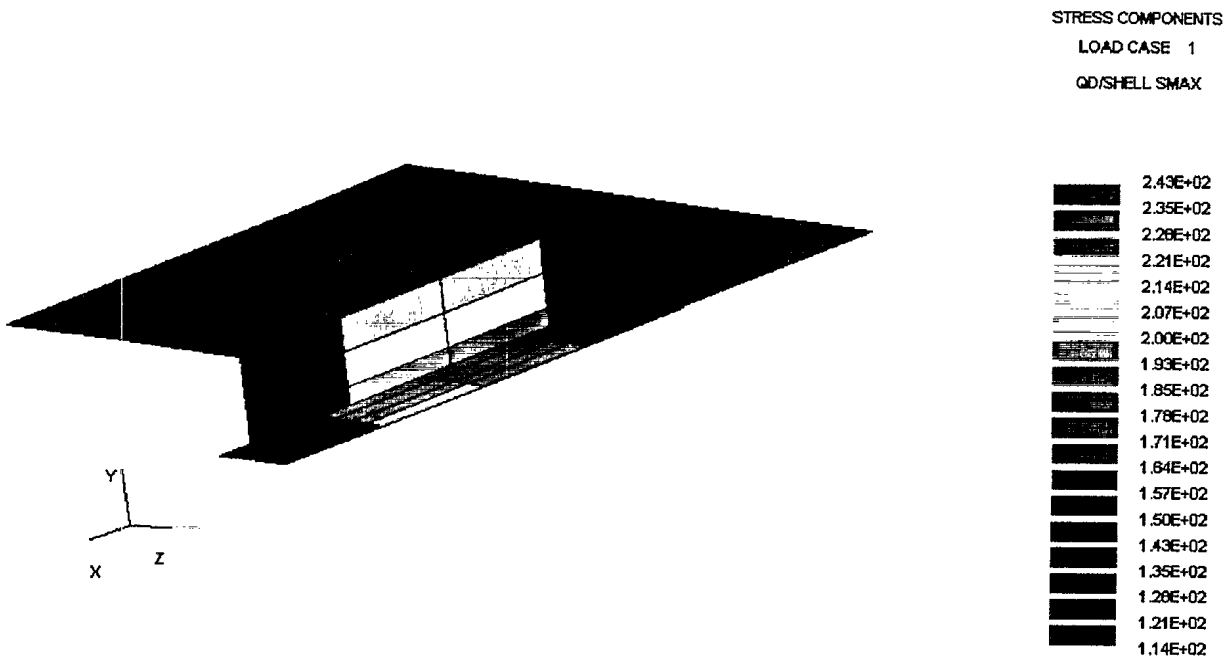

Figure 57: The Stresses (MPa) in the Corroded Stiffener Due to the Sagging Load

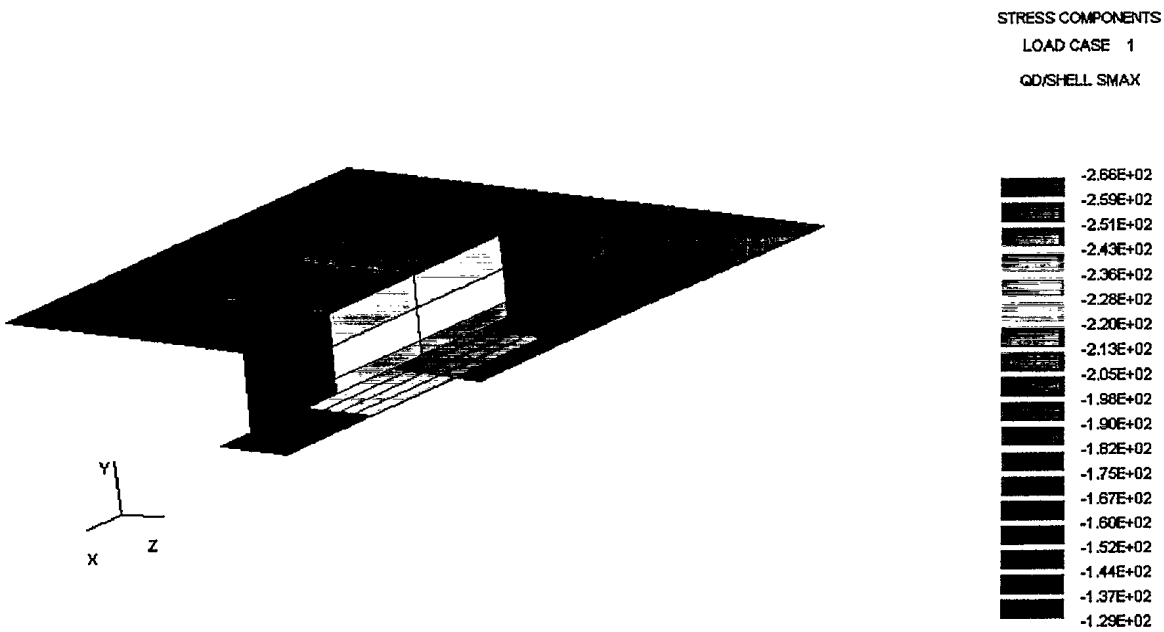

Figure 58: The Stresses (MPa) in the Corroded Stiffener Due to the Hogging Load

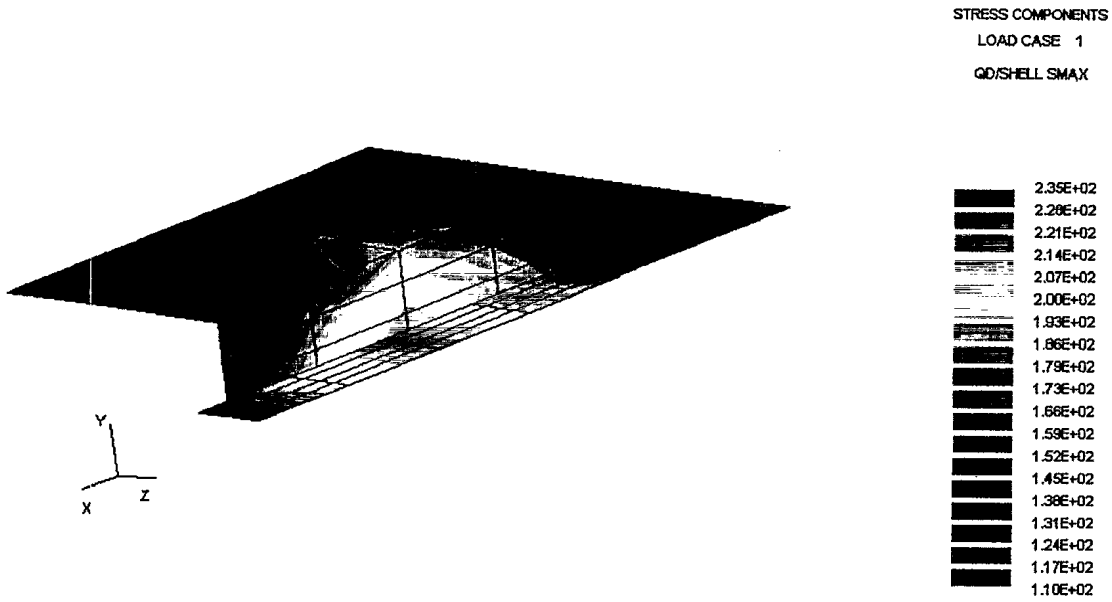

Figure 59: A Fringe Plot of the Stresses (MPa) in the Corroded Stiffener Due to the Hogging Load

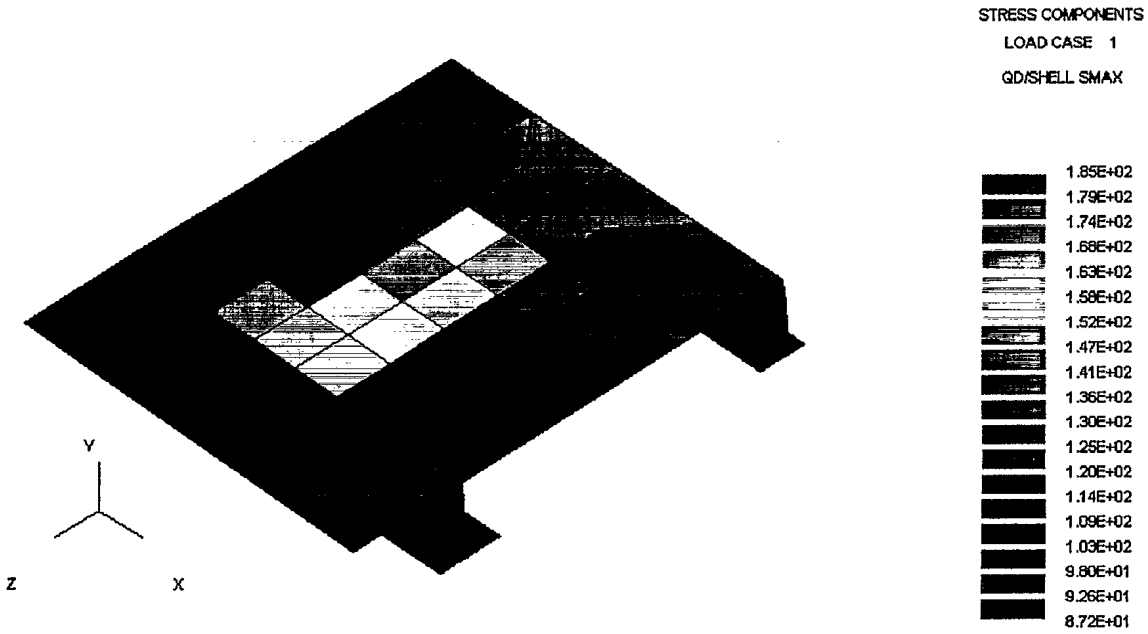

Figure 60: The Stresses (MPa) in the Corrosion Pit Due to the Hogging Load

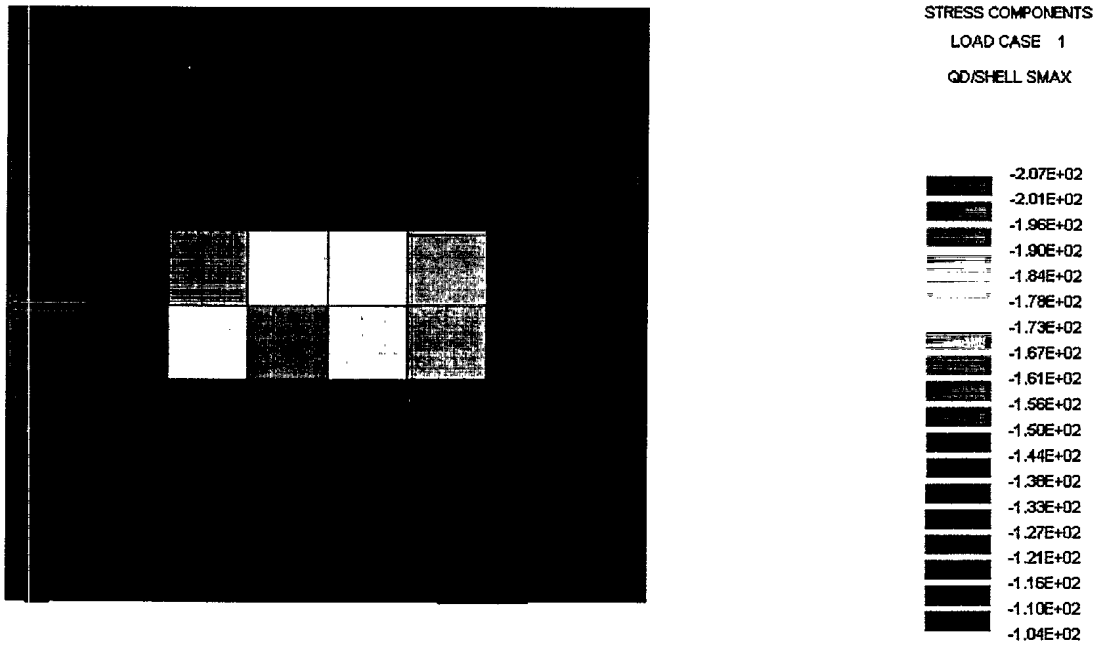

Figure 61: The Stresses (MPa) in the Corrosion Pit Due to the Sagging Load

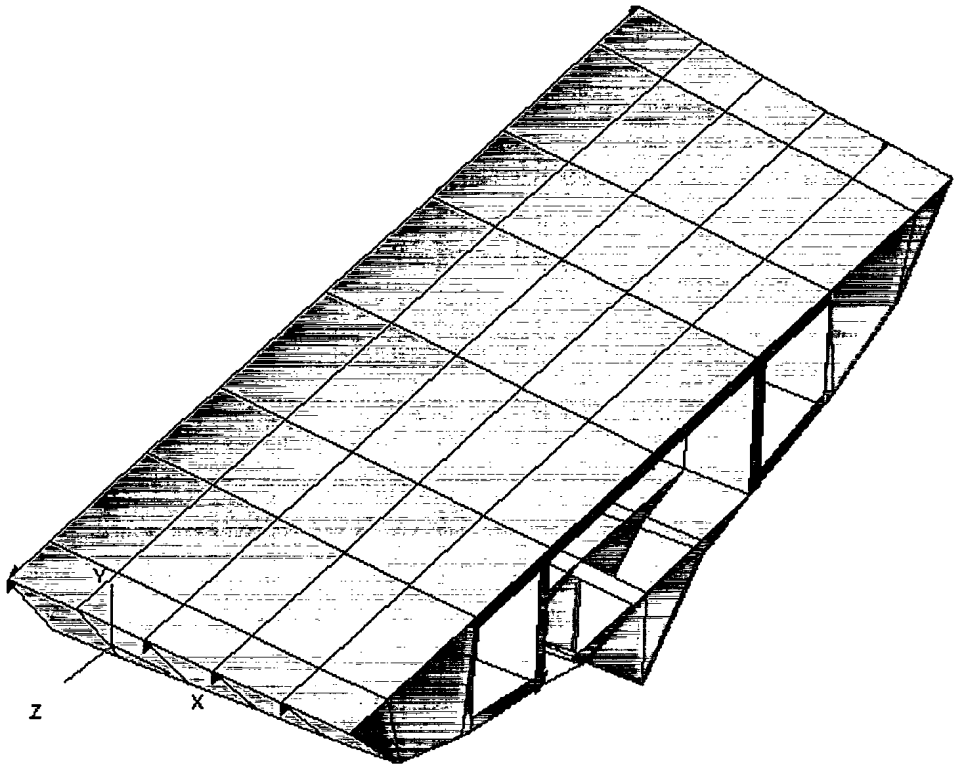

Figure 62: Region 4 of Bottom, Including Gray Water Tank, Extracted from the MAESTRO Model

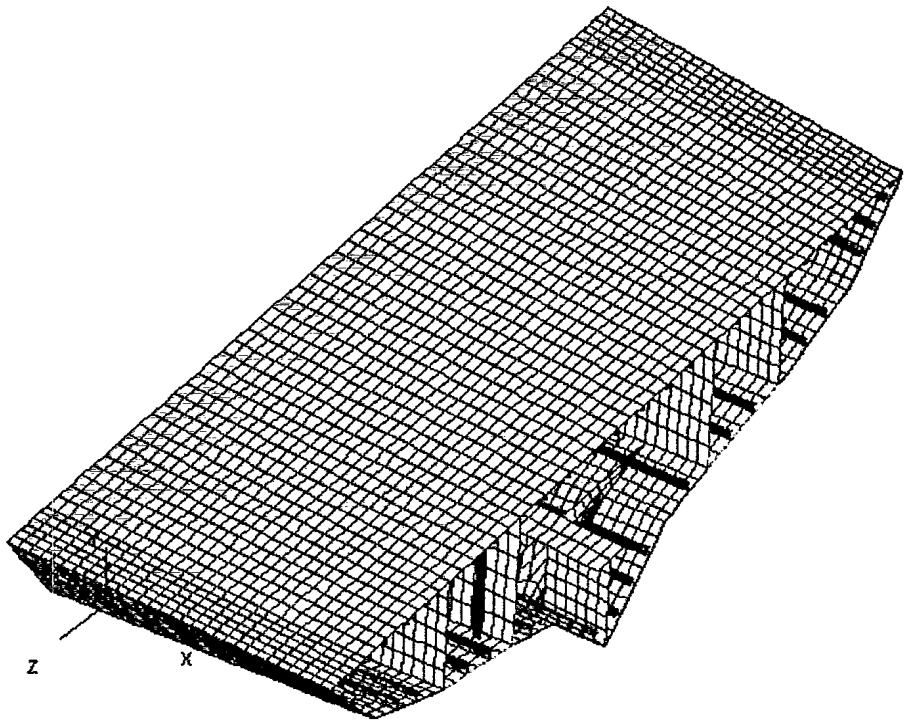

Figure 63: The Refined Model of Region 4

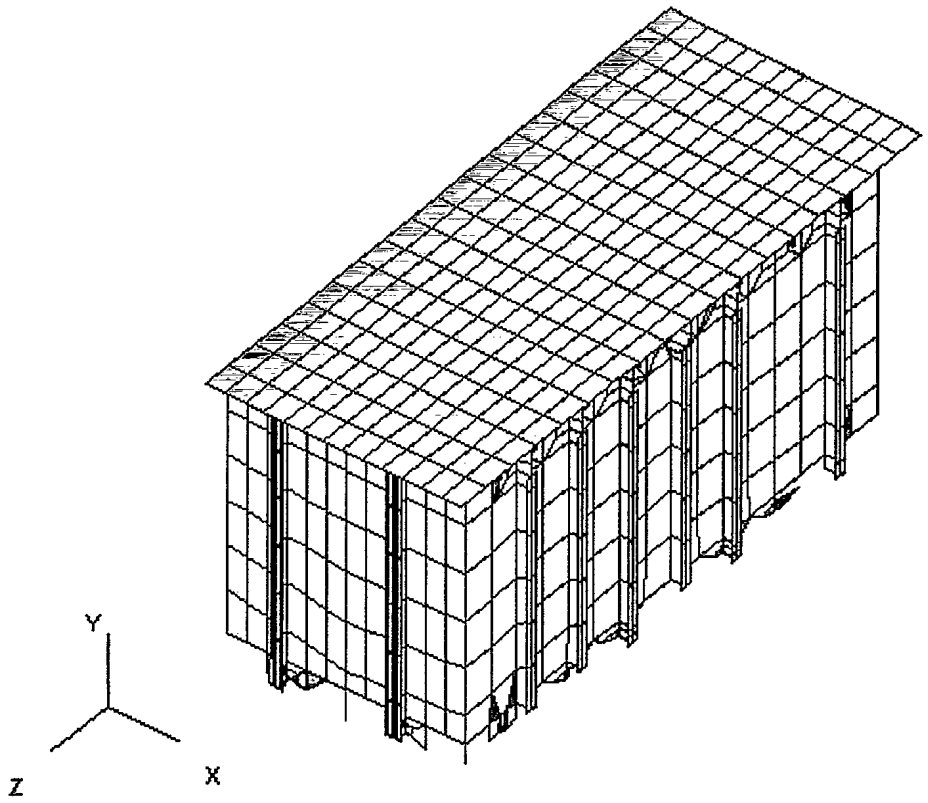

Figure 64: The Refined Gray Water Tank of Region 4

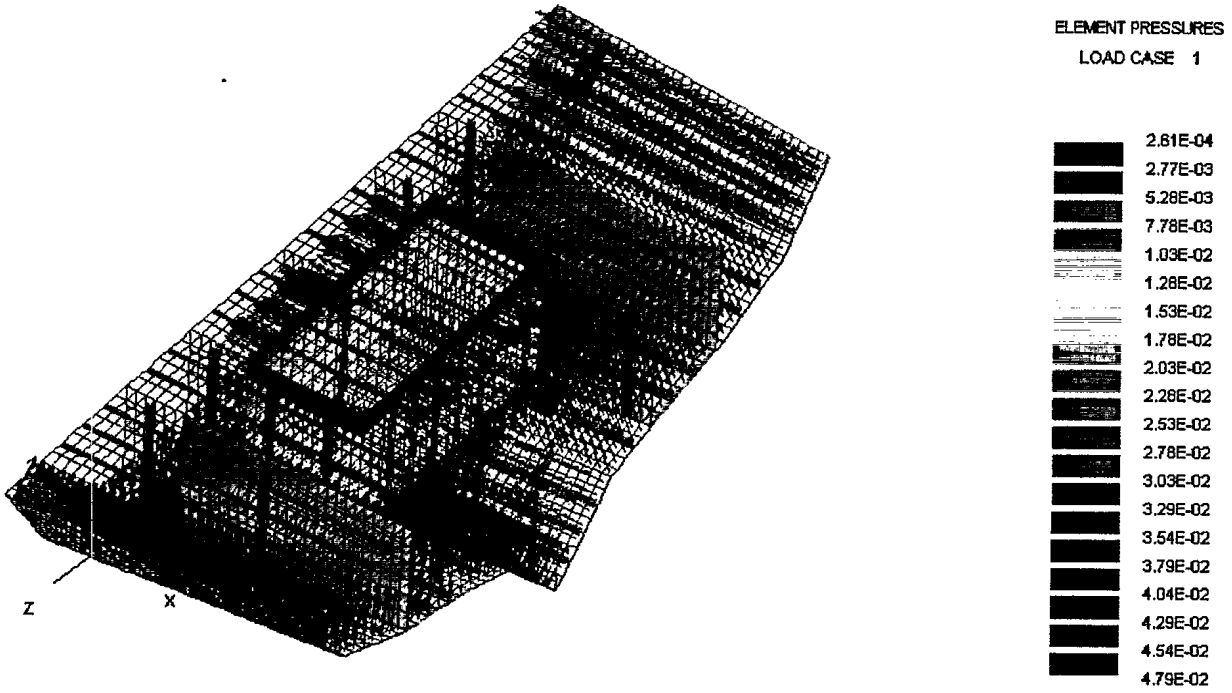

Figure 65: The Loading of the Refined Model of Region 4

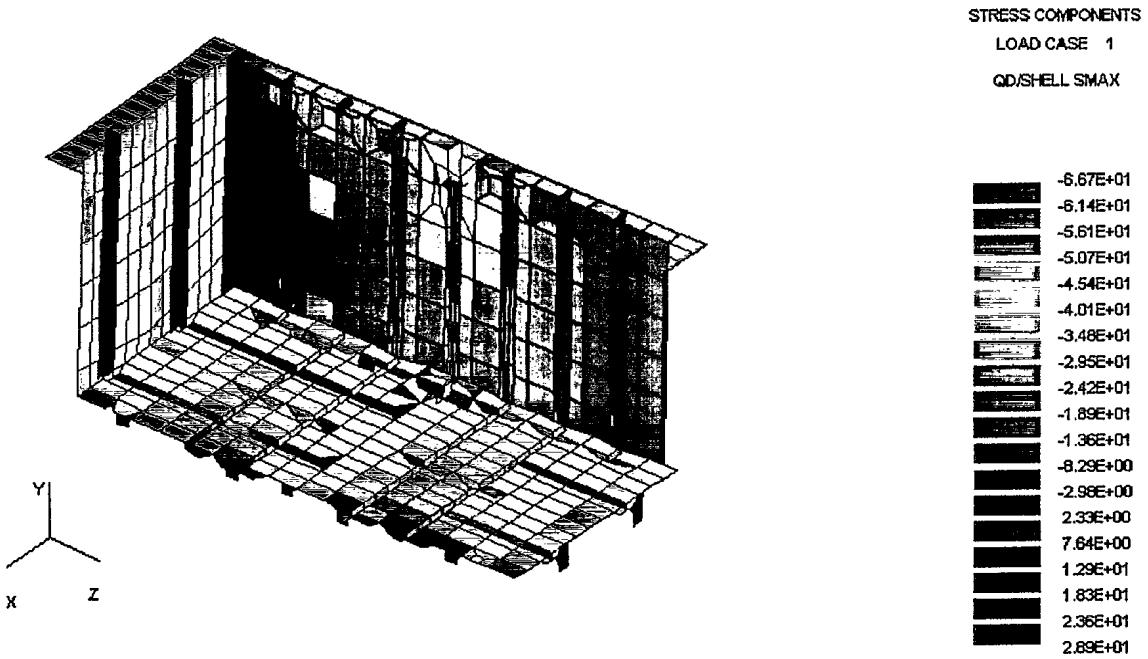

Figure 66: Hogging Stresses (MPa) in the Empty Gray Water Tank

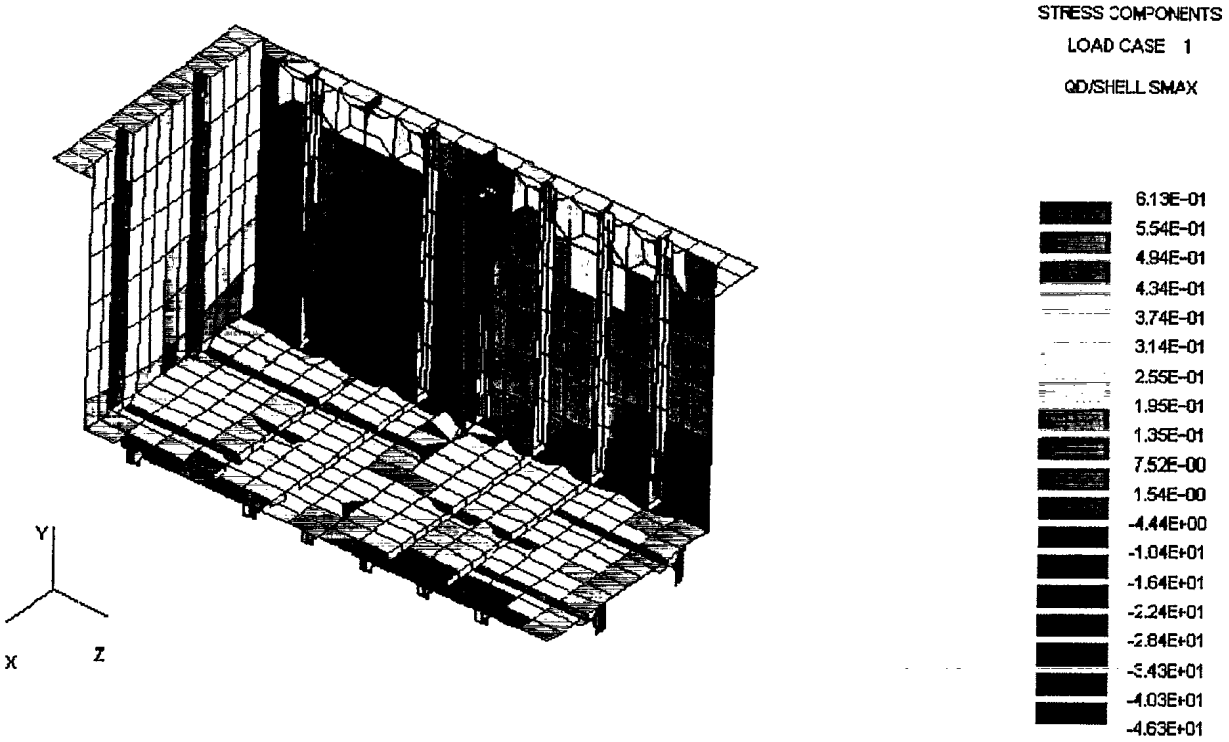

Figure 67: Hogging Stresses (MPa) in the Empty Gray Water Tank

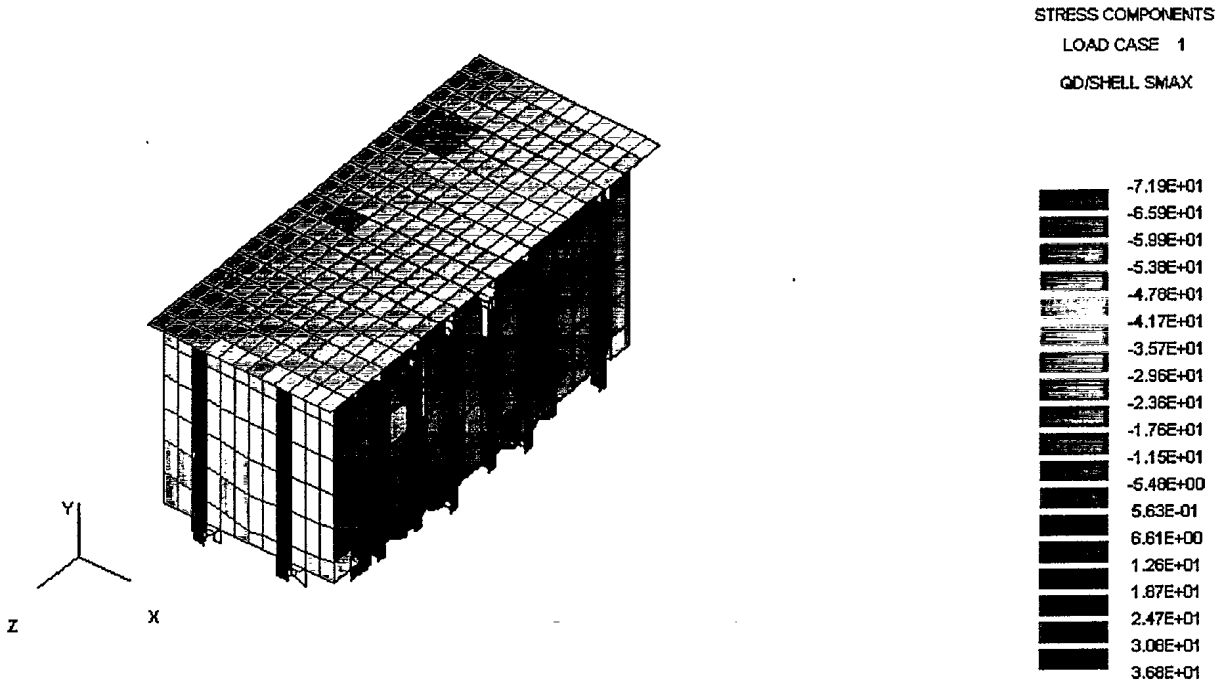

Figure 68: Hogging Plus Fluid Load Stresses (MPa) in the Port Side of the Gray Water Tank

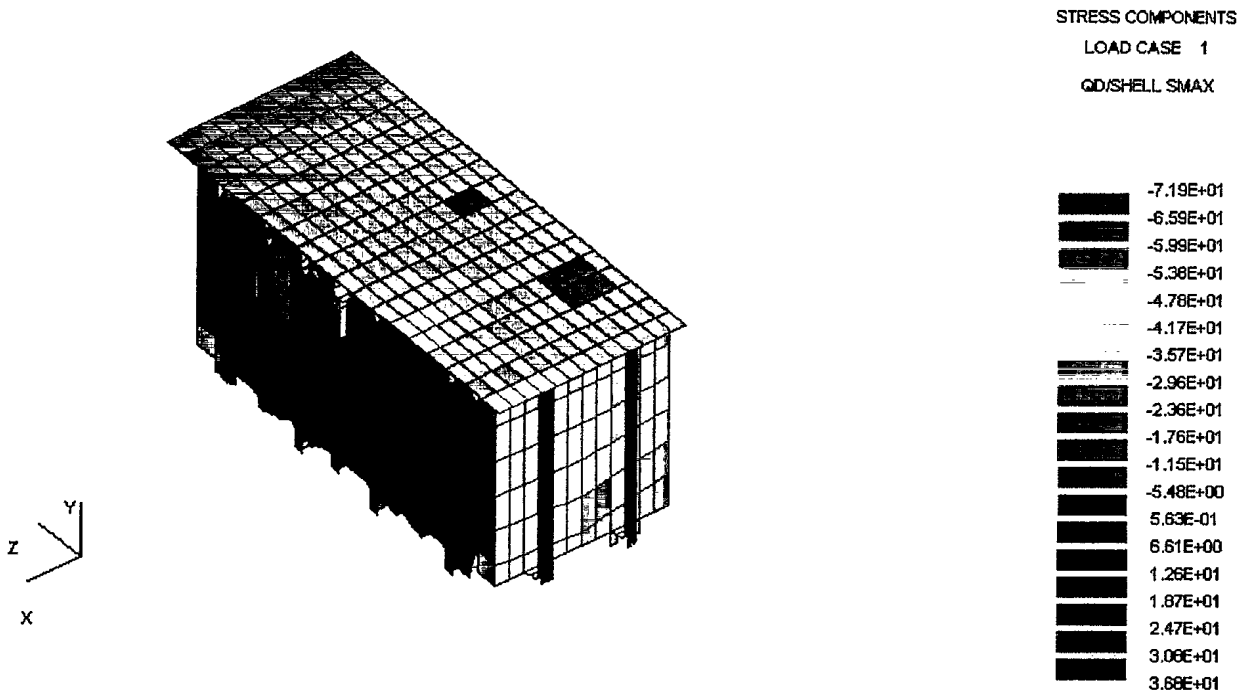

Figure 69: Hogging Plus Fluid Stresses (MPa) in the Starboard Side of the Gray Water Tank

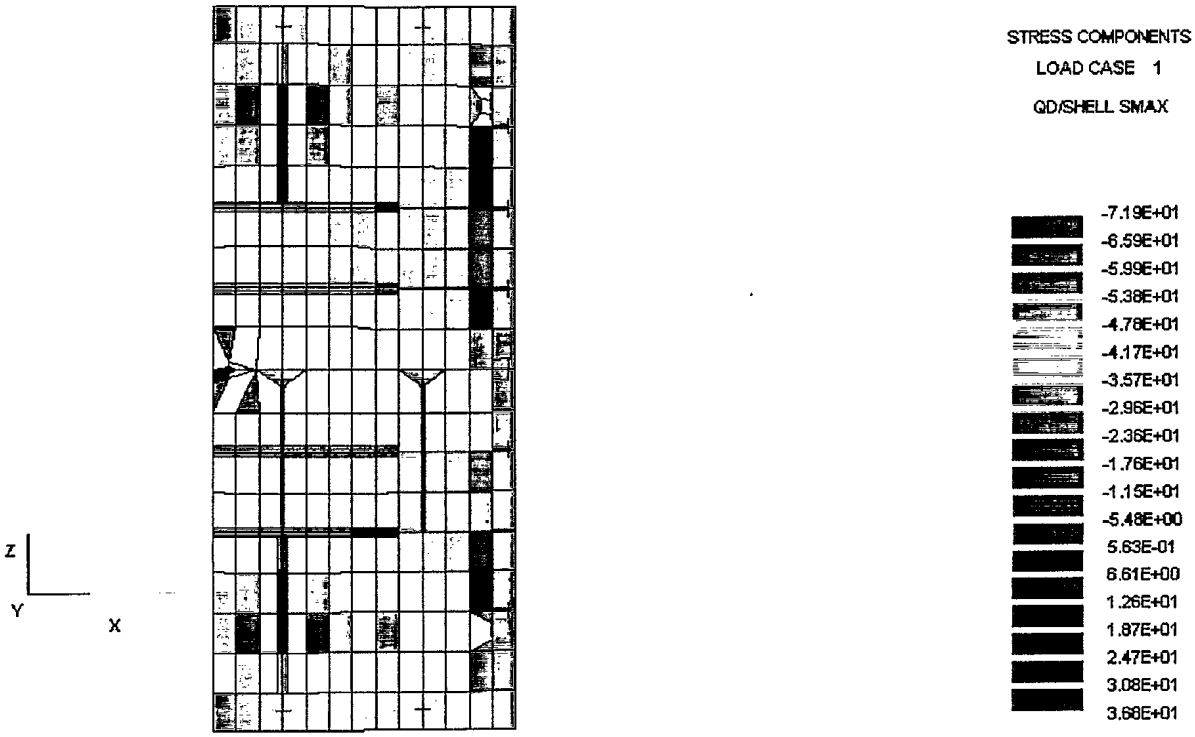

Figure 70: Hogging Plus Fluid Load Stresses (MPa) in the Bottom of the Gray Water Tank

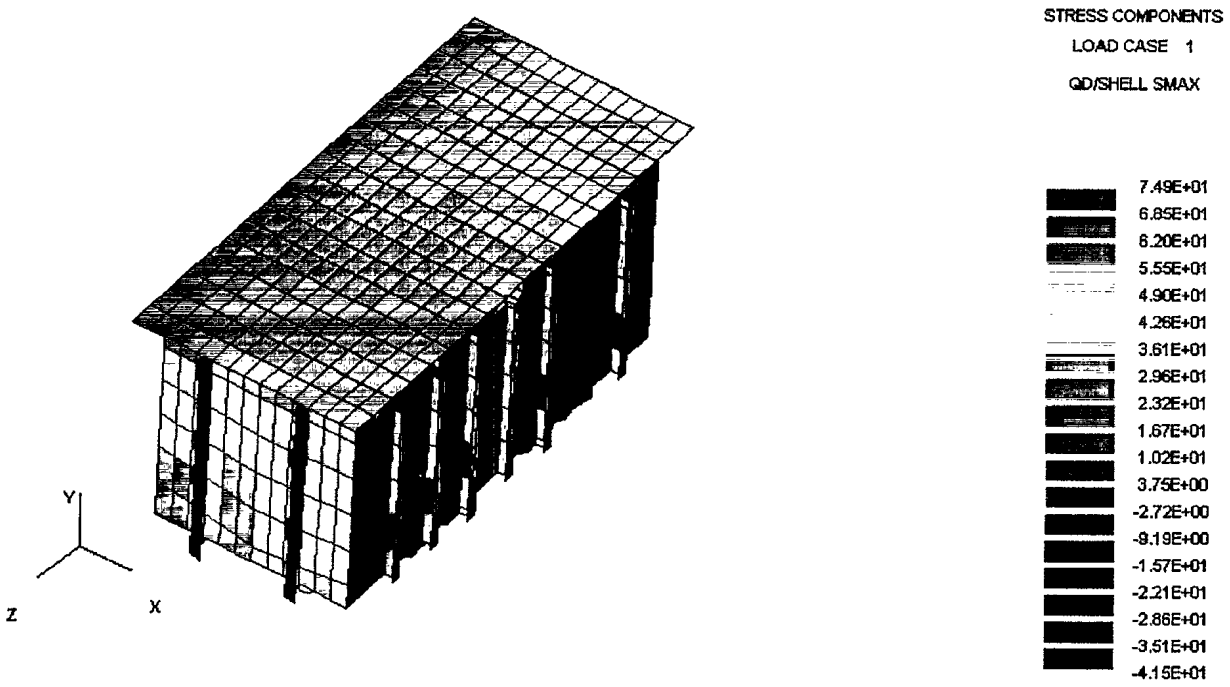

Figure 71: Sagging Plus Fluid Load Stresses (MPa) in the Port Side of the Gray Water Tank

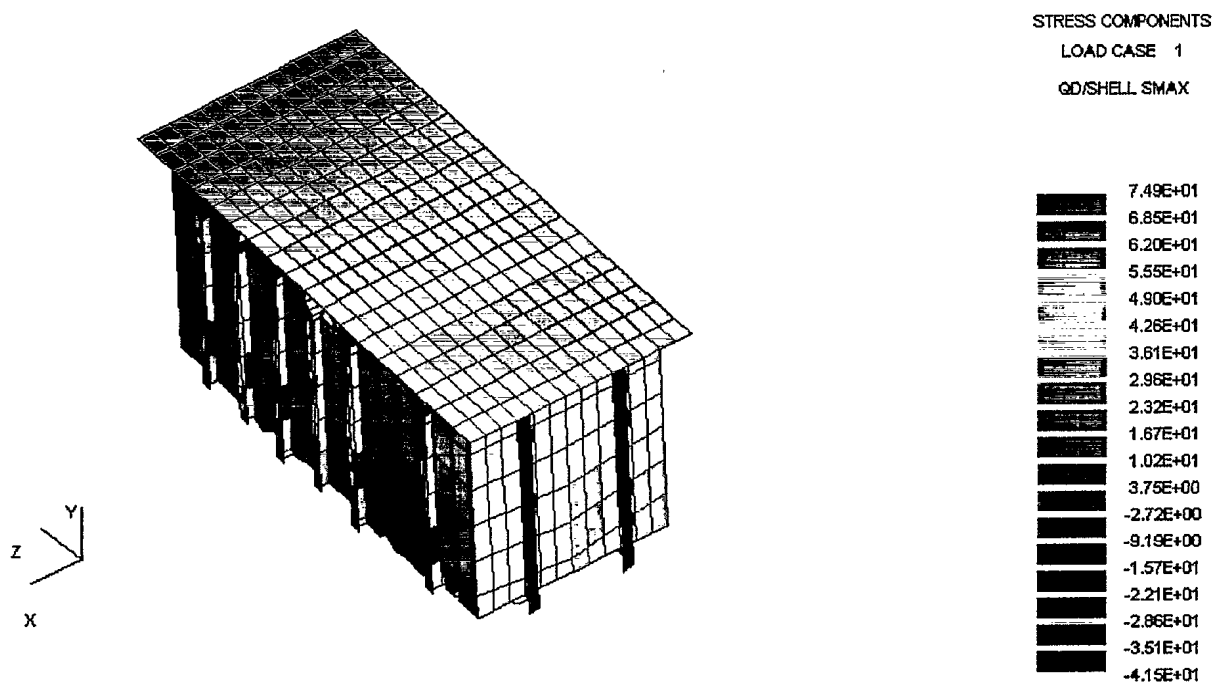

Figure 72: Sagging Plus Fluid Load Stresses (MPa) in the Starboard Side of the Gray Water Tank

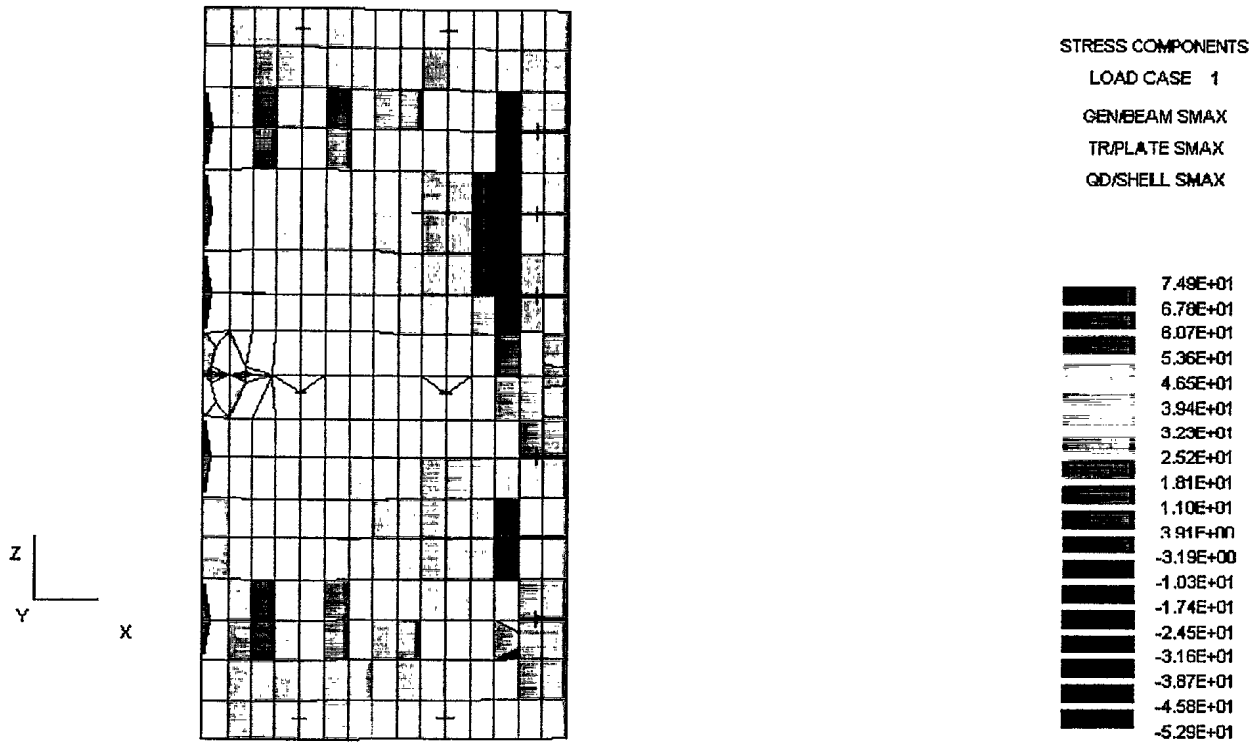

Figure 73: Sagging Plus Fluid Load Stresses (MPa) in the Bottom of the Gray Water Tank

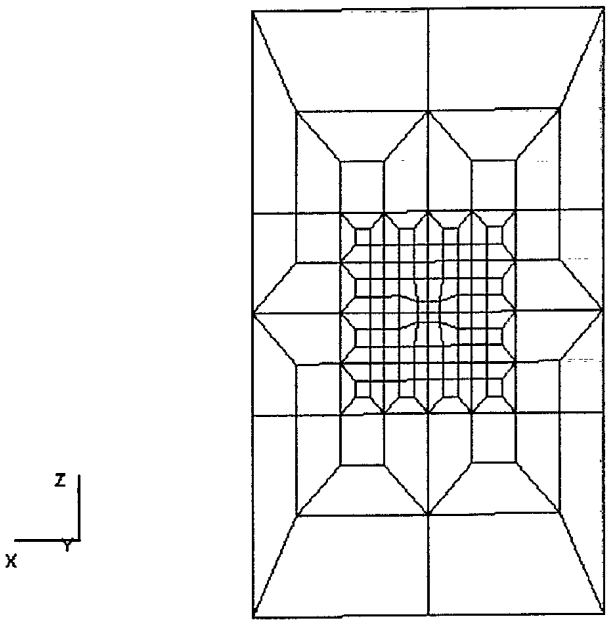

Figure 74: A Corrosion Pit Formed Using Elements to Effect the Transition Between the Coarse and Fine Grids

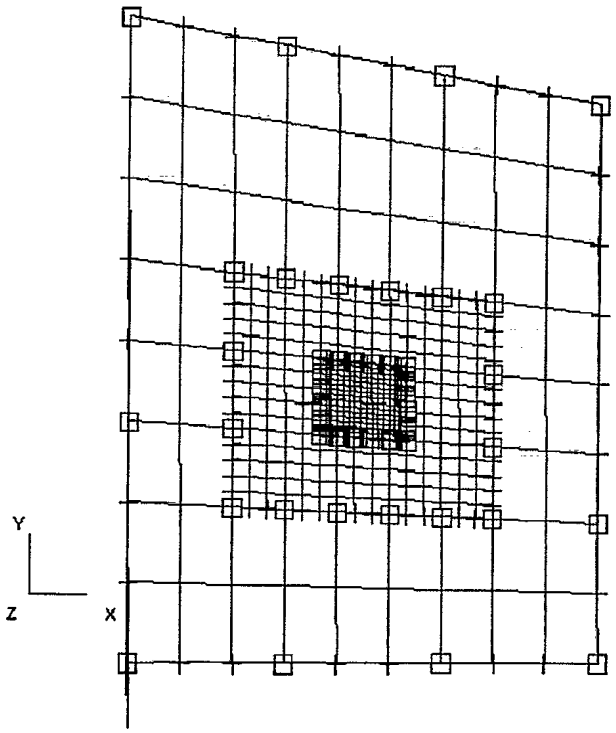

Figure 75: A Corrosion Pit Formed in the Port Side Using Multi-point Constraints to Accomplish the Transition Between Coarse and Fine Grid

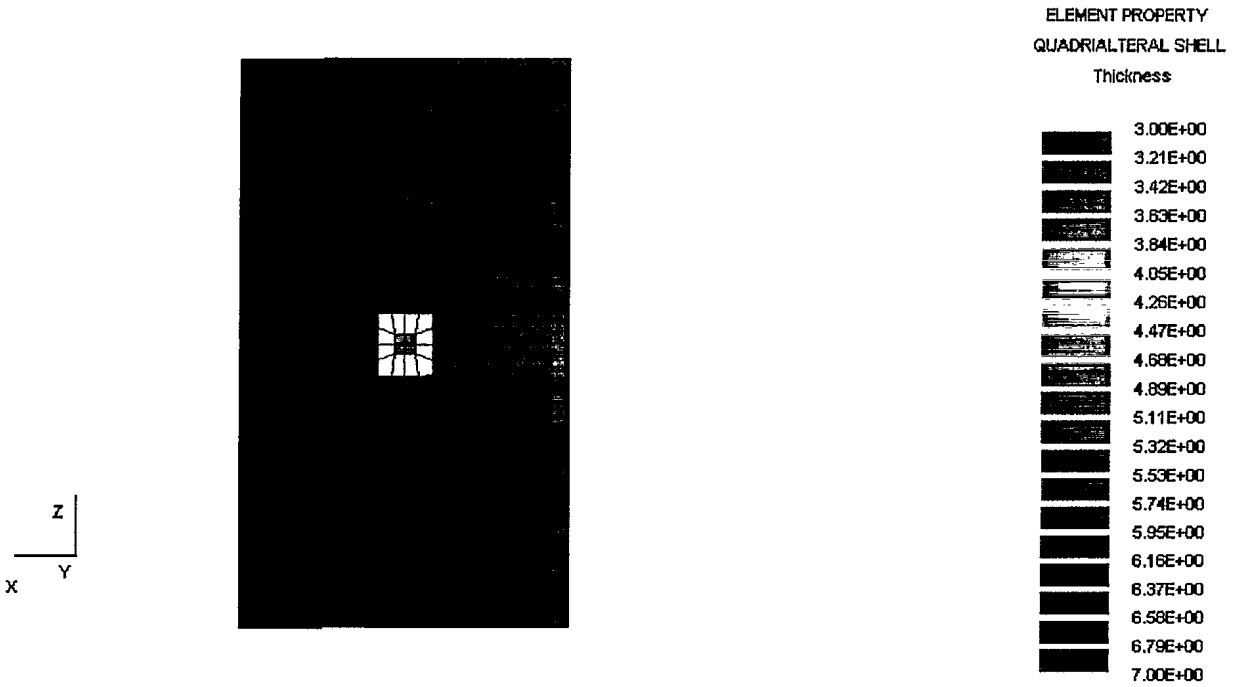

Figure 76: A Typical Element Grid Showing the Variation in the Plate Thickness in the Corrosion Pit in the Bottom of the Gray Water Tank

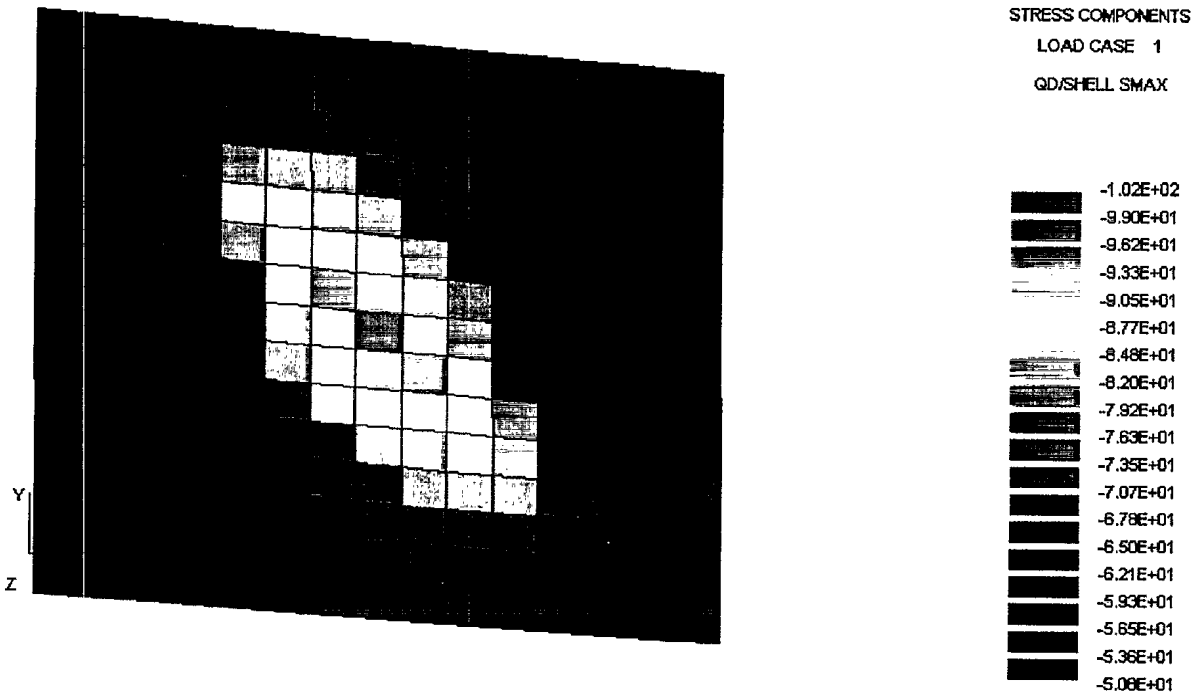

Figure 77: Hogging Plus Fluid Load Stresses (MPa) in the Corrosion Pit, Port Side of the Gray Water Tank, Using Multi-point Constraints

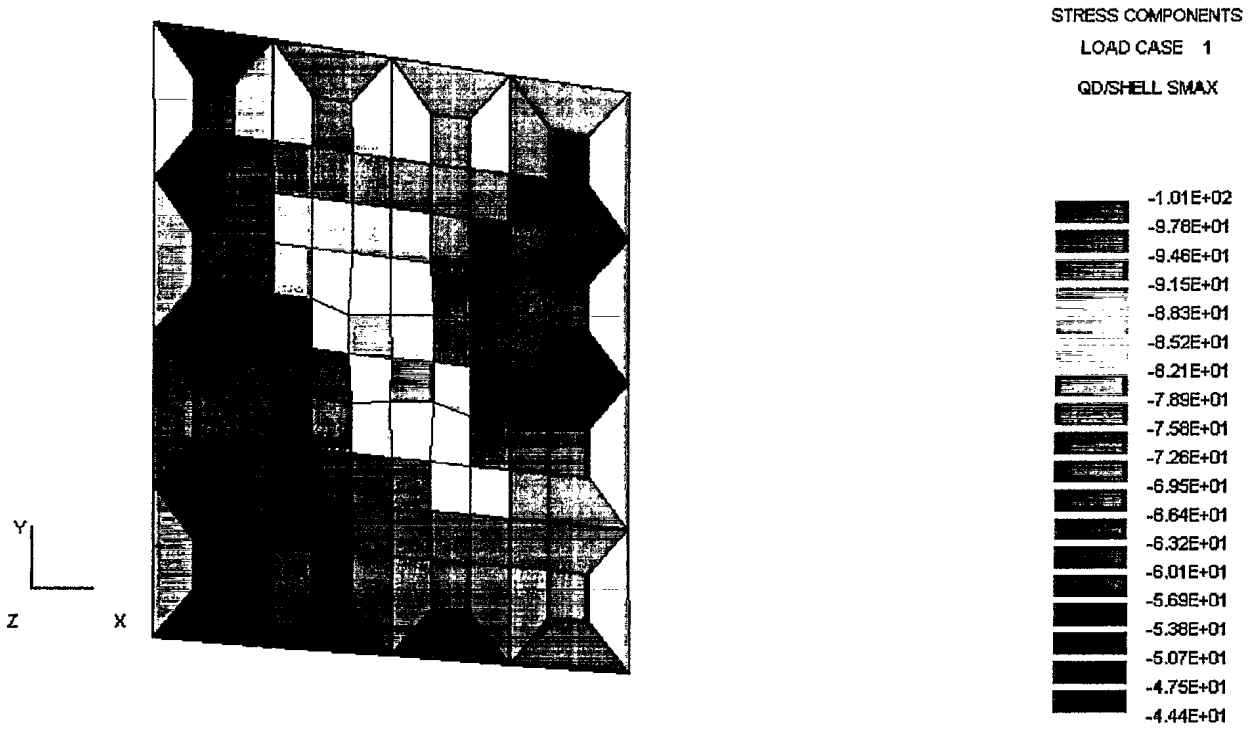

Figure 78: Hogging Plus Fluid Load Stresses (MPa) in the Corrosion Pit Starboard Side of the Gray Water Tank

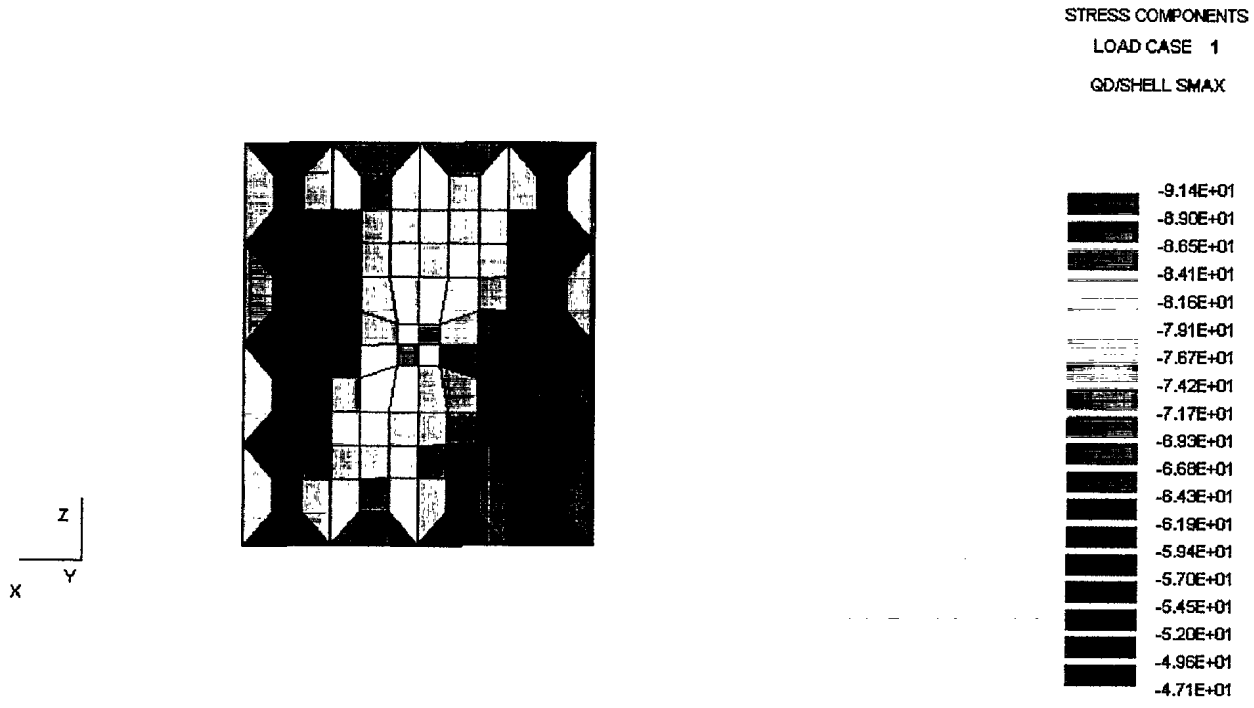

Figure 79: Hogging Plus Fluid Load Stresses (MPa) in the Corrosion Pit in Bottom of the Gray Water Tank

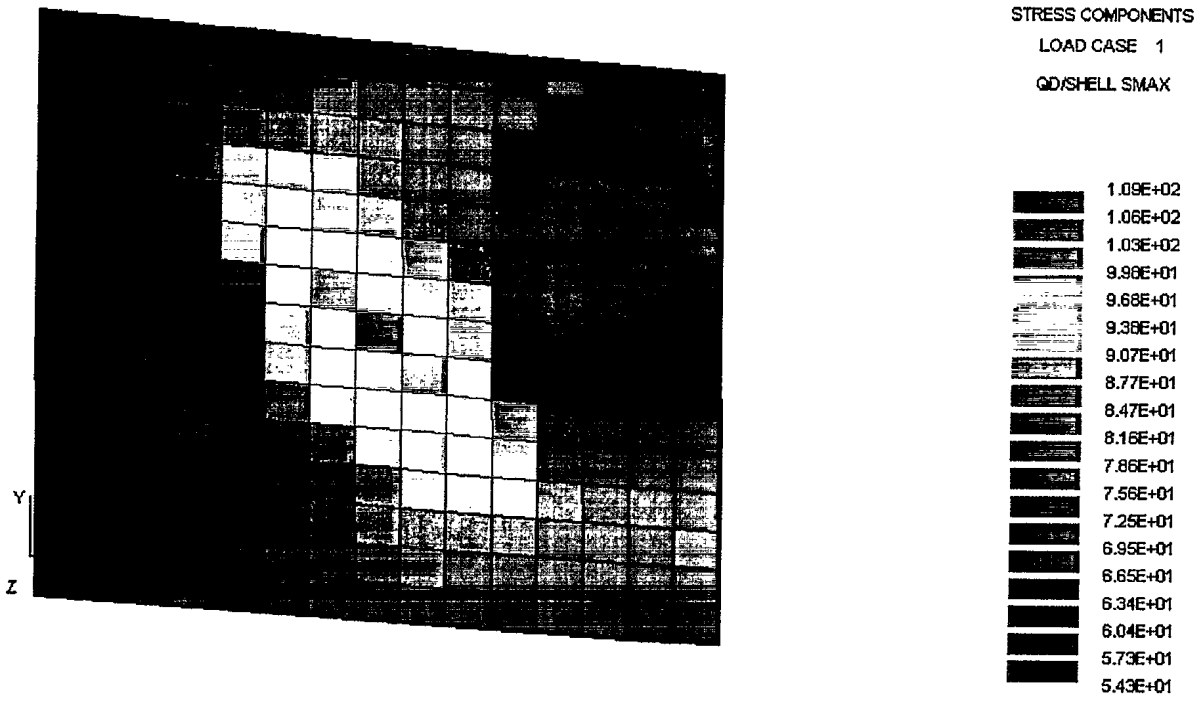

Figure 80: Sagging Plus Fluid Load Stresses (MPa)in the Corrosion Pit, Port Side of the Gray Water Tank, Using Multi-point Constraint

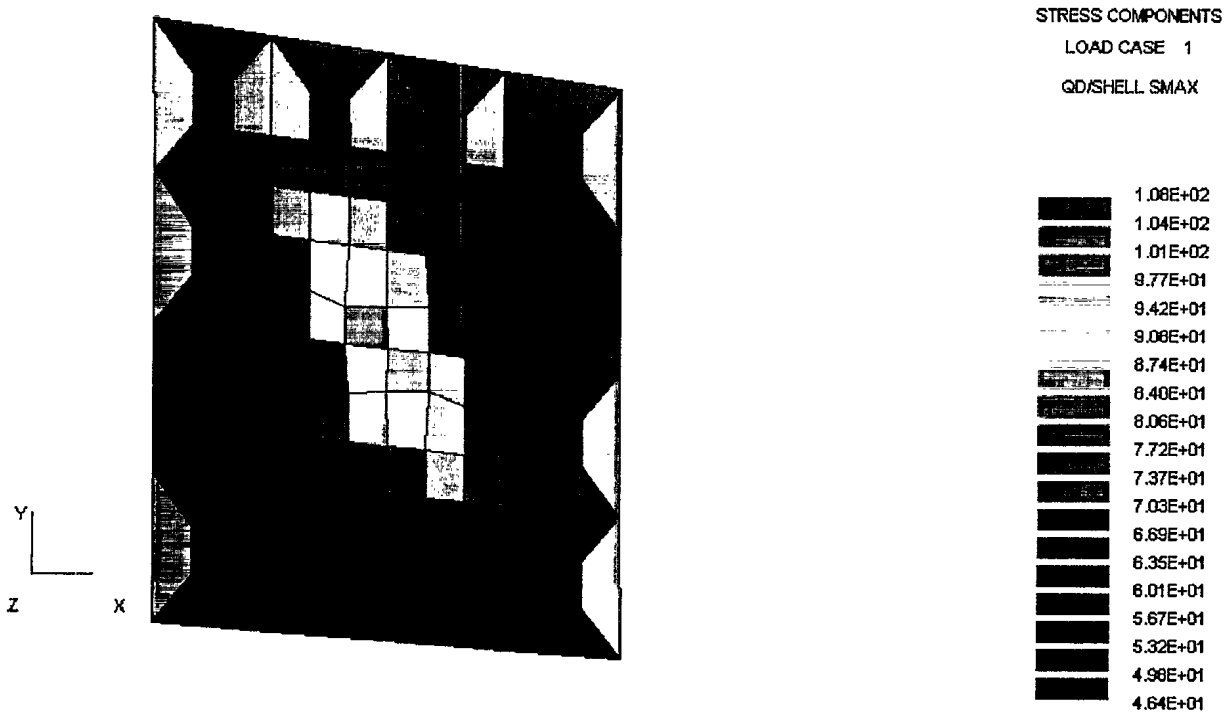

Figure 81: Sagging Plus Fluid Load Stresses (MPa) in the Corrosion Pit Starboard Side of the Gray Water Tank

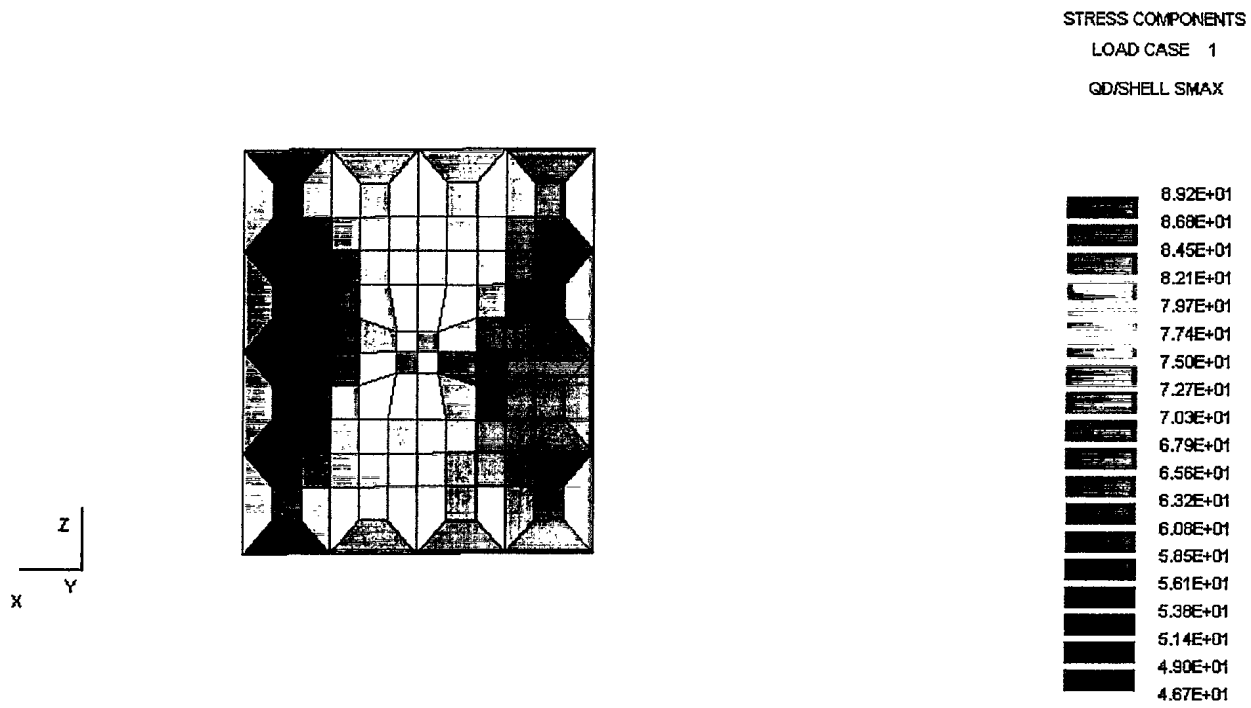

Figure 82: Sagging Plus Fluid Load Stresses (MPa) in the Corrosion Pit in Bottom of the Gray Water Tank

A CPF MAESTRO Load File (Deep Hog)

```
LOADSET 1  " DRAFT = 2.789 M"
N  1.0
IMMERSION  2789.0  0.0  1.1382  WAVE  -4000.00  124000.00  180.0  0.0
0  0  0
0  0  0
0  0  0
0  0  0
0  0  0
0  0  0
0  0  0
0  0  0
0  0  0
0  0  0
0  0  0
0  0  0
0  0  0
0  0  0
0  0  0
0  0  0
LOADSET 2  " WEIGHT ONLY"
N  1.0
0  0  0                                                    ! ( SS1-M1)
WEIGHT
   0   9  21  33  45  58  34  4
  41  77 114 151
4  0  0                                                    ! ( SS1-M2)
 12  1  0.0   -34421.0  0.0
 12  2  0.0   -34421.0  0.0
 13  1  0.0   -34421.0  0.0
 13  2  0.0   -34421.0  0.0
WEIGHT
 142  60  98 137 175 214
0  26  0                                                   ! ( SS1-M3)
$ ITEM 21, DFO NO. 1
DATUM    23   4100   10  13   ,  -8.335E-06
DATUM    22   4100   10  13   ,  -8.335E-06
DATUM    96   4100   10  13   ,  -8.335E-06
DATUM   100   4100   10  13   ,  -8.335E-06
DATUM   104   4100   10  13   ,  -8.335E-06
DATUM   106   4100   10  13   ,  -8.335E-06
$ ITEM 23, DFO NO. 1
DATUM    20   4100   10  13   ,  -8.335E-06
DATUM    21   4100   10  13   ,  -8.335E-06
DATUM    98   4100   10  13   ,  -8.335E-06
DATUM   102   4100   10  13   ,  -8.335E-06
```

```
DATUM   105   4100   10  13   ,  -8.335E-06
DATUM   107   4100   10  13   ,  -8.335E-06
$ ITEM 20, DFO NO. 2
DATUM    94   2600    1   1   ,  -8.335E-06
DATUM    97   2600    1   1   ,  -8.335E-06
DATUM    22   2600    2   9   ,  -8.335E-06
DATUM    96   2600    2   9   ,  -8.335E-06
DATUM   100   2600    2   9   ,  -8.335E-06
DATUM   104   2600    2   9   ,  -8.335E-06
DATUM   106   2600    1   9   ,  -8.335E-06
$ ITEM 22, DFO NO. 2
DATUM    95   2600    1   1   ,  -8.335E-06
DATUM    99   2600    1   1   ,  -8.335E-06
DATUM    21   2600    2   9   ,  -8.335E-06
DATUM    98   2600    2   9   ,  -8.335E-06
DATUM   102   2600    2   9   ,  -8.335E-06
DATUM   105   2600    2   9   ,  -8.335E-06
DATUM   107   2600    1   9   ,  -8.335E-06
WEIGHT
 240  54  96 138 179  250  292  127
 127  171  216  260  304
6  40  0                                                  ! ( SS1-M4)
 28  6  0.0   -23572.0  0.0
 28  8  0.0   -23572.0  0.0
 28 10  0.0   -23572.0  0.0
 54  6  0.0   -23572.0  0.0
 54  8  0.0   -23572.0  0.0
 54 10  0.0   -23572.0  0.0
$ ITEM 24, DFO NO.3
DATUM    28   3700    1   4   ,  -8.335E-06
DATUM   113   3700    1   4   ,  -8.335E-06
DATUM   114   3700    1   4   ,  -8.335E-06
DATUM   139   3700    1   4   ,  -8.335E-06
DATUM    97   3700    1   4   ,  -8.335E-06
DATUM    29   3700    2   4   ,  -8.335E-06
DATUM   111   3700    1   2   ,  -8.335E-06
DATUM   129   3700    3   4   ,  -8.335E-06
DATUM    23   3700    3   4   ,   8.335E-06
$ ITEM 25, DFO NO.4
DATUM    31   3700    1   4   ,  -8.335E-06
DATUM   116   3700    1   4   ,  -8.335E-06
DATUM   117   3700    1   4   ,  -8.335E-06
DATUM   137   3700    1   4   ,  -8.335E-06
DATUM    98   3700    1   4   ,  -8.335E-06
DATUM   121   3700    1   4   ,   8.335E-06
DATUM   110   3700    1   2   ,  -8.335E-06
DATUM   138   3700    2   4   ,  -8.335E-06
DATUM    24   3700    2   4   ,   8.335E-06
$ ITEM 26, DFO NO. 5
```

```
DATUM    130   1020   5  17   ,  -8.335E-06
DATUM     29   1020   5  17   ,  -8.335E-06
DATUM    139   1020   5  17   ,  -8.335E-06
DATUM    141   1020   5  17   ,  -8.335E-06
DATUM    142   1020   5  17   ,  -8.335E-06
$ ITEM 27, DFO NO. 5
DATUM    112   4150  13  17   ,  -8.335E-06
DATUM    113   4150  13  17   ,  -8.335E-06
DATUM    114   4150  13  17   ,  -8.335E-06
DATUM    130   4150  13  17   ,  -8.335E-06
DATUM    148   4150  13  17   ,   8.335E-06
DATUM    146   4150  13  17   ,  -8.335E-06
$ ITEM 28, DFO NO. 6
DATUM    131   1020   5  17   ,  -8.335E-06
DATUM    138   1020   5  17   ,  -8.335E-06
DATUM    137   1020   5  17   ,  -8.335E-06
DATUM    133   1020   5  17   ,  -8.335E-06
DATUM     30   1200   5  17   ,  -8.335E-06
$ ITEM 29, DFO NO. 6
DATUM    115   4150  13  17   ,  -8.335E-06
DATUM    116   4150  13  17   ,  -8.335E-06
DATUM    117   4150  13  17   ,  -8.335E-06
DATUM    147   4150  13  17   ,  -8.335E-06
DATUM    149   4150  13  17   ,   8.335E-06
DATUM    131   4150  13  17   ,  -8.335E-06
WEIGHT
 307  303  321  338  355  373  362  326
 334  342  350  359  343  250  312  374
 436
4  22  0                                          ! ( SS1-M5)
 49  3  0.0  -103309.0  0.0
 49  5  0.0  -103309.0  0.0
 50  3  0.0  -103309.0  0.0
 50  5  0.0  -103309.0  0.0
$ITEM 30, DFO NO. 7
DATUM     64   1270   ,   ,   ,  -8.335E-06
DATUM     25   1270   ,   ,   ,  -8.335E-06
DATUM     24   1270   ,   ,   ,  -8.335E-06
DATUM     29   1270   ,   ,   ,  -8.335E-06
DATUM     42   1270   ,   ,   ,  -8.335E-06
DATUM     55   1270   ,   ,   ,  -8.335E-06
DATUM     56   1270   ,   ,   ,  -8.335E-06
DATUM     41   1270   ,   ,   ,  -8.335E-06
DATUM     40   1270   ,   ,   ,  -8.335E-06
DATUM     62   1270   ,   ,   ,  -8.335E-06
DATUM     60   1270   ,   ,   ,  -8.335E-06
$ITEM 31, DFO NO. 8
DATUM     65   1270   ,   ,   ,  -8.335E-06
DATUM     26   1270   ,   ,   ,  -8.335E-06
```

```
DATUM    27   1270   ,   ,    ,  -8.335E-06
DATUM    35   1270   ,   ,    ,  -8.335E-06
DATUM    43   1270   ,   ,    ,  -8.335E-06
DATUM    57   1270   ,   ,    ,  -8.335E-06
DATUM    58   1270   ,   ,    ,  -8.335E-06
DATUM    44   1270   ,   ,    ,  -8.335E-06
DATUM    45   1270   ,   ,    ,  -8.335E-06
DATUM    63   1270   ,   ,    ,  -8.335E-06
DATUM    61   1270   ,   ,    ,  -8.335E-06
WEIGHT
498  560  453  436  429  423  416  410
428  421
176  10  0                                                    ! ( SS1-M6)
 34 10  0.0   -65974.0  0.0
 34 11  0.0   -65974.0  0.0
 34 12  0.0   -65974.0  0.0
 34 13  0.0   -65974.0  0.0
 34 14  0.0   -65974.0  0.0
 36 10  0.0   -65974.0  0.0
 36 11  0.0   -65974.0  0.0
 36 12  0.0   -65974.0  0.0
 36 13  0.0   -65974.0  0.0
 36 14  0.0   -65974.0  0.0
 38 10  0.0   -65974.0  0.0
 38 11  0.0   -65974.0  0.0
 38 12  0.0   -65974.0  0.0
 38 13  0.0   -65974.0  0.0
 38 14  0.0   -65974.0  0.0
 40 10  0.0   -65974.0  0.0
 40 11  0.0   -65974.0  0.0
 40 12  0.0   -65974.0  0.0
 40 13  0.0   -65974.0  0.0
 40 14  0.0   -65974.0  0.0
 35  2  0.0   -25153.0  0.0
 35  3  0.0   -25153.0  0.0
 35  4  0.0   -25153.0  0.0
 35  5  0.0   -25153.0  0.0
 35  6  0.0   -25153.0  0.0
 35  7  0.0   -25153.0  0.0
 35  8  0.0   -25153.0  0.0
 35  9  0.0   -25153.0  0.0
 36  2  0.0   -25153.0  0.0
 36  3  0.0   -25153.0  0.0
 36  5  0.0   -25153.0  0.0
 36  6  0.0   -25153.0  0.0
 36  7  0.0   -25153.0  0.0
 36  8  0.0   -25153.0  0.0
 36  9  0.0   -25153.0  0.0
 38  2  0.0   -25153.0  0.0
```

```
38  3  0.0   -25153.0  0.0
38  5  0.0   -25153.0  0.0
38  6  0.0   -25153.0  0.0
38  7  0.0   -25153.0  0.0
38  8  0.0   -25153.0  0.0
38  9  0.0   -25153.0  0.0
39  2  0.0   -25153.0  0.0
39  3  0.0   -25153.0  0.0
39  4  0.0   -25153.0  0.0
39  5  0.0   -25153.0  0.0
39  6  0.0   -25153.0  0.0
39  7  0.0   -25153.0  0.0
39  8  0.0   -25153.0  0.0
39  9  0.0   -25153.0  0.0
34  0  0.0    -4004.0  0.0
34  1  0.0    -4004.0  0.0
34  2  0.0    -4004.0  0.0
34  3  0.0    -4004.0  0.0
34  4  0.0    -4004.0  0.0
34  5  0.0    -4004.0  0.0
34  6  0.0    -4004.0  0.0
34  7  0.0    -4004.0  0.0
34  8  0.0    -4004.0  0.0
34  9  0.0    -4004.0  0.0
34 10  0.0    -4004.0  0.0
34 11  0.0    -4004.0  0.0
34 12  0.0    -4004.0  0.0
34 13  0.0    -4004.0  0.0
34 14  0.0    -4004.0  0.0
34 15  0.0    -4004.0  0.0
34 16  0.0    -4004.0  0.0
34 17  0.0    -4004.0  0.0
35  0  0.0    -4004.0  0.0
35  1  0.0    -4004.0  0.0
35  2  0.0    -4004.0  0.0
35  3  0.0    -4004.0  0.0
35  4  0.0    -4004.0  0.0
35  5  0.0    -4004.0  0.0
35  6  0.0    -4004.0  0.0
35  7  0.0    -4004.0  0.0
35  8  0.0    -4004.0  0.0
35  9  0.0    -4004.0  0.0
35 10  0.0    -4004.0  0.0
35 11  0.0    -4004.0  0.0
35 12  0.0    -4004.0  0.0
35 13  0.0    -4004.0  0.0
35 14  0.0    -4004.0  0.0
35 15  0.0    -4004.0  0.0
35 16  0.0    -4004.0  0.0
```

```
35 17  0.0    -4004.0  0.0
36  0  0.0    -4004.0  0.0
36  1  0.0    -4004.0  0.0
36  2  0.0    -4004.0  0.0
36  3  0.0    -4004.0  0.0
36  4  0.0    -4004.0  0.0
36  5  0.0    -4004.0  0.0
36  6  0.0    -4004.0  0.0
36  7  0.0    -4004.0  0.0
36  8  0.0    -4004.0  0.0
36  9  0.0    -4004.0  0.0
36 10  0.0    -4004.0  0.0
36 11  0.0    -4004.0  0.0
36 12  0.0    -4004.0  0.0
36 13  0.0    -4004.0  0.0
36 14  0.0    -4004.0  0.0
36 15  0.0    -4004.0  0.0
36 16  0.0    -4004.0  0.0
36 17  0.0    -4004.0  0.0
37  0  0.0    -4004.0  0.0
37  1  0.0    -4004.0  0.0
37  2  0.0    -4004.0  0.0
37  3  0.0    -4004.0  0.0
37  4  0.0    -4004.0  0.0
37  5  0.0    -4004.0  0.0
37  6  0.0    -4004.0  0.0
37  7  0.0    -4004.0  0.0
37  8  0.0    -4004.0  0.0
37  9  0.0    -4004.0  0.0
37 10  0.0    -4004.0  0.0
37 11  0.0    -4004.0  0.0
37 12  0.0    -4004.0  0.0
37 13  0.0    -4004.0  0.0
37 14  0.0    -4004.0  0.0
37 15  0.0    -4004.0  0.0
37 16  0.0    -4004.0  0.0
37 17  0.0    -4004.0  0.0
38  0  0.0    -4004.0  0.0
38  1  0.0    -4004.0  0.0
38  2  0.0    -4004.0  0.0
38  3  0.0    -4004.0  0.0
38  4  0.0    -4004.0  0.0
38  5  0.0    -4004.0  0.0
38  6  0.0    -4004.0  0.0
38  7  0.0    -4004.0  0.0
38  8  0.0    -4004.0  0.0
38  9  0.0    -4004.0  0.0
38 10  0.0    -4004.0  0.0
38 11  0.0    -4004.0  0.0
```

```
 38 12  0.0    -4004.0  0.0
 38 13  0.0    -4004.0  0.0
 38 14  0.0    -4004.0  0.0
 38 15  0.0    -4004.0  0.0
 38 16  0.0    -4004.0  0.0
 38 17  0.0    -4004.0  0.0
 39  0  0.0    -4004.0  0.0
 39  1  0.0    -4004.0  0.0
 39  2  0.0    -4004.0  0.0
 39  3  0.0    -4004.0  0.0
 39  4  0.0    -4004.0  0.0
 39  5  0.0    -4004.0  0.0
 39  6  0.0    -4004.0  0.0
 39  7  0.0    -4004.0  0.0
 39  8  0.0    -4004.0  0.0
 39  9  0.0    -4004.0  0.0
 39 10  0.0    -4004.0  0.0
 39 11  0.0    -4004.0  0.0
 39 12  0.0    -4004.0  0.0
 39 13  0.0    -4004.0  0.0
 39 14  0.0    -4004.0  0.0
 39 15  0.0    -4004.0  0.0
 39 16  0.0    -4004.0  0.0
 39 17  0.0    -4004.0  0.0
 40  0  0.0    -4004.0  0.0
 40  1  0.0    -4004.0  0.0
 40  2  0.0    -4004.0  0.0
 40  3  0.0    -4004.0  0.0
 40  4  0.0    -4004.0  0.0
 40  5  0.0    -4004.0  0.0
 40  6  0.0    -4004.0  0.0
 40  7  0.0    -4004.0  0.0
 40  8  0.0    -4004.0  0.0
 40  9  0.0    -4004.0  0.0
 40 10  0.0    -4004.0  0.0
 40 11  0.0    -4004.0  0.0
 40 12  0.0    -4004.0  0.0
 40 13  0.0    -4004.0  0.0
 40 14  0.0    -4004.0  0.0
 40 15  0.0    -4004.0  0.0
 40 16  0.0    -4004.0  0.0
 40 17  0.0    -4004.0  0.0
$ ITEM 36, DFO SERV. NO.1
DATUM    20   3325   1   7    ,  -8.335E-06
DATUM    74   3325   1   7    ,  -8.335E-06
DATUM    75   3325   1   7    ,  -8.335E-06
DATUM    71   3325   1   7    ,  -8.335E-06
DATUM    32   3325   1   7    ,  -8.335E-06
$ ITEM 37, DFO SERV. NO.2
```

```
DATUM    78   3325   1   7    ,  -8.335E-06
DATUM    77   3325   1   7    ,  -8.335E-06
DATUM    76   3325   1   7    ,  -8.335E-06
DATUM    48   3325   1   7    ,  -8.335E-06
DATUM    70   3325   1   7    ,  -8.335E-06
WEIGHT
402  383  364  345  382  429  451  439
427  415  388  443  455  456  457  459
459
90  0  0                                                    ! ( SS2-M1)
 27  9  0.0   -73158.0  0.0
 31  9  0.0   -73158.0  0.0
 28  1  0.0   -41311.0  0.0
 28  2  0.0   -41311.0  0.0
 28  3  0.0   -41311.0  0.0
 28  4  0.0   -41311.0  0.0
 28  5  0.0   -41311.0  0.0
 28  6  0.0   -41311.0  0.0
 28  7  0.0   -41311.0  0.0
 28  8  0.0   -41311.0  0.0
 28  9  0.0   -41311.0  0.0
 30  1  0.0   -41311.0  0.0
 30  2  0.0   -41311.0  0.0
 30  3  0.0   -41311.0  0.0
 30  4  0.0   -41311.0  0.0
 30  5  0.0   -41311.0  0.0
 30  6  0.0   -41311.0  0.0
 30  7  0.0   -41311.0  0.0
 30  8  0.0   -41311.0  0.0
 30  9  0.0   -41311.0  0.0
 26  1  0.0    -4004.0  0.0
 26  2  0.0    -4004.0  0.0
 26  3  0.0    -4004.0  0.0
 26  4  0.0    -4004.0  0.0
 26  5  0.0    -4004.0  0.0
 26  6  0.0    -4004.0  0.0
 26  7  0.0    -4004.0  0.0
 26  8  0.0    -4004.0  0.0
 26  9  0.0    -4004.0  0.0
 26 10  0.0    -4004.0  0.0
 27 1  0.0    -4004.0  0.0
 27 2  0.0    -4004.0  0.0
 27  3  0.0    -4004.0  0.0
 27  4  0.0    -4004.0  0.0
 27  5  0.0    -4004.0  0.0
 27  6  0.0    -4004.0  0.0
 27  7  0.0    -4004.0  0.0
 27  8  0.0    -4004.0  0.0
 27  9  0.0    -4004.0  0.0
```

```
26 10  0.0    -4004.0  0.0
28  1  0.0    -4004.0  0.0
28  2  0.0    -4004.0  0.0
28  3  0.0    -4004.0  0.0
28  4  0.0    -4004.0  0.0
28  5  0.0    -4004.0  0.0
28  6  0.0    -4004.0  0.0
28  7  0.0    -4004.0  0.0
28  8  0.0    -4004.0  0.0
28  9  0.0    -4004.0  0.0
26 10  0.0    -4004.0  0.0
29  1  0.0    -4004.0  0.0
29  2  0.0    -4004.0  0.0
29  3  0.0    -4004.0  0.0
29  4  0.0    -4004.0  0.0
29  5  0.0    -4004.0  0.0
29  6  0.0    -4004.0  0.0
29  7  0.0    -4004.0  0.0
29  8  0.0    -4004.0  0.0
29  9  0.0    -4004.0  0.0
29 10  0.0    -4004.0  0.0
30  1  0.0    -4004.0  0.0
30  2  0.0    -4004.0  0.0
30  3  0.0    -4004.0  0.0
30  4  0.0    -4004.0  0.0
30  5  0.0    -4004.0  0.0
30  6  0.0    -4004.0  0.0
30  7  0.0    -4004.0  0.0
30  8  0.0    -4004.0  0.0
30  9  0.0    -4004.0  0.0
30 10  0.0    -4004.0  0.0
31  1  0.0    -4004.0  0.0
31  2  0.0    -4004.0  0.0
31  3  0.0    -4004.0  0.0
31  4  0.0    -4004.0  0.0
31  5  0.0    -4004.0  0.0
31  6  0.0    -4004.0  0.0
31  7  0.0    -4004.0  0.0
31  8  0.0    -4004.0  0.0
31  9  0.0    -4004.0  0.0
31 10  0.0    -4004.0  0.0
32  1  0.0    -4004.0  0.0
32  2  0.0    -4004.0  0.0
32  3  0.0    -4004.0  0.0
32  4  0.0    -4004.0  0.0
32  5  0.0    -4004.0  0.0
32  6  0.0    -4004.0  0.0
32  7  0.0    -4004.0  0.0
32  8  0.0    -4004.0  0.0
```

```
 32  9  0.0    -4004.0  0.0
 32 10  0.0    -4004.0  0.0
WEIGHT
 427  422  418  413  409  404  420  417
 408  399
3  14  0                                                    ! ( SS2-M2)
 29  3  0.0  -137745.0  0.0
 29  4  0.0  -137745.0  0.0
 29  5  0.0  -137745.0  0.0
$ ITEM 38, DFO SETTLING NO. 1
DATUM    92   1220    ,  ,  ,  -8.335E-06
DATUM    96   1220    1  1  ,  -8.335E-06
DATUM    91   1220    2  8  ,  -8.335E-06
DATUM    95   1220    1  1  ,  -8.335E-06
DATUM    31   1220    2  8  ,  -8.335E-06
DATUM    30   1220    1  7  ,  -8.335E-06
DATUM    35   1220    ,  ,  ,  -8.335E-06
$ ITEM 39, DFO SETTLING NO. 2
DATUM    32   1220    ,  ,  ,  -8.335E-06
DATUM    97   1220    1  1  ,  -8.335E-06
DATUM    89   1220    2  8  ,  -8.335E-06
DATUM    98   1220    1  1  ,  -8.335E-06
DATUM    90   1220    2  8  ,  -8.335E-06
DATUM    33   1220    1  7  ,  -8.335E-06
DATUM    35   1220    ,  ,  ,  -8.335E-06
WEIGHT
 399  390  457  488  460  432  403  375
2  34  0                                                    ! ( SS2-M3)
 31   2   0.00  -29332  0.00
 35   2   0.00  -29332  0.00
$ ITEM 32 & 33, DFO NO. 9
DATUM   118   3400    5    9  ,  -8.335E-06
DATUM   117   3400    5    9  ,  -8.335E-06
DATUM    35   3400    5    9  ,  -8.335E-06
DATUM   116   3400    5    9  ,  -8.335E-06
DATUM   115   3400    5    9  ,  -8.335E-06
DATUM    36   3400    5    9  ,  -8.335E-06
$ ITEM 18, FW NO.1
DATUM    48   3350    1   3   ,  -9.806E-06
DATUM    53   3350    5   8   ,  -9.806E-06
DATUM    32   3350    1   8   ,  -9.806E-06
DATUM    33   3350    1   8   ,  -9.806E-06
DATUM   114   3350    1   8   ,  -9.806E-06
DATUM   119   3350    1   8   ,  -9.806E-06
$ ITEM 19, FW NO.2
DATUM    52   3350    1   3   ,  -9.806E-06
DATUM    56   3350    5   8   ,  -9.806E-06
DATUM   120   3350    1   8   ,  -9.806E-06
DATUM   113   3350    1   8   ,  -9.806E-06
```

```
DATUM    43   3350    1   8   ,  -9.806E-06
DATUM    44   3350    1   8   ,  -9.806E-06
$ ITEM 40, JP-5 NO.1
DATUM   118   3610   10  12   ,  -8.335E-06
DATUM   117   3610   10  11   ,  -8.335E-06
DATUM    35   3610   10  12   ,  -8.335E-06
DATUM    34   3610   10  12   ,  -8.335E-06
DATUM   119   3610   10  11   ,  -8.335E-06
DATUM   114   3610   10  12   ,  -8.335E-06
DATUM    33   3610   10  11   ,  -8.335E-06
DATUM    32   3610   10  12   ,  -8.335E-06
$ ITEM 41, JP-5 NO.2
DATUM   116   3610   10  12   ,  -8.335E-06
DATUM   115   3610   10  11   ,  -8.335E-06
DATUM    36   3610   10  12   ,  -8.335E-06
DATUM    37   3610   10  12   ,  -8.335E-06
DATUM   120   3610   10  11   ,  -8.335E-06
DATUM   113   3610   10  12   ,  -8.335E-06
DATUM    44   3610   10  12   ,  -8.335E-06
DATUM    43   3610   10  11   ,  -8.335E-06
WEIGHT
 382  432  421  409  398  387  380  389
 363  337  311  285
4  8  0                                              ! ( SS2-M4)
 25   3   0.00  -54225.0  0.00
 25   4   0.00  -54225.0  0.00
 29   3   0.00  -54225.0  0.00
 29   4   0.00  -54225.0  0.00
$ ITEM 34, DFO NO.10
DATUM    27   3600   1   7   ,  -8.335E-06
DATUM    72   3600   1   7   ,  -8.335E-06
DATUM    28   3600   1   7   ,  -8.335E-06
DATUM    35   3600   1   7   ,  -8.335E-06
$ ITEM 35, DFO NO.10
DATUM    26   3600   1   7   ,  -8.335E-06
DATUM    73   3600   1   7   ,  -8.335E-06
DATUM    25   3600   1   7   ,  -8.335E-06
DATUM    30   3600   1   7   ,  -8.335E-06
WEIGHT
 295  445  406  341  277  212  148  197
2  0  0                                              ! ( SS2-M5)
 17   5   0.00 -219891.0  0.00
 21   5   0.00 -219891.0  0.00
WEIGHT
 238  235  232  229  184 293 379 309
 239 169
4  0  0                                              ! ( SS2-M6)
  9   5   0.00  -72457.0  0.00
  9   6   0.00  -72457.0  0.00
```

```
 19   3   0.00  -52000.0  0.00
 21   3   0.00  -52000.0  0.00
WEIGHT
 100 103 305 272 239 206 173 140
0  0  0                                                    ! ( SS3-M1)
0  0  0                                                    ! ( SS3-M2)
0  0  0                                                    ! ( SS3-M3)
0  0  0                                                    ! ( SS3-M4)
0  0  0                                                    ! ( SS3-M5)
LOADSET 3 "APPENDAGE BUOYANCY"
N 1.0 0
$ XIX(D) MODULE LOADS
0  0  0                  !  1-1
0  0  0                  !  1-2
0  0  0                  !  1-3
4  0  0                  !  1-4
30  0  0  22500  0         !  SONAR DOME BUOYANCY
30  1  0  22500  0         !  9.184 TONNES
30  2  0  22500  0
30  3  0  22500  0
0  0  0                  !  1-5
0  0  0                  !  1-6
0  0  0                  !  2-1
0  0  0                  !  2-2
0  0  0                  !  2-3
0  0  0                  !  2-4
2  0  0                  !  2-5
17  4  0  101773  0        !  SHAFTING ETC. BUOYANCY
21  4  0  101773  0        !  20.8 TONNES
2  0  0                  !  2-6
20  3  0  40317.2  0       !  RUDDER BUOYANCY
20  4  0  40317.2  0       !  8.228 TONNES
0  0  0                  !  3-1
0  0  0                  !  3-2
0  0  0                  !  3-3
0  0  0                  !  3-4
0  0  0                  !  3-5
END
CASE 1 "  FULL LOAD CONDITION  "
1.0  1  2  3
$BALANCE 1  2
 0.0  0.0  0.0  0.0
 0.0  0.0
ENDLOAD
```

B CPF MAESTRO Load File (Light Sag)

```
LOADSET 1  " DRAFT = 6.631.60 M"
N  1.0
IMMERSION  6631.60  0.0  -1.0014  WAVE  -4000.00  124000.00  0.0  0.0
0  0  0
0  0  0
0  0  0
0  0  0
0  0  0
0  0  0
0  0  0
0  0  0
0  0  0
0  0  0
0  0  0
0  0  0
0  0  0
0  0  0
0  0  0
0  0  0
LOADSET 2  " WEIGHT ONLY"                                    !  OPERATIONAL LIGHT SAGGING
N  1.0
0  0  0                                                      ! ( SS1-M1)
WEIGHT
   0   9  21  33  45  58  34  2
  39  76 113 150
4  0  0                                                      ! ( SS1-M2)
$ ITEM 16  CHAIN ANCHOR STBD
 12  1  0.0  -34421.0  0.0
 13  1  0.0  -34421.0  0.0
 12  2  0.0  -34421.0  0.0
 13  2  0.0  -34421.0  0.0
WEIGHT
 145  67  98 128 159 189
0  12  0                                                     ! ( SS1-M3)
$ ITEM 20, DFO NO. 1
DATUM    23   2930   10  13   ,  -8.335E-06
DATUM    22   2930   10  13   ,  -8.335E-06
DATUM    96   2930   10  13   ,  -8.335E-06
DATUM   100   2930   10  13   ,  -8.335E-06
DATUM   104   2930   10  13   ,  -8.335E-06
DATUM   106   2930   10  13   ,  -8.335E-06
$ ITEM 21, DFO NO. 2
DATUM    20   2930   10  13   ,  -8.335E-06
DATUM    21   2930   10  13   ,  -8.335E-06
DATUM    98   2930   10  13   ,  -8.335E-06
```

```
DATUM   102   2930   10  13   ,  -8.335E-06
DATUM   105   2930   10  13   ,  -8.335E-06
DATUM   107   2930   10  13   ,  -8.335E-06
WEIGHT
 209  49  91 133 175 246 287 126
 124 165 207 248 290
0  10  0                                          ! ( SS1-M4)
$ ITEM 22, DFO NO. 5
DATUM    130    970   5  17   ,  -8.335E-06
DATUM     29    970   5  17   ,  -8.335E-06
DATUM    139    970   5  17   ,  -8.335E-06
DATUM    141    970   5  17   ,  -8.335E-06
DATUM    142    970   5  17   ,  -8.335E-06
$ ITEM 23, DFO NO. 6
DATUM    131    970   5  17   ,  -8.335E-06
DATUM    138    970   5  17   ,  -8.335E-06
DATUM    137    970   5  17   ,  -8.335E-06
DATUM    133    970   5  17   ,  -8.335E-06
DATUM     30    970   5  17   ,  -8.335E-06
WEIGHT
 336 346 342 339 336 333 319 308
 320 331 342 353 342 241 287 332
 378
4  22  0                                          ! ( SS1-M5)
$ ITEM 12, 850 KW DG SET FWD
 49  3  0.0  -103309.0  0.0
 49  5  0.0  -103309.0  0.0
 50  3  0.0  -103309.0  0.0
 50  5  0.0  -103309.0  0.0
$ITEM 24, DFO NO. 7
DATUM    64    850   ,   ,    ,  -8.335E-06
DATUM    25    850   ,   ,    ,  -8.335E-06
DATUM    24    850   ,   ,    ,  -8.335E-06
DATUM    29    850   ,   ,    ,  -8.335E-06
DATUM    42    850   ,   ,    ,  -8.335E-06
DATUM    55    850   ,   ,    ,  -8.335E-06
DATUM    56    850   ,   ,    ,  -8.335E-06
DATUM    41    850   ,   ,    ,  -8.335E-06
DATUM    40    850   ,   ,    ,  -8.335E-06
DATUM    62    850   ,   ,    ,  -8.335E-06
DATUM    60    850   ,   ,    ,  -8.335E-06
$ITEM 25, DFO NO. 8
DATUM    65    850   ,   ,    ,  -8.335E-06
DATUM    26    850   ,   ,    ,  -8.335E-06
DATUM    27    850   ,   ,    ,  -8.335E-06
DATUM    35    850   ,   ,    ,  -8.335E-06
DATUM    43    850   ,   ,    ,  -8.335E-06
DATUM    57    850   ,   ,    ,  -8.335E-06
DATUM    58    850   ,   ,    ,  -8.335E-06
```

```
DATUM    44    850   ,   ,    ,  -8.335E-06
DATUM    45    850   ,   ,    ,  -8.335E-06
DATUM    63    850   ,   ,    ,  -8.335E-06
DATUM    61    850   ,   ,    ,  -8.335E-06
WEIGHT
 424 469 448 438 431 424 417 411
 380 379
176  0  0                                                    ! ( SS1-M6)
$ ITEM 5,6 AND 1/2 OF 7  MAIN GEARING AND SHAFT
 34 10  0.0   -65974.0  0.0
 34 11  0.0   -65974.0  0.0
 34 12  0.0   -65974.0  0.0
 34 13  0.0   -65974.0  0.0
 34 14  0.0   -65974.0  0.0
 36 10  0.0   -65974.0  0.0
 36 11  0.0   -65974.0  0.0
 36 12  0.0   -65974.0  0.0
 36 13  0.0   -65974.0  0.0
 36 14  0.0   -65974.0  0.0
 38 10  0.0   -65974.0  0.0
 38 11  0.0   -65974.0  0.0
 38 12  0.0   -65974.0  0.0
 38 13  0.0   -65974.0  0.0
 38 14  0.0   -65974.0  0.0
 40 10  0.0   -65974.0  0.0
 40 11  0.0   -65974.0  0.0
 40 12  0.0   -65974.0  0.0
 40 13  0.0   -65974.0  0.0
 40 14  0.0   -65974.0  0.0
$ ITEM 2,3,4  GAS TURBINE AND RAFT
 35  2  0.0   -25153.0  0.0
 35  3  0.0   -25153.0  0.0
 35  4  0.0   -25153.0  0.0
 35  5  0.0   -25153.0  0.0
 35  6  0.0   -25153.0  0.0
 35  7  0.0   -25153.0  0.0
 35  8  0.0   -25153.0  0.0
 35  9  0.0   -25153.0  0.0
 36  2  0.0   -25153.0  0.0
 36  3  0.0   -25153.0  0.0
 36  5  0.0   -25153.0  0.0
 36  6  0.0   -25153.0  0.0
 36  7  0.0   -25153.0  0.0
 36  8  0.0   -25153.0  0.0
 36  9  0.0   -25153.0  0.0
 38  2  0.0   -25153.0  0.0
 38  3  0.0   -25153.0  0.0
 38  5  0.0   -25153.0  0.0
 38  6  0.0   -25153.0  0.0
```

```
 38  7  0.0   -25153.0  0.0
 38  8  0.0   -25153.0  0.0
 38  9  0.0   -25153.0  0.0
 39  2  0.0   -25153.0  0.0
 39  3  0.0   -25153.0  0.0
 39  4  0.0   -25153.0  0.0
 39  5  0.0   -25153.0  0.0
 39  6  0.0   -25153.0  0.0
 39  7  0.0   -25153.0  0.0
 39  8  0.0   -25153.0  0.0
 39  9  0.0   -25153.0  0.0
$ FUTURE GROWTH
 34  0  0.0    -4004.0  0.0
 34  1  0.0    -4004.0  0.0
 34  2  0.0    -4004.0  0.0
 34  3  0.0    -4004.0  0.0
 34  4  0.0    -4004.0  0.0
 34  5  0.0    -4004.0  0.0
 34  6  0.0    -4004.0  0.0
 34  7  0.0    -4004.0  0.0
 34  8  0.0    -4004.0  0.0
 34  9  0.0    -4004.0  0.0
 34 10  0.0    -4004.0  0.0
 34 11  0.0    -4004.0  0.0
 34 12  0.0    -4004.0  0.0
 34 13  0.0    -4004.0  0.0
 34 14  0.0    -4004.0  0.0
 34 15  0.0    -4004.0  0.0
 34 16  0.0    -4004.0  0.0
 34 17  0.0    -4004.0  0.0
 35  0  0.0    -4004.0  0.0
 35  1  0.0    -4004.0  0.0
 35  2  0.0    -4004.0  0.0
 35  3  0.0    -4004.0  0.0
 35  4  0.0    -4004.0  0.0
 35  5  0.0    -4004.0  0.0
 35  6  0.0    -4004.0  0.0
 35  7  0.0    -4004.0  0.0
 35  8  0.0    -4004.0  0.0
 35  9  0.0    -4004.0  0.0
 35 10  0.0    -4004.0  0.0
 35 11  0.0    -4004.0  0.0
 35 12  0.0    -4004.0  0.0
 35 13  0.0    -4004.0  0.0
 35 14  0.0    -4004.0  0.0
 35 15  0.0    -4004.0  0.0
 35 16  0.0    -4004.0  0.0
 35 17  0.0    -4004.0  0.0
 36  0  0.0    -4004.0  0.0
```

```
36  1  0.0    -4004.0  0.0
36  2  0.0    -4004.0  0.0
36  3  0.0    -4004.0  0.0
36  4  0.0    -4004.0  0.0
36  5  0.0    -4004.0  0.0
36  6  0.0    -4004.0  0.0
36  7  0.0    -4004.0  0.0
36  8  0.0    -4004.0  0.0
36  9  0.0    -4004.0  0.0
36 10  0.0    -4004.0  0.0
36 11  0.0    -4004.0  0.0
36 12  0.0    -4004.0  0.0
36 13  0.0    -4004.0  0.0
36 14  0.0    -4004.0  0.0
36 15  0.0    -4004.0  0.0
36 16  0.0    -4004.0  0.0
36 17  0.0    -4004.0  0.0
37  0  0.0    -4004.0  0.0
37  1  0.0    -4004.0  0.0
37  2  0.0    -4004.0  0.0
37  3  0.0    -4004.0  0.0
37  4  0.0    -4004.0  0.0
37  5  0.0    -4004.0  0.0
37  6  0.0    -4004.0  0.0
37  7  0.0    -4004.0  0.0
37  8  0.0    -4004.0  0.0
37  9  0.0    -4004.0  0.0
37 10  0.0    -4004.0  0.0
37 11  0.0    -4004.0  0.0
37 12  0.0    -4004.0  0.0
37 13  0.0    -4004.0  0.0
37 14  0.0    -4004.0  0.0
37 15  0.0    -4004.0  0.0
37 16  0.0    -4004.0  0.0
37 17  0.0    -4004.0  0.0
38  0  0.0    -4004.0  0.0
38  1  0.0    -4004.0  0.0
38  2  0.0    -4004.0  0.0
38  3  0.0    -4004.0  0.0
38  4  0.0    -4004.0  0.0
38  5  0.0    -4004.0  0.0
38  6  0.0    -4004.0  0.0
38  7  0.0    -4004.0  0.0
38  8  0.0    -4004.0  0.0
38  9  0.0    -4004.0  0.0
38 10  0.0    -4004.0  0.0
38 11  0.0    -4004.0  0.0
38 12  0.0    -4004.0  0.0
38 13  0.0    -4004.0  0.0
```

```
 38 14   0.0     -4004.0   0.0
 38 15   0.0     -4004.0   0.0
 38 16   0.0     -4004.0   0.0
 38 17   0.0     -4004.0   0.0
 39  0   0.0     -4004.0   0.0
 39  1   0.0     -4004.0   0.0
 39  2   0.0     -4004.0   0.0
 39  3   0.0     -4004.0   0.0
 39  4   0.0     -4004.0   0.0
 39  5   0.0     -4004.0   0.0
 39  6   0.0     -4004.0   0.0
 39  7   0.0     -4004.0   0.0
 39  8   0.0     -4004.0   0.0
 39  9   0.0     -4004.0   0.0
 39 10   0.0     -4004.0   0.0
 39 11   0.0     -4004.0   0.0
 39 12   0.0     -4004.0   0.0
 39 13   0.0     -4004.0   0.0
 39 14   0.0     -4004.0   0.0
 39 15   0.0     -4004.0   0.0
 39 16   0.0     -4004.0   0.0
 39 17   0.0     -4004.0   0.0
 40  0   0.0     -4004.0   0.0
 40  1   0.0     -4004.0   0.0
 40  2   0.0     -4004.0   0.0
 40  3   0.0     -4004.0   0.0
 40  4   0.0     -4004.0   0.0
 40  5   0.0     -4004.0   0.0
 40  6   0.0     -4004.0   0.0
 40  7   0.0     -4004.0   0.0
 40  8   0.0     -4004.0   0.0
 40  9   0.0     -4004.0   0.0
 40 10   0.0     -4004.0   0.0
 40 11   0.0     -4004.0   0.0
 40 12   0.0     -4004.0   0.0
 40 13   0.0     -4004.0   0.0
 40 14   0.0     -4004.0   0.0
 40 15   0.0     -4004.0   0.0
 40 16   0.0     -4004.0   0.0
 40 17   0.0     -4004.0   0.0
WEIGHT
 391 403 415 428 410 381 415 415
 416 416 399 447 442 449 444 440
 435
90  0  0                                          ! ( SS2-M1)
$ 1/2 OF ITEM 7, INT SHAFT
 27  9  0.0   -73158.0  0.0
 31  9  0.0   -73158.0  0.0
$ ITEM 1, CRUISE DIESEL ENGINE
```

```
 28  1  0.0   -41311.0  0.0
 28  2  0.0   -41311.0  0.0
 28  3  0.0   -41311.0  0.0
 28  4  0.0   -41311.0  0.0
 28  5  0.0   -41311.0  0.0
 28  6  0.0   -41311.0  0.0
 28  7  0.0   -41311.0  0.0
 28  8  0.0   -41311.0  0.0
 28  9  0.0   -41311.0  0.0
 30  1  0.0   -41311.0  0.0
 30  2  0.0   -41311.0  0.0
 30  3  0.0   -41311.0  0.0
 30  4  0.0   -41311.0  0.0
 30  5  0.0   -41311.0  0.0
 30  6  0.0   -41311.0  0.0
 30  7  0.0   -41311.0  0.0
 30  8  0.0   -41311.0  0.0
 30  9  0.0   -41311.0  0.0
$ FUTURE GROWTH
 26  1  0.0    -4004.0  0.0
 26  2  0.0    -4004.0  0.0
 26  3  0.0    -4004.0  0.0
 26  4  0.0    -4004.0  0.0
 26  5  0.0    -4004.0  0.0
 26  6  0.0    -4004.0  0.0
 26  7  0.0    -4004.0  0.0
 26  8  0.0    -4004.0  0.0
 26  9  0.0    -4004.0  0.0
 26 10  0.0    -4004.0  0.0
 27  1  0.0    -4004.0  0.0
 27  2  0.0    -4004.0  0.0
 27  3  0.0    -4004.0  0.0
 27  4  0.0    -4004.0  0.0
 27  5  0.0    -4004.0  0.0
 27  6  0.0    -4004.0  0.0
 27  7  0.0    -4004.0  0.0
 27  8  0.0    -4004.0  0.0
 27  9  0.0    -4004.0  0.0
 26 10  0.0    -4004.0  0.0
 28  1  0.0    -4004.0  0.0
 28  2  0.0    -4004.0  0.0
 28  3  0.0    -4004.0  0.0
 28  4  0.0    -4004.0  0.0
 28  5  0.0    -4004.0  0.0
 28  6  0.0    -4004.0  0.0
 28  7  0.0    -4004.0  0.0
 28  8  0.0    -4004.0  0.0
 28  9  0.0    -4004.0  0.0
 26 10  0.0    -4004.0  0.0
```

```
29  1  0.0    -4004.0  0.0
29  2  0.0    -4004.0  0.0
29  3  0.0    -4004.0  0.0
29  4  0.0    -4004.0  0.0
29  5  0.0    -4004.0  0.0
29  6  0.0    -4004.0  0.0
29  7  0.0    -4004.0  0.0
29  8  0.0    -4004.0  0.0
29  9  0.0    -4004.0  0.0
29 10  0.0    -4004.0  0.0
30  1  0.0    -4004.0  0.0
30  2  0.0    -4004.0  0.0
30  3  0.0    -4004.0  0.0
30  4  0.0    -4004.0  0.0
30  5  0.0    -4004.0  0.0
30  6  0.0    -4004.0  0.0
30  7  0.0    -4004.0  0.0
30  8  0.0    -4004.0  0.0
30  9  0.0    -4004.0  0.0
30 10  0.0    -4004.0  0.0
31  1  0.0    -4004.0  0.0
31  2  0.0    -4004.0  0.0
31  3  0.0    -4004.0  0.0
31  4  0.0    -4004.0  0.0
31  5  0.0    -4004.0  0.0
31  6  0.0    -4004.0  0.0
31  7  0.0    -4004.0  0.0
31  8  0.0    -4004.0  0.0
31  9  0.0    -4004.0  0.0
31 10  0.0    -4004.0  0.0
32  1  0.0    -4004.0  0.0
32  2  0.0    -4004.0  0.0
32  3  0.0    -4004.0  0.0
32  4  0.0    -4004.0  0.0
32  5  0.0    -4004.0  0.0
32  6  0.0    -4004.0  0.0
32  7  0.0    -4004.0  0.0
32  8  0.0    -4004.0  0.0
32  9  0.0    -4004.0  0.0
32 10  0.0    -4004.0  0.0
WEIGHT
 428 423 418 413 408 403 429 419
 399 378
3  0  0                                          ! ( SS2-M2)
$ ITEM 13, DIESEL GEN AFT
 29  3  0.0  -137745.0  0.0
 29  4  0.0  -137745.0  0.0
 29  5  0.0  -137745.0  0.0
WEIGHT
```

```
 366 345 470 538 493 449 404 360
8  15  0                                                    ! ( SS2-M3)
$ ITEM 9, STERN TUBE
 31   2   0.00  -29332  0.00
$ ITEM 19, BW/GW COLLECT TANK
 32   1   0.00  -24754  0.00
 32   2   0.00  -24754  0.00
 32   3   0.00  -24754  0.00
 33   1   0.00  -24754  0.00
 33   2   0.00  -24754  0.00
 33   3   0.00  -24754  0.00
$ ITEM 9, STERN TUBE
 35   2   0.00  -29332  0.00
$ ITEM 26, DFO NO. 9
DATUM   118   2550    5    9  ,  -8.335E-06
DATUM   117   2550    5    9  ,  -8.335E-06
DATUM    35   2550    5    9  ,  -8.335E-06
$ ITEM 17, FW NO.1
DATUM    48   3170    1   3   ,  -9.806E-06
DATUM    53   3170    5   8   ,  -9.806E-06
DATUM    32   3170    1   8   ,  -9.806E-06
DATUM    33   3170    1   8   ,  -9.806E-06
DATUM   114   3170    1   8   ,  -9.806E-06
DATUM   119   3170    1   8   ,  -9.806E-06
$ ITEM 18, FW NO.2
DATUM    52   3170    1   3   ,  -9.806E-06
DATUM    56   3170    5   8   ,  -9.806E-06
DATUM   120   3170    1   8   ,  -9.806E-06
DATUM   113   3170    1   8   ,  -9.806E-06
DATUM    43   3170    1   8   ,  -9.806E-06
DATUM    44   3170    1   8   ,  -9.806E-06
WEIGHT
 360 426 420 414 409 403 400 395
 361 326 291 257
4  8  0                                                    ! ( SS2-M4)
$ ITEM 8 AND 9, STERN TUBE AND PROP SHAFT
 25   3   0.00  -54225.0  0.00
 25   4   0.00  -54225.0  0.00
 29   3   0.00  -54225.0  0.00
 29   4   0.00  -54225.0  0.00
$ ITEM 27, DFO NO.10
DATUM    27   2740   1   7   ,  -8.335E-06
DATUM    72   2740   1   7   ,  -8.335E-06
DATUM    28   2740   1   7   ,  -8.335E-06
DATUM    35   2740   1   7   ,  -8.335E-06
$ ITEM 28, DFO NO.10
DATUM    26   2740   1   7   ,  -8.335E-06
DATUM    73   2740   1   7   ,  -8.335E-06
DATUM    25   2740   1   7   ,  -8.335E-06
```

```
DATUM    30   2740   1   7   ,  -8.335E-06
WEIGHT
 216 335 400 337 273 209 146 194
2  0  0                                                    ! ( SS2-M5)
$ ITEM 8 AND 10, PROPELLER AND PROP SHAFT
 17   5   0.00 -219891.0  0.00
 21   5   0.00 -219891.0  0.00
WEIGHT
 236 233 230 227 182 292 379 309
 239 169
4  0  0                                                    ! ( SS2-M6)
$ ITEM 14  TACTAS HANDLING
  9   5   0.00  -72457.0  0.00
  9   6   0.00  -72457.0  0.00
$ ITEM 15  RUDDER STOCK
 19   3   0.00  -52000.0  0.00
 21   3   0.00  -52000.0  0.00
WEIGHT
 100 103 307 272 238 203 169 135
0  0  0                                                    ! ( SS3-M1)
0  0  0                                                    ! ( SS3-M2)
0  0  0                                                    ! ( SS3-M3)
0  0  0                                                    ! ( SS3-M4)
0  0  0                                                    ! ( SS3-M5)
LOADSET 3 "APPENDAGE BUOYANCY"
N 1.0 0
$ XIX(D) MODULE LOADS
0  0  0                 !  1-1
0  0  0                 !  1-2
0  0  0                 !  1-3
4  0  0                 !  1-4
30  0  0  22500  0         !  SONAR DOME BUOYANCY
30  1  0  22500  0         !  9.184 TONNES
30  2  0  22500  0
30  3  0  22500  0
0  0  0                 !  1-5
0  0  0                 !  1-6
0  0  0                 !  2-1
0  0  0                 !  2-2
0  0  0                 !  2-3
0  0  0                 !  2-4
2  0  0                 !  2-5
17  4  0  101773  0         !  SHAFTING ETC. BUOYANCY
21  4  0  101773  0         !  20.8 TONNES
2  0  0                 !  2-6
20  3  0  40317.2  0         !  RUDDER BUOYANCY
20  4  0  40317.2  0         !  8.228 TONNES
0  0  0                 !  3-1
0  0  0                 !  3-2
```

```
0  0  0                    !  3-3
0  0  0                    !  3-4
0  0  0                    !  3-5
END
CASE 1 "  T = 6631.60, TRIM= -1.0014 Deg   "
1.0  1  2  3
$BALANCE  1  1
 0.0  0.0  0.0  0.0
 0.0  0.0
ENDLOADS
```

References

[1] "MAESTRO,-Method for Analysis Evaluation and Structural Optimization, User's Manual Version 6.0,", distributed by Ross McNatt Naval Architects, Annapolis, MD., July 1992.

[2] "Vibration And Strength Analysis Program(VAST): User's Manual Version 6.0", Martec Ltd., Halifax, Nova Scotia , September, 1990.

[3] "MAESTRO/DSA,"Martec Ltd. Halifax, Nova Scotia.

UNCLASSIFIED
SECURITY CLASSIFICATION OF FORM
(highest classification of Title, Abstract, Keywords)

DOCUMENT CONTROL DATA

(Security classification of title, body of abstract and indexing annotation must be entered when the overall document is classified)

1. ORIGINATOR (the name and address of the organization preparing the document.. Organizations for whom the document was prepared. e.g. Establishment sponsoring a contractor's report. or tasking agency. are entered in section 8.)

D.R. Smith
Suite 707. 5959 Spring Garden Road
Halifax, N.S.

2. SECURITY CLASSIFICATION (overall security classification of the document including special warning terms if applicable).

Unclassified

3. TITLE (the complete document title as indicated on the title page. Its classification should be indicated by the appropriate abbreviation (S.C.R or U) in parentheses after the title).

A Procedure for Assessing the Structure of the CPF Considering the Loss of Strength Due to Corrosion

4. AUTHORS (Last name. first name. middle initial. If military. show rank. e.g. Doe. Maj. John E.)

D.R. Smith

5. DATE OF PUBLICATION (month and year of publication of document)	6a. NO .OF PAGES (total containing information Include Annexes. Appendices. etc).	6b. NO. OF REFS (total cited in document)
April 99	107	3

7. DESCRIPTIVE NOTES (the category of the document. e.g. technical report. technical note or memorandum. If appropriate. enter the type of report. e.g. interim. progress. summary, annual or final. Give the inclusive dates when a specific reporting period is covered).

DREA Contractor Report

8. SPONSORING ACTIVITY (the name of the department project office or laboratory sponsoring the research and development. Include address).

Defence Research Establishment Atlantic
P.O. Box 1012
Dartmouth, N.S. B2Y 3Z7

9a. PROJECT OR GRANT NO. (if appropriate. the applicable research and development project or grant number under which the document was written. Please specify whether project or grant).	9b. CONTRACT NO. (if appropriate. the applicable number under which the document was written).
1gc	W7707-8-5853

10a ORIGINATOR'S DOCUMENT NUMBER (the official document number by which the document is identified by the originating activity. This number must be unique to this document.)	10b OTHER DOCUMENT NOs. (Any other numbers which may be assigned this document either by the originator or by the sponsor.)
DREA CR 1999-111	

11. DOCUMENT AVAILABILITY (any limitations on further dissemination of the document, other than those imposed by security classification)

(x) Unlimited distribution
( ) Defence departments and defence contractors; further distribution only as approved
( ) Defence departments and Canadian defence contractors; further distribution only as approved
( ) Government departments and agencies; further distribution only as approved
( ) Defence departments; further distribution only as approved
( ) Other (please specify):

12. DOCUMENT ANNOUNCEMENT (any limitation to the bibliographic announcement of this document. This will normally correspond to the Document Availability (11). However. where further distribution (beyond the audience specified in (11) is possible. a wider announcement audience may be selected).

Full unlimited

UNCLASSIFIED
SECURITY CLASSIFICATION OF FORM

13. ABSTRACT (a brief and factual summary of the document. It may also appear elsewhere in the body of the document itself. It is highly desirable that the abstract of classified documents be unclassified. Each paragraph of the abstract shall begin with an indication of the security classification of the information in the paragraph (unless the document itself is unclassified) represented as (S), (C), (R), or (U). It is not necessary to include here abstracts in both official languages unless the text is bilingual).

The report describes the effect of possible corrosion of the hull plating and stiffeners on the structural strength of the Canadian Patrol Frigate in deep departure hogging and light operational sagging conditions. Balance on an eight meter wave was the sea state loading case considered. A MAESTRO analysis was carried out to obtain the initial structural strength, then the effects of corrision were assessed. To model corrosion, areas of plating and the attached stiffeners were reduced in cross-section and modelled in detail. After each reduction, the structure was analysed using the finite element analysis program, VAST, to determine the effect on strength when applying the boundary conditions and loading from the MAESTRO analysis. The adequacy paramaters and stresses with and without corrosion are presented in graphical form as a measure of the hull strength.

14. KEYWORDS, DESCRIPTORS or IDENTIFIERS (technically meaningful terms or short phrases that characterize a document and could be helpful in cataloguing the document. They should be selected so that no security classification is required. Identifiers, such as equipment model designation, trade name, military project code name, geographic location may also be included. If possible keywords should be selected from a published thesaurus. e.g. Thesaurus of Engineering and Scientific Terms (TEST) and that thesaurus-identified. If it not possible to select indexing terms which are Unclassified, the classification of each should be indicated as with the title).

corrosion
ship structures
hull
strength
MAESTRO
finite element
plating
stiffeners
VAST
structural analysis
adqeuacy parameter

The Defence Research
and Development Branch
provides Science and
Technology leadership
in the advancement and
maintenance of Canada's
defence capabilities.

Leader en sciences et
technologie de la défense,
la Direction de la recherche
et du développement pour
la défense contribue
à maintenir et à
accroître les compétences
du Canada dans
ce domaine.

#513041

DEFENCE R&D DÉFENSE

www.crad.dnd.ca